AD-A106 890 NAVAL POSTGRADUATE SCHOOL MONTEREY CA F/G 14/2
AN ANALYTICAL AND EXPERIMENTAL ANALYSIS OF FACTORS AFFECTING EX--ETC(U)
DEC 72 D L BAILEY

UNCLASSIFIED NL

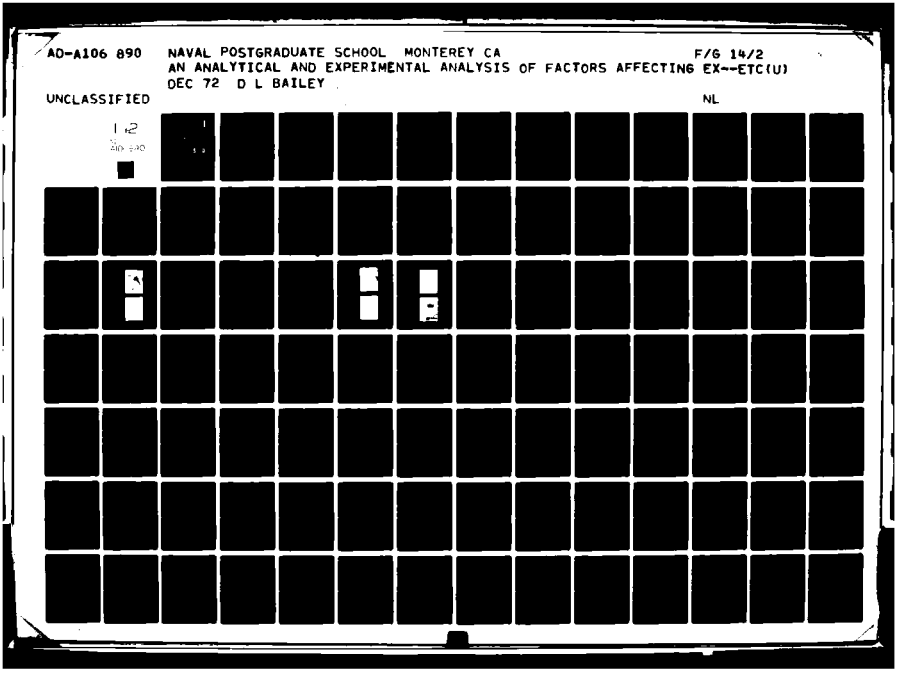

PHOTOGRAPH THIS SHEET

AD A106890

DTIC ACCESSION NUMBER

II

LEVEL

Naval Postgraduate School
Monterey, CA

I

INVENTORY

An Analytical and Experimental Analysis of Factors Affecting Exhaust System Performance in Sea Level Static Jet Engine Test Facilities.

DOCUMENT IDENTIFICATION

Dec. 72

Bailey, David L;

DISTRIBUTION STATEMENT A
Approved for public release;
Distribution Unlimited

DISTRIBUTION STATEMENT

ACCESSION FOR	
NTIS	GRA&I
DTIC	TAB
UNANNOUNCED	
JUSTIFICATION	
BY	
DISTRIBUTION /	
AVAILABILITY CODES	
DIST	AVAIL AND/OR SPECIAL
A	

DISTRIBUTION STAMP

DTIC
ELECTE
S NOV 9 1981 D
D

DATE ACCESSIONED

DATE RECEIVED IN DTIC

PHOTOGRAPH THIS SHEET AND RETURN TO DTIC-DDA-2

DTIC FORM OCT 79 70A

DOCUMENT PROCESSING SHEET

NAVAL POSTGRADUATE SCHOOL
Monterey, California

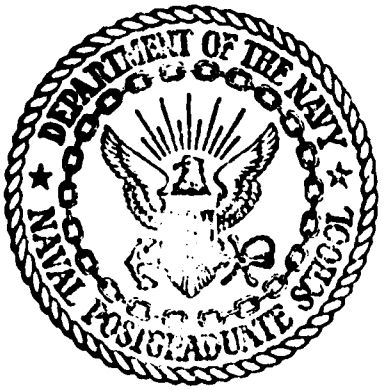

THESIS

An Analytical and Experimental Analysis
of
Factors Affecting Exhaust System Performance
in
Sea Level Static Jet Engine Test Facilities

by

David Laurence Bailey

Thesis Advisor: A. E. Fuhs

December 1972

An Analytical and Experimental Analysis of Factors Affecting Exhaust System Performance in Sea Level Static Jet Engine Test Facilities

by

David Laurence Bailey
Lieutenant, United States Navy
B.S., United States Naval Academy, 1965

Submitted in partial fulfillment of the requirements for the degree of

AERONAUTICAL ENGINEER

from the

NAVAL POSTGRADUATE SCHOOL
December 1972

Author : David Laurence Bailey

Approved by: Allen E. Fuhs
Thesis Advisor

D. W. Boltze
Chairman, Department of Aeronautics

Academic Dean

ABSTRACT

The study was motivated by a request from the Naval Air Rework Facility, NAS North Island, that work be conducted to obtain information on parameters affecting exhaust system performance in sea level static jet engine test facilities. The cost of pollution abatement devices makes it mandatory that accurate knowledge of flow parameters be developed. The study investigated by theory and experiment certain parameters of test cell design. A computer program based on the one-dimensional mass, momentum and energy conservation equations was developed. Components were designed to test on a scale of 24:1 the effects of varying exhaust system configurations. Theoretical results were found to be in good agreement with experimental data, indicating that the program may be used to analyze full scale systems. Recommendations for further development in the analysis and experimental program were made.

TABLE OF CONTENTS

I.	INTRODUCTION	8
II.	BACKGROUND	10
	A. MILITARY CONSTRUCTION PROJECT P-135	10
	B. ENGINE TECHNOLOGY	10
	C. SUMMARY OF TEST FACILITY REQUIREMENTS	13
III.	THEORETICAL ANALYSIS	16
IV.	EXPERIMENTAL DEVELOPMENT	21
	A. MODEL CONSTRUCTION	21
	B. AUXILIARY EQUIPMENT	29
	C. EXPERIMENTAL PROCEDURE	34
	D. DATA REDUCTION PROCEDURES	36
V.	ANALYSIS OF RESULTS AND CONCLUSIONS	37
	A. RESULTS	37
	B. CONCLUSIONS AND RECOMMENDATIONS	65
APPENDIX A:	TEST CELL EXHAUST SYSTEM	68
APPENDIX B:	THEORETICAL ANALYSIS	87
APPENDIX C:	DATA REDUCTION PROGRAMS	102
MAIN COMPUTER PROGRAM		110
PROGRAM M1DOT		116
PROGRAM AUG1		117
LIST OF REFERENCES		119
INITIAL DISTRIBUTION LIST		125
FORM DD 1473		127

LIST OF TABLES

Table No.		
I	Exhaust System Test Configuration Code	35
II	Experimental Results	38
III	Dual Mode Inlet Configurations	42
IV	Inlet Configuration Identification Code	43
V	Inlet Configuration Effects	52
B-I	Symbols for Main Computer Program	99
C-I	Symbols for Program M1DOT	106
C-II	Symbols for Program AUG1	109

LIST OF FIGURES

Figure No.		
1	Future Test Cell Requirements	14
2	Station Designation and Ideal Velocity Profiles for Jet Pump Analysis	18
3	Jet Mixing Zones	19
4	Station Designation (a) 15" Augmenter (b) 25" Augmenter	24
5	Position of Holes in Colander Models	25
6	Colanders Designed for Experiment	26
7	Colander Mounted on Apparatus	26
8	Inlet Schematics (a) Conical Inlet (b) Restricted Inlet	28
9	Dual Mode Installation	30
10	Nozzle and Augmenter	30
11	Inlet of Apparatus and Primary Air Piping	31
12	Primary Nozzle	31
13	Schematic of Dual Power Mode of Operation	32
14	Variation of Nozzle Total Pressure with Total Pressure at Orifice Inlet	44
15	Velocity Profiles for Configuration 210.15, P_{T_1} = 2.1 atm	45
16	Centerline Velocity Decay, P_{T_1} = 2.1 atm	47
17	Nondimensional velocity profiles, P_{T_1} = 2.1 atm	48

Figure No.		
18	Nondimensional Velocity Profile, Station 4, Configuration 200.19, Run 6.930	49
19	Secondary Mass Flow vs Primary Mass Flow for Configuration 200.13	50
20	Variation of Augmentation Ratio with P_{T_1}, Configuration 200.13	53
21	P_1 vs P_{T_1} for Configuration 200.13	54
22	Variation of Augmentation Ratio with Nozzle Exit Pressure, Configuration 200.13	55
23	Augmentation Ratio vs A_3/A_1, P_{T_1} = 1.6 atm	57
24	Augmentation Ratio vs Nozzle Displacement	58
25	Augmentation Ratio vs Augmenter Back Pressure, P_{T_1} = 1.45 atm	60
26	Augmenter Pressure Rise with Colanders Installed	61
27	Effect of Colanders on Nondimensional Velocity Profile, P_{T_1} = 1.45 atm	62
28	Effect of Colander on Nondimensional Velocity Profile, P_{T_1} = 2.1 atm	63
29	Jet Spread Parameter as a Function of A_3/A_1	64
30	Test Cells 13 and 14, NAS North Island	70
31	Test Cells 19 and 20, NAS North Island	71
32	Test Cell Pressure Profile	76

ACKNOWLEDGEMENT

The author wishes to express his sincere appreciation and gratitude to Professor Allen E. Fuhs of the Naval Postgraduate School for his guidance in the preparation and execution of this study; to Mr. B. Funk of the Department of Aeronautics for his invaluable assistance in the fabrication of model components; to the Commanding Officer and personnel, particularly Mr. Frank Freeman, of the Naval Air Rework Facility, NAS North Island for the knowledge gained during the six-week Experience Tour; and especially to his wife for her support and patience during the long endeavor. This work was funded in part by AIRTASK Number A330330C/551B/2F00-432-302.

I. INTRODUCTION

Funding is planned for Fiscal Year 1975 for MILCON P-135 at the Naval Air Rework Facility at NAS North Island. The project will include construction of two large turbojet or turbofan test cells as well as the modernization of two existing cells. All four cells will be equipped with pollution abatement devices to meet local environmental protection requirements as required by Executive Order 11282, May 26, 1966.

Useful design life for modern jet engine test facilities is approximately 20 years. This may be extended by proper planning for advances in engine size and flow characteristics.

Because of the cost of test cell construction and pollution abatement systems, flexibility is of the utmost importance. Air flow requirements will range from that required by a small turbojet at idle power to that required by a large turbofan at full power. Exhaust cooling requirements will range from none to whatever is needed for a large afterburning engine.

A jet engine operates as a jet pump when installed in a sea level static test facility. Many studies have been accomplished on jet pumps [Refs. 1 - 7], but little empirical information is available on engine test facility flow systems. The aim of this project was to study by analysis and experiment the factors which determine the performance of such a system.

Parameters which may vary in a jet test facility include augmenter length and diameter, engine position and size relative to the augmenter, and back pressures as determined by exhaust treatment facilities and aerodynamic design. Each individual engine type has characteristic flow properties at innumerable operating points, and these properties will vary significantly between engine types.

A computer program based on one-dimensional analysis of the conservation of mass, momentum and energy was developed for the Naval Postgraduate School IBM-360/67 digital computer. In this program the significant parameters could be varied,and predictions could be made of test cell flow properties based on engine operating points.

An experimental exhaust system was designed to match the inlet and test section experimental apparatus designed by Tower [Ref. 8]. Experimental work was carried out to check the validity of the computer program as well as to obtain empirical evidence of the effects of the physical variables in test cell design and construction.

II. BACKGROUND

A. MILITARY CONSTRUCTION PROJECT P-135

The primary motivation for this study was the need for an analysis to be conducted prior to the final project definition of MILCON P-135. This project is for the previously described jet engine test facilities at the Naval Air Rework Facility, NAS North Island.

B. ENGINE TECHNOLOGY

In the past, several different aircraft types were powered by similar engines. New technological developments have changed this situation dramatically, as evidenced by the differences between characteristics of high bypass ratio turbofans and afterburning turbojets. Future changes and developments will require more precise matching of engines and airframes for specific missions. Because of the vast differences of engine types, it may not prove feasible to build a single test cell capable of testing every engine in the Navy's inventory. Present Navy policy is to assign the overhaul and repair responsibility of a particular engine type to each NARF.

The first advanced technology engines for Navy fighter aircraft will be used in the F-14 Tomcat. Early versions will use the Pratt and Whitney TF-30 412 engine, while F-14B models will be equipped with the more powerful F401 PW 400 engines. The latter engine is in the 20,000 - 30,000 pound thrust category and will have an air flow rate at full power of about 300 pounds per second. If a test cell augmentation

ratio of 2:1 is chosen, a cell flow rate of about 900 pounds per second can be expected. Test cell augmentation ratio is defined as the total cell airflow less engine airflow divided by engine airflow.

Further fighter aircraft development will bring to the Navy the Advanced Deck Launched Interceptor. The ADLI will utilize an advanced technology engine with turbine inlet temperatures in excess of 3,000° F. Also, advanced hybrid multicycle engines are being developed and will be introduced to operational use during the life of test cells built in the present decade [Ref. 9]. Turboramjets or supercharged ejector ramjets may also be introduced.

Future attack aircraft must combine the capability of high subsonic cruise speeds with the ability to loiter for long periods over target areas. Non-afterburning turbofan engines are presently in use for attack missions, and their continued development and refinement are predicted.

The U. S. Marine Corps presently has the Harrier (AV-8A) in operational use. The Navy may move toward procurement of Harrier in the near future and advanced vectored thrust V/STOL aircraft within 10 to 15 years. The Harrier utilizes the Pegasus turbofan engine with variable nozzles. The advanced Pegasus 15 engine will have 25,000 pounds of thrust and an airflow requirement of 450 pounds per second. A requirement for testing these engines is that shrouds and ducts be installed for directing the exhaust streams of the individual nozzles into a common exhauster [Ref. 10]. With a 1:1 augmentation ratio, total cell flow requirements for this engine will be 900 pounds per second.

The Navy is currently developing the S-3 carrier based ASW aircraft, which is powered by the General Electric TF-34 turbofan engine. This is a 9,000 pound thrust engine with an airflow capacity of about 300 pounds per second and will be the first engine that will be tested in a cell in the same configuration as it is mounted on the aircraft. That is, it will be pylon mounted, thereby requiring an overhead thrust bed. The TF-34 has a bypass ratio greater than 6:1. Because of the exhaust characteristics of turbofan engines, care must be taken in matching the engine and the augmenter to avoid excess air entrainment over that which is required for cooling purposes. Excess air entrainment increases the cell depression [Ref. 11]. Cell depression is the difference between cell ambient pressure and atmospheric pressure, and a large difference may cause a redistribution of pressures acting on the engine and result in erroneous thrust measurements.

Future patrol aircraft developed and introduced in the 1980's may utilize large fan engines. Other aircraft using the same type of engines may be developed to replace the Navy's present transport fleet. Military transports with STOL capability will require turbofans in the 25,000 - 30,000 pound thrust category [Ref. 12]. The airflow through an engine of this size will be on the order of 1,000 pounds per second, and total cell airflow could run as high as 2,000 pounds per second, depending on the augmenter design.

Smaller logistic aircraft, successors to the C-2 COD aircraft, may use turbofans in the 5,000 - 10,000 pound thrust category. These will be similar to the above-mentioned TF-34 in flow requirements, and the test facility requirements will be similar as well.

In order to minimize drag associated with nozzle and airframe interaction, non-axisymmetric nozzles may be employed in the future. This possibility implies a requirement for an augmenter tube designed to permit replacement of the receptor bellmouth.

Knowledge of systems on the horizon which may eventually become operational is essential to provide flexibility and long life for projected test facilities.

C. SUMMARY OF TEST FACILITY REQUIREMENTS

Figure 1 from Ref. 13 is the summary of test cell requirements available from current sources. As with any forecast, it includes some uncertainty;but the information included is as authoritative as possible, having been collected from engine manufacturers, Department of Defense planning agencies, published reports of service sponsored research and interviews with facilities planners for several test cell operators.

Gerend [Ref. 14] provides a simple method of predicting turbine engine weights and dimensions. This method was used to confirm the validity of this summary information. This projection is confined to facilities for sea level testing only. References 15 and 16 provide forecasts of requirements for altitude test facilities.

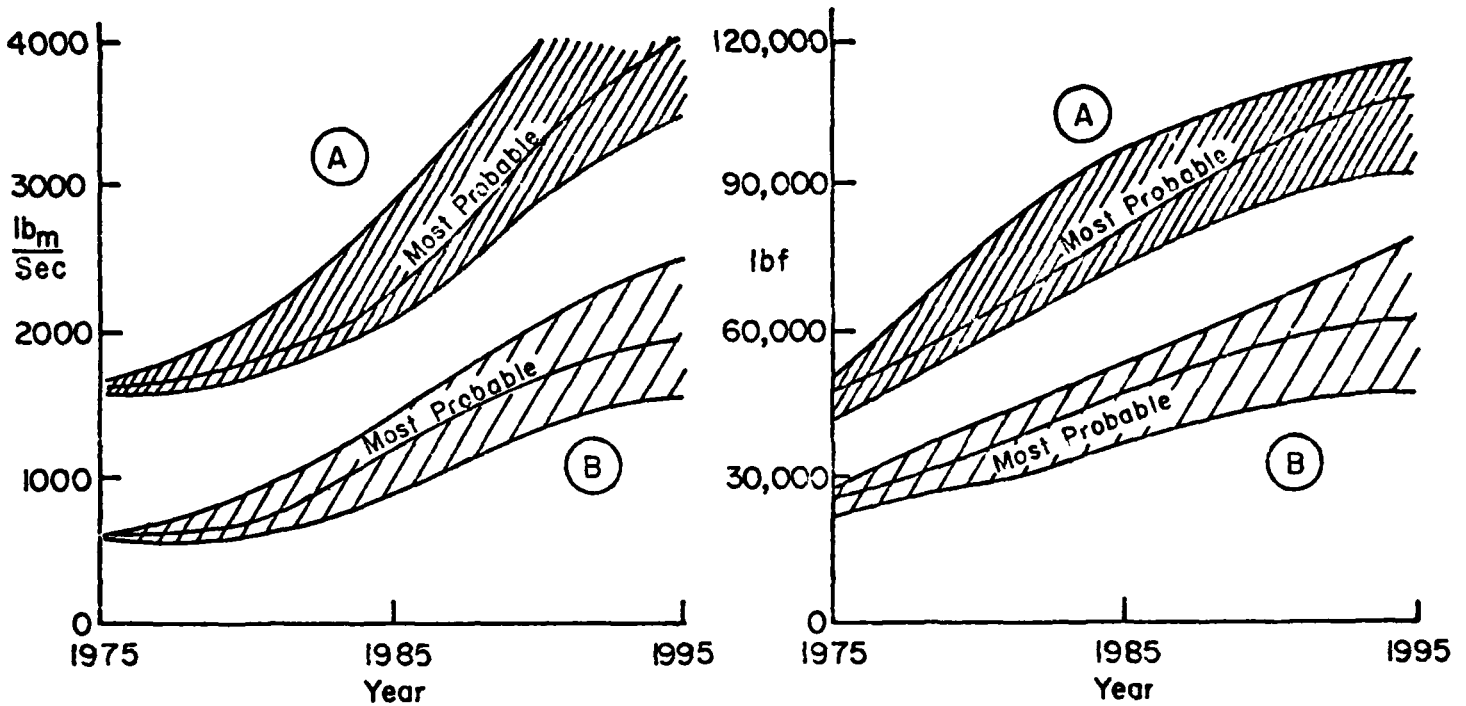

FIGURE 1 FUTURE TEST CELL REQUIREMENTS

Readers unfamiliar with test cell design philosophy may find it useful to scan Appendix A before proceeding. This section contains a detailed discussion of present and future design criteria for test facilities, and will familiarize the reader with test cell terminology.

III. THEORETICAL ANALYSIS

The analysis developed to study the augmenter flow was based on the one-dimensional conservation of mass, energy and momentum. Krenkel and Lipowsky [Ref. 5] have previously illustrated the usefulness of applying a one-dimensional analysis for solving problems involving ejectors. The procedure has been found to be particularly useful in problems involving constant pressure or constant area mixing.

Details involving the actual mixing processes have been omitted. Much work in describing the mixing process has been accomplished [Refs. 17-25]. These analyses are generally similar to those involving free jets, and most involve a boundary layer type analysis of the mixing region between two streams. According to Hanbury [Ref. 26], these procedures are very complex, and solutions depend both on the control parameters and the actual flow geometry. Because this study was intended to find trends in flow properties rather than to find exact data, the one-dimensional analysis was chosen. The following assumptions were made for the analysis used in this work:

1. Flow is one-dimensional and steady.
2. Flow is adiabatic.
3. Flow properties are uniform at a cross section.
4. All gases are treated as ideal gases.
5. The mixing is accomplished in a constant area.

Figure 2 illustrates the ideal one-dimensional jet pump. Stations 1 and 2 are coplanar and are the primary and secondary flow nozzles. Station 3 is the augmentor exit. The analysis assumed complete mixing at station 3. The velocity profiles of Fig. 2 were used in the continuity equations. The equation for conservation of mass

$$\rho_1 U_1 A_1 + \rho_2 U_2 A_2 = \rho_3 U_3 A_3 \qquad \text{(III-1)}$$

The equation for momentum is

$$(P_1 + \rho_1 U_1^2) A_1 + (P_2 + \rho_2 U_2^2) A_2 = (P_3 + \rho_3 U_3^2) A_3 \qquad \text{(III-2)}$$

Conservation of energy is expressed by

$$(\rho_1 U_1^2 A_1)(C_p T_1 + U_1^2/2) + (\rho_2 U_2^2 A_2)(C_p T_2 + U_2^2/2) =$$

$$(\rho_3 U_3^2 A_3)(C_p T_3 + U_3^2/2) \qquad \text{(III-3)}$$

Appendix B contains detailed developments of the computational procedure. The basic program solves for two values of temperature at station 3 and iterates until the two values are within one degree Rankine of one another.

Input data include primary and secondary stagnation values and outlet static pressure. Primary and secondary static pressures at stations 1 and 2 were assumed to be equal.

The method of handling the relative positions of the primary and secondary nozzles involved modeling the behavior of the expanding primary jet and the velocity profile in the mixing zone. Figure 3

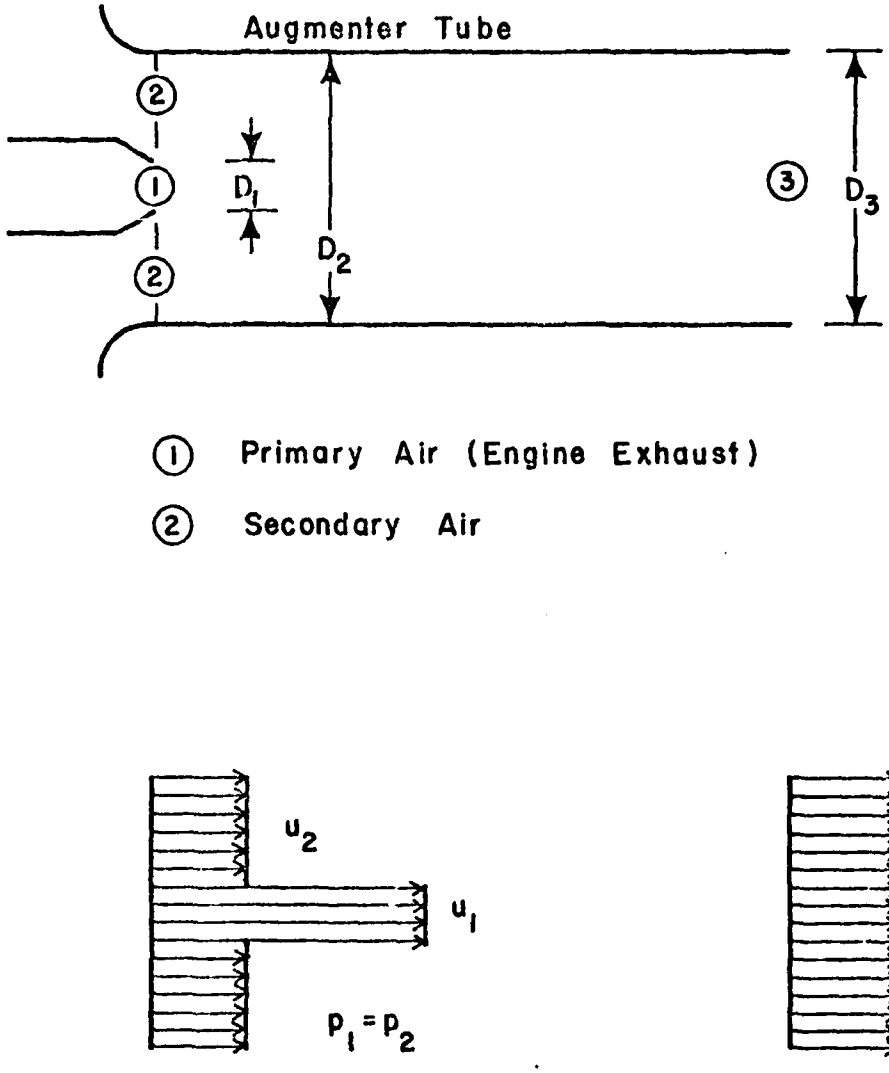

FIGURE 2 STATION DESIGNATION AND IDEAL VELOCITY PROFILES FOR JET PUMP ANALYSIS

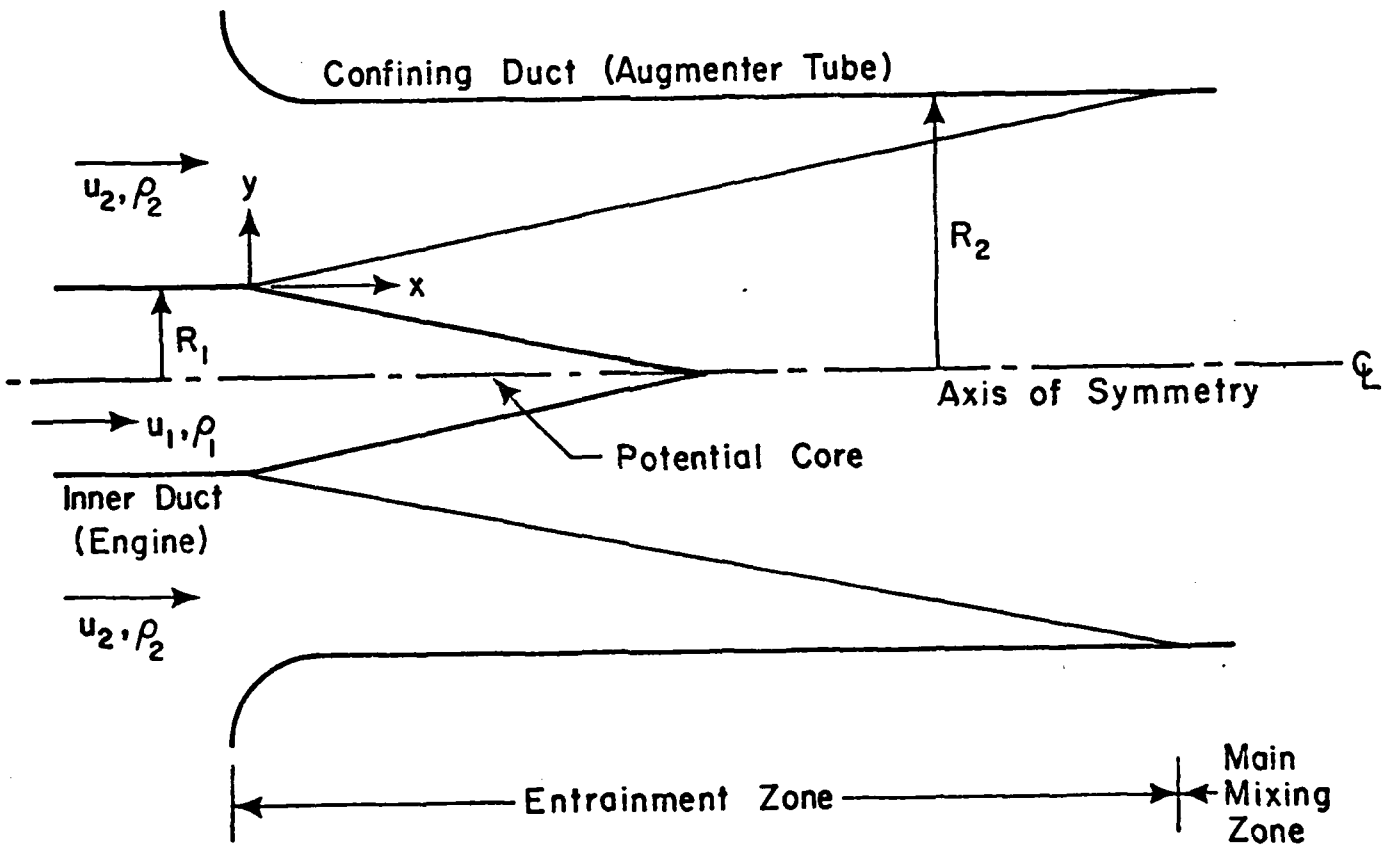

FIGURE 3 JET MIXING ZONES

illustrates the nomenclature of the mixing zones. Bauer [Ref. 27] discusses a nondimensional jet spread parameter σ . He has shown that Abramovich's model for σ is a good approximation to empirical data.

$$\sigma = 24\ U_{mean}/U_{\infty} \qquad \text{(III-4)}$$

As shown by Bauer [Ref. 27] and Korst and Chow [Ref. 19] the velocity profile in the mixing region was approximated by an error function.

A computer routine was developed to determine the effect of augmenter length on the jet pump. Values of wall friction were computed using flat plate drag coefficients and viscosity values from Schlichting [Ref. 28].

Reference 29 lists ducting parameters for losses caused by components in the exhaust system. Computations were made to determine the effect of augmenter entry design using loss coefficients for re-entry and bellmouth inlets.

The exhaust system back pressure was set arbitrarily in the computer routine but could be varied by use of a loop command. The Main Computer Program is included in the computer program section following Appendix C.

IV. EXPERIMENTAL DEVELOPMENT

A. MODEL CONSTRUCTION

The size of the simulated exhaust system was determined by the scale of the model developed by Tower [Ref. 8] and by the mass flow required for proper simulation. The inlet and test section components of Tower's model were designed as a 24:1 scale model of a 24' x 24' test cell.

Much of the distortion present at the compressor face in a cell mounted engine is due to vortices formed either by turning the flow or by the presence of flow treatment devices both acoustic and mechanical in nature.

The size of the model was determined by balancing the predicted mass flow which would be produced when a simulated engine was driven by one of the available compressed air supplies with the size required for meaningful distortion data collection. The compressed air source is discussed in Section IV B.

The model was constructed entirely of plexiglass. This material was chosen because of its ready availability and the ease with which components could be constructed. The material is light so that parts may be easily interchanged. Finally, the choice allowed appropriate flow visualization techniques to be used throughout the model.

The size of the augmenter also was determined by available material. A section of 5.0" inner diameter molded acrylic tubing was

chosen. Outer diameter was 5.5". Two sections of different length were constructed; the lengths were 15" and 25". Each section was equipped with 7 data collection stations positioned as shown in Fig. 4. Each station consisted of three static pressure ports positioned 120° apart on a circumference. The diameter of the ports was 0.062". A threaded mounting block was positioned at each station for the purpose of securing the probes used to measure total pressure and temperature.

In order to increase the back pressure of the system and to study the effect of different designs, two model colanders were built from the same tubing as that used for the augmenter tubes. Each colander was 6.25" long. One model was drilled with 12 rows of 5 holes each which produced a 35 percent increase in flow area. The holes were spaced 30° apart. The second model was drilled with 15 rows of 5 holes each, producing a 69 percent increase in flow area. The rows were 24° apart for the second model. All holes were 0.75" in diameter. Figure 5 illustrates the position of the holes. One end of each colander was capped with a 7.5" square section of 1/4" plexiglass.

The open end of each colander and one end of each augmenter were equipped with identical end plates for fastening purposes. The end plates were also 7.5" square sections of 1/4" plexiglass with 5.5" circular cutouts. Bolt holes were drilled in each corner of the end plates. The colanders are shown in Fig 6, and Fig. 7 shows a colander mounted for testing.

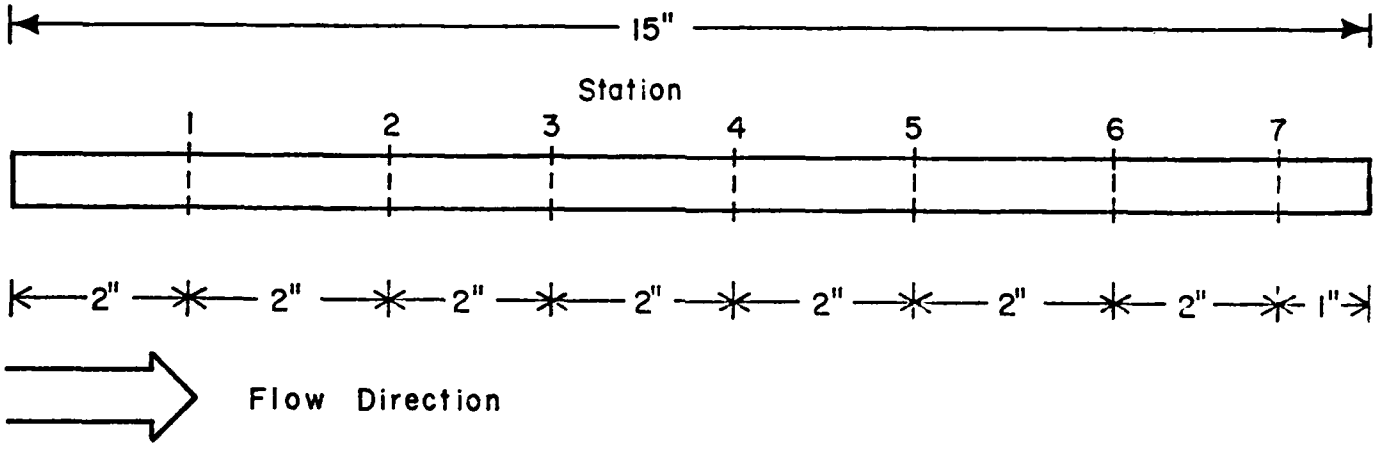

(a) 15" Augmenter

FIGURE 4 STATION DESIGNATION

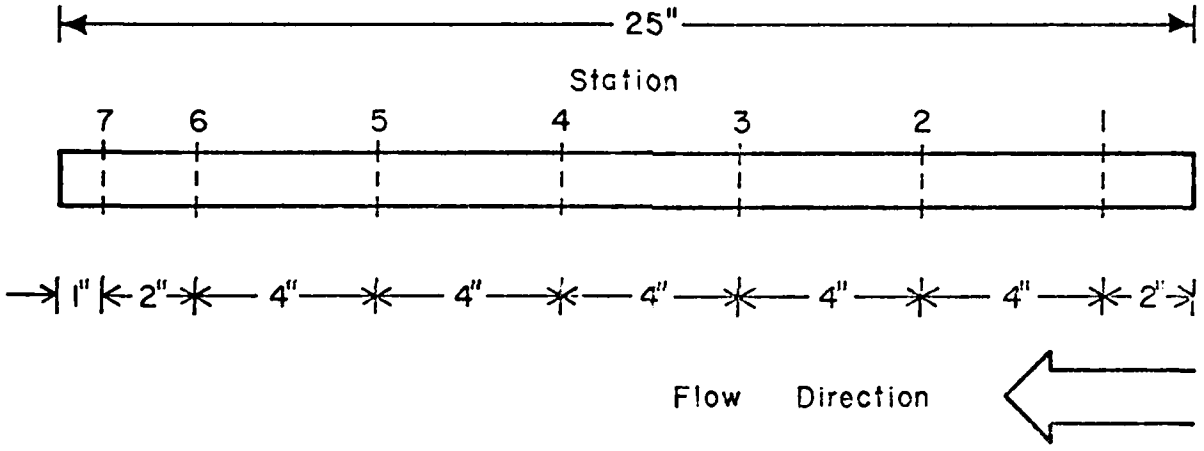

(b) 25" Augmenter

FIGURE 4 STATION DESIGNATION (continued)

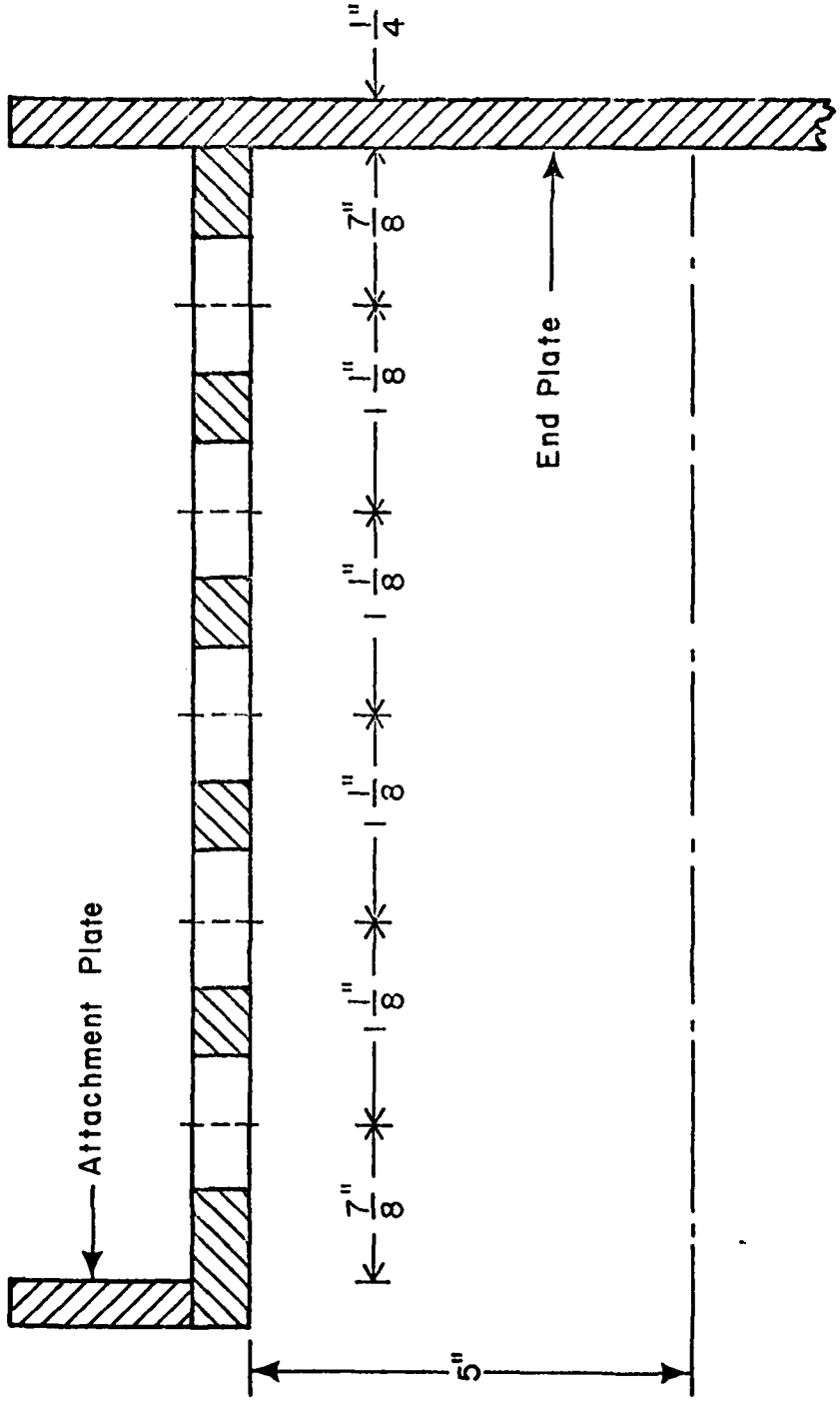

FIGURE 5 POSITION OF HOLES IN COLANDER MODELS

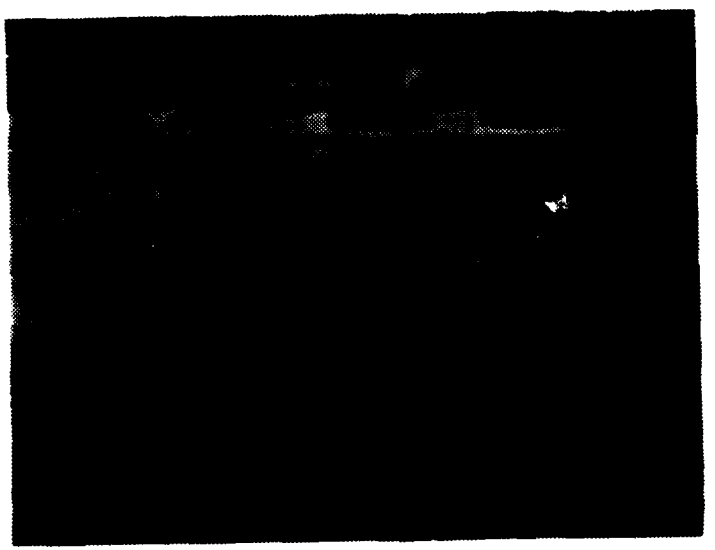

FIGURE 6 COLANDERS DESIGNED FOR EXPERIMENT

FIGURE 7 COLANDER MOUNTED ON APPARATUS

A conical inlet to the augmenter was fashioned from a 1" thick speciman of plexiglass and was designed for quick installation and removal. The maximum diameter of the inlet cap is 7.0" and closes to 5.0" on a 45° angle. The conical inlet is illustrated in Fig. 8a.

A restricted inlet was designed to simulate the orifice installation used in one test facility to limit the cell augmentation ratio. This inlet was also fashioned from a 1" thick piece of plexiglass on a lathe. The diameter of the restricted inlet is 3.0" as illustrated in Fig. 8b.

The end section of the model test cell was designed as a simple box structure 15" long with a square 12" x 12" cross section. The top piece had a cutout to accommodate the pipe which carried the primary air to the installed nozzle.

A spacer section holder was constructed to vary the linear distance between the nozzle and the inlet to the augmenter tube. The section was designed such that combinations of sections properly installed allowed the distance to be varied over a range of 5" in 1/2" increments. The nozzle with no spacers installed was positioned 1" inside the augmenter.

An aluminum cross brace was designed to serve the dual purpose of adjusting and securing the augmenter and colander sections. The brace was clamped to the table holding the model and was adjustable in the vertical as well as the horizontal direction. The end plate of the

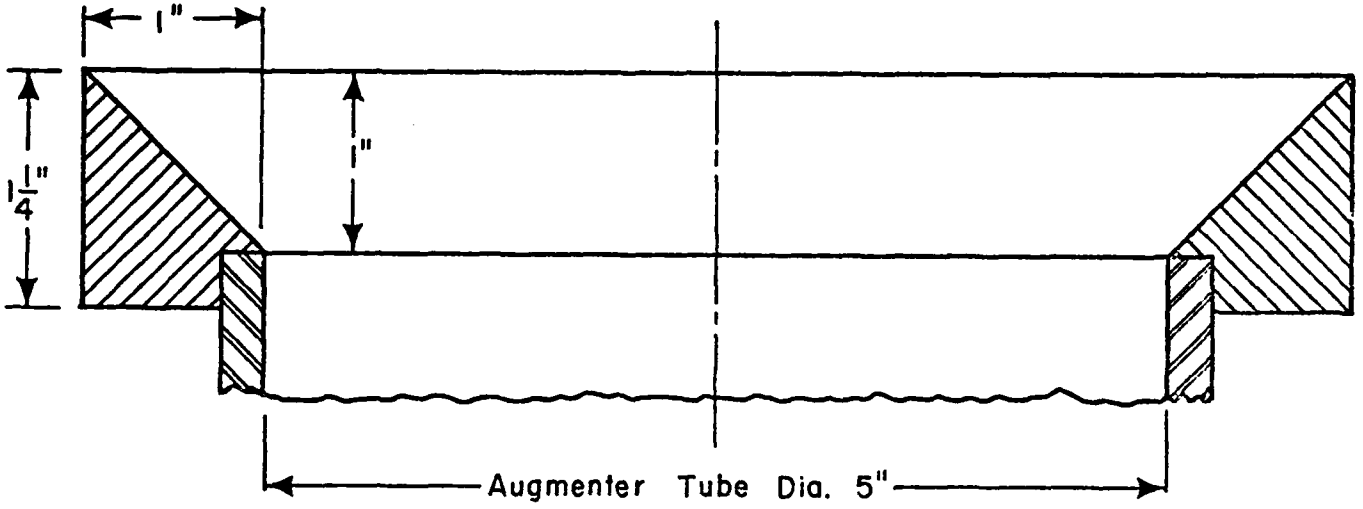

(a) Conical Inlet

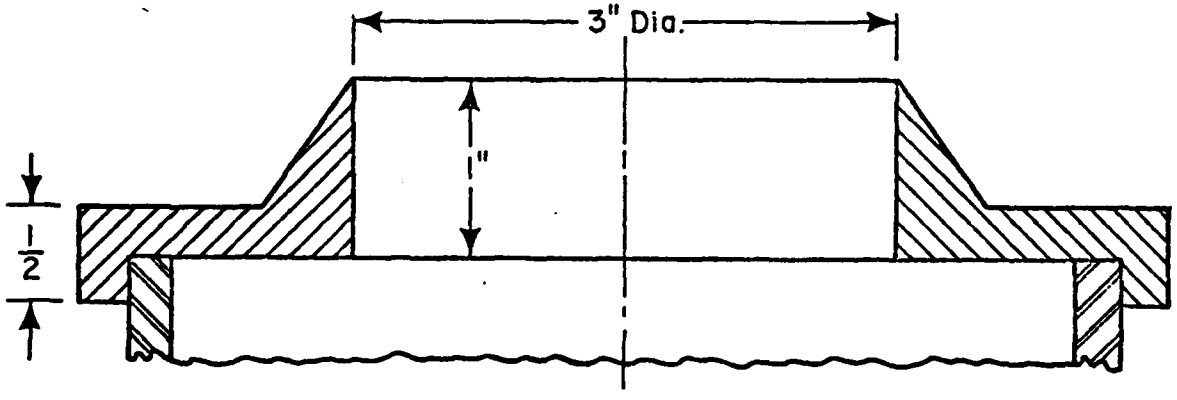

(b) Restricted Inlet

FIGURE 8 INLET SCHEMATICS

last section installed was bolted to the cross brace. Figures 7, 9 and 10 show the cross brace. Figures 9 through 11 show various views of the model as the tests were run in the laboratory.

The primary nozzle was taken from an earlier experiment involving jet pumps conducted by Wade [Ref. 7]. The nozzle exit diameter was enlarged to 1.0" for this experiment. It will be possible in future experiments to use the same nozzle with a larger diameter by machining off progressively greater amounts of material. The nozzle is of the converging type and is made of stainless steel. Figure 12 pictures the nozzle installed in the test model.

The experiments were run using various inlet configurations designed and discussed by Tower [Ref. 8]. Tower utilized a 1/2 horsepower squirrel cage blower to suck air through the simulated engine inlet which was instrumented to obtain distortion data. The mass flow removed from the test cell by the blower was nearly equal to the mass flow passing through the nozzle at full power, so that the total mass flow through the inlet was nearly equal to the mass flow through the augmenter. A schematic of the dual power mode of operation is shown in Fig. 13.

B. AUXILIARY EQUIPMENT

The two stage Carrier compressor located in Building 230 of the Naval Postgraduate School supplied air for the primary nozzle. This compressor is nominally rated at an outlet pressure of 29 psia with a

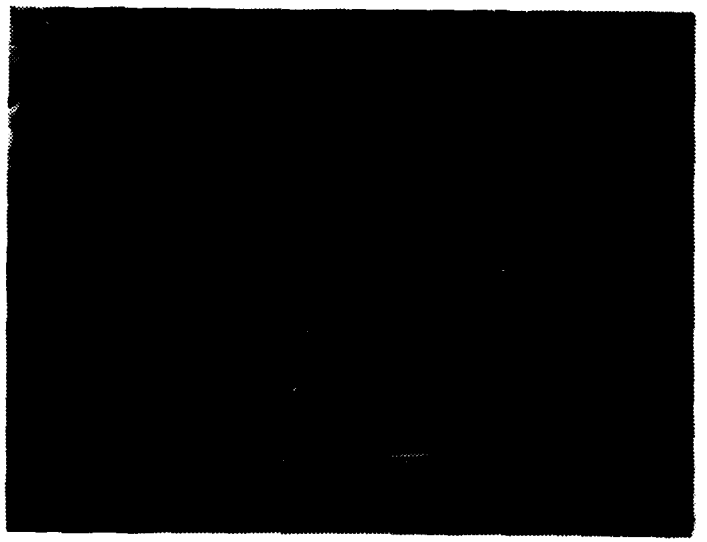

FIGURE 9 DUAL MODE INSTALLATION

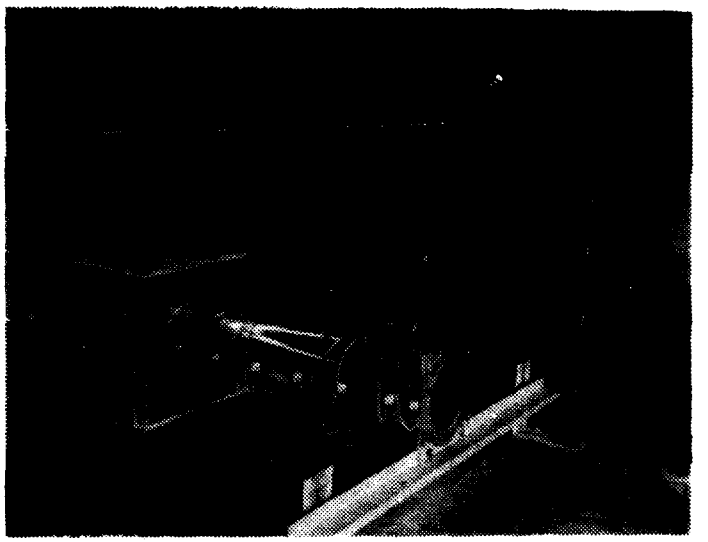

FIGURE 10 NOZZLE AND AUGMENTER

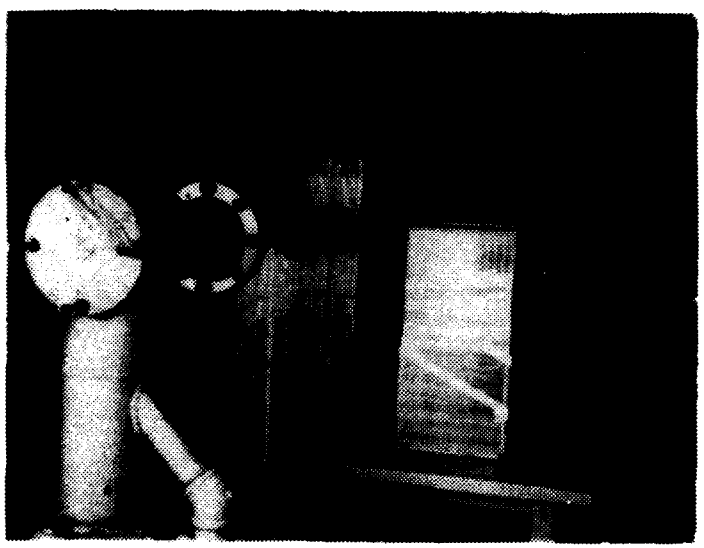

FIGURE 11 INLET OF APPARATUS AND PRIMARY AIR PIPING

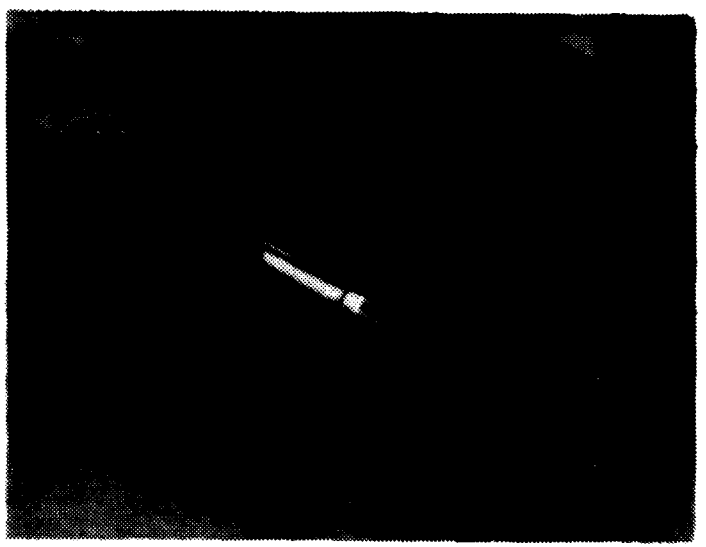

FIGURE 12 PRIMARY NOZZLE

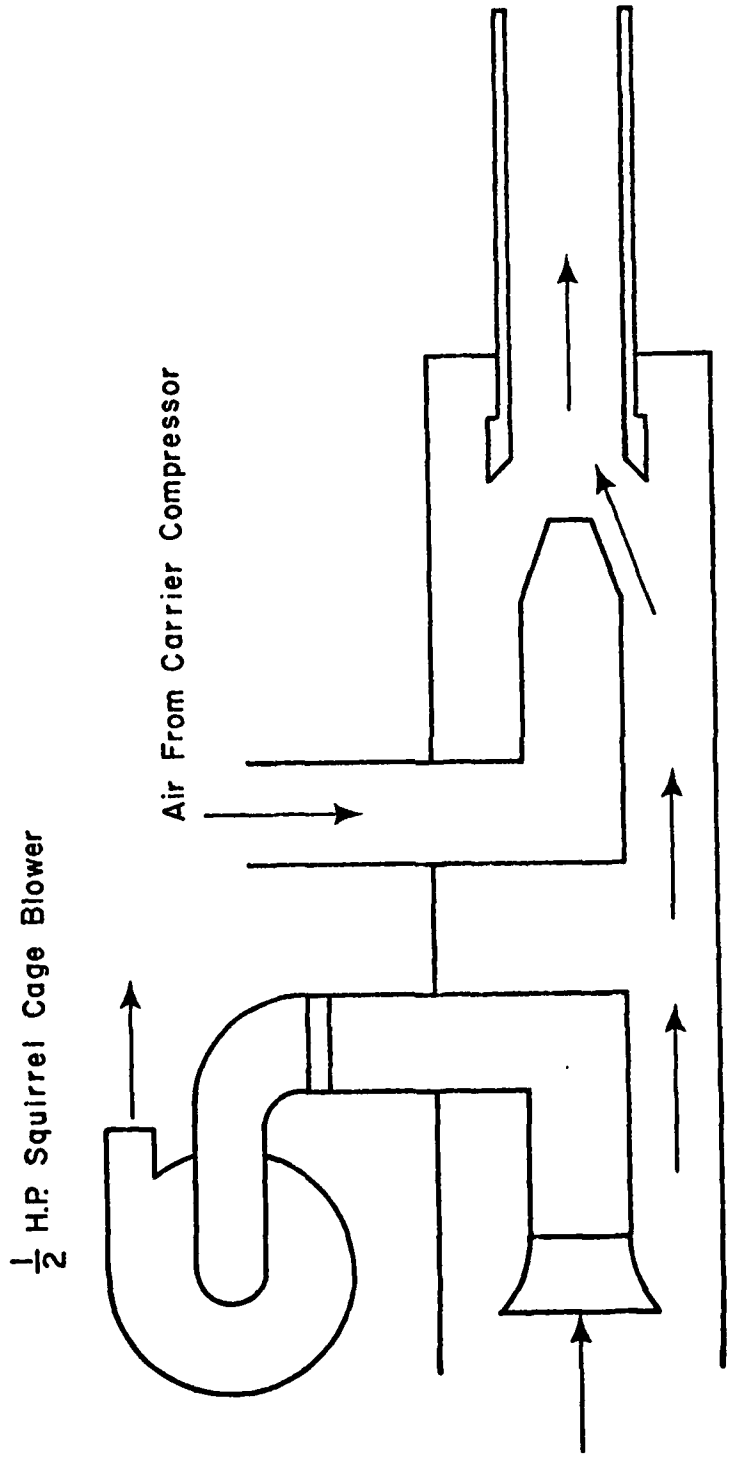

FIGURE 13 SCHEMATIC OF DUAL POWER MODE OF OPERATION

maximum flow capacity of about 4.5 pounds per second. Higher pressures were measured in this experiment however. Pressure taps at the flow orifice inlet indicated a maximum pressure of 35" of mercury gage, or almost 32 psia. Excess air was piped to the atmosphere through a separate valve system. Flow rate for the nozzle was controlled by valves in Building 249 where the experimental apparatus was installed. The air was piped underground from Building 230 to Building 249.

A stainless steel sharp edge orifice was installed in a 3" pipe to measure the mass flow through the nozzle. The installation met ASME standards for orifices. Flow rates were calculated according to Ref. 30; the calculations are discussed in detail in Appendix C. The pressure readings at the orifice were measured by flange taps. The inlet pressure was measured with a mercury manometer, and the pressure drop through the orifice was measured with a water manometer. The temperature upstream of the orifice was measured by a chromel-alumel thermocouple with a readout from a Leeds and Northrop millivolt potentiometer.

A Kiel probe was used to measure total pressure in the augmenter, and an iron-constantan thermocouple was used to measure total temperature. To obtain mass flow rate in the augmenter, pressure and temperature readings were taken at 1/4" radial increments starting at the centerline. The probes were held in place by the mounting blocks discussed in the preceding section. The pressures were measured on a water manometer when possible and on a mercury manometer when the range of the water manometer was exceeded. The recorded values were

used in the computer program AUG1 to determine the flow rate. This computer program is discussed in Appendix C.

Using water manometers, static pressures were measured at each of the seven augmenter stations. The three static ports at each axial position were joined in a single manifold to average out fluctuations.

C. EXPERIMENTAL PROCEDURE

Several test configurations were investigated. Table I shows the method of designating the configuration. A configuration designated 200.15 indicates the use of the 25" augmenter with no colander or inlet cap, a nozzle diameter of 1" and a spacer combination totaling 2".

Prior to starting the compressor, it was necessary to insure that all valves leading to other experiments were closed and that the excess air dump valve was fully open. It was also necessary to pre-oil the compressor bearings for a 30 minute period prior to starting.

After starting the compressor for the first run of the day, it was necessary to wait 5 to 10 minutes to allow the inlet temperature to stabilize. Once the temperature was stable, a typical run consisted of the following steps:

1. Set the inlet pressure as measured at the orifice inlet flange taps.
2. Record the inlet temperature and pressure and the pressure drop across the orifice.
3. Record static pressures at 7 axial stations on the augmenter.

Table 1 Exhaust System Test Configuration Code

ABC.DE

A: Augmenter Length
1.....15"
2.....25"
3.....40"

B: Inlet Configuration
0.....None
1.....Conical
2.....Restricted

C: Colander
1.....None
2..1.35 x Aug Area
3..1.69 x Aug Area

D: Nozzle Diameter
1.....1"
2.....1.25"
3.....1.5"

E: Displacement (Spacers)
1.....0"
2.....1/2"
3.....1"
4.....1-1/2"
5.....2"
6.....2-1/2"
7.....3"
8.....3-1/2"
9.....4"

4. Record total pressures and temperatures while traversing the augmenter at a given station.

5. Repeat step 4 at other stations as desired to determine velocity profiles or to confirm flow rate calculations.

6. Set a new inlet pressure,and repeat steps 2 through 5.

D. DATA REDUCTION PROCEDURES

The primary mass flow through the nozzle was calculated according to specifications set in Ref. 30. Calculations are discussed in detail in Appendix C. The total mass flow in the augmenter was determined by a procedure which divided the flow area into 10 concentric areas divided by circles 1/4" apart. It was assumed that the velocity was constant in each small area. It was also assumed that the static pressure was constant at all points on a cross section of the augmenter.

Using isentropic flow relations and the perfect gas law, it was possible to determine the density and velocity at each point where the total temperature and pressure had been measured. Mass flows were calculated for each incremental area and totaled to find the total augmenter mass flow. Program AUG1 computes the mass flows on the IBM-360/67 digital computer and is discussed in Appendix C.

V. ANALYSIS OF RESULTS AND CONCLUSIONS

A. RESULTS

Table II summarizes the data obtained from the experimental apparatus discussed in the previous section. Runs 1.929 through 4.929, 1.004 through 3.004, 1.006 through 5.006, and 1.011 through 5.011 were run with Tower to study the effects of changing the inlet configuration. Analysis of the data indicates two factors which affected the performance. Inlet acoustic treatments in the form of either flat or staggered baffles cut the augmentation ratio by a factor of 1/3. Compare run 1.004 with 5.006. It is seen that the installation of acoustic treatments, which is necessary if cells are to conform with local anti-noise ordinances, also helps to maintain the augmentation ratio at a reasonable level.

The second major factor that was found to affect test cell performance was the presence of turning vanes. Turning vanes are necessary in some installations to reduce compressor face inlet distortion. Large fan engines are particularly susceptible to distortion. Tower [Ref. 8] discussed distortion limits for various engines. Results indicate that the decreased turbulence level obtained when turning vanes are installed leads to a decrease in total cell mass flow. This occurs because the mixing process in the augmenter becomes less effective. Increased turbulence in either the secondary or primary stream causes mixing to occur more rapidly as evidenced by the centerline velocity decay. Compare run 1.929 with run 1.004.

Table II Experimental Results

Configuration	Run	Station	$\dot{m}_1$ (pps)	$\dot{m}_3$ (pps)	$\dot{m}_2/\dot{m}_1$	P_{noz}/P_{atm}	U_{cl} (fps)
200.11	1.929	4	0.51	2.50	3.92	2.1	909
200.11	2.929	4	0.52	1.61	2.10	2.1	859
200.11	3.929	4	0.54	2.34	3.33	2.1	935
200.11	4.929	4	0.53	2.55	3.78	2.1	839
200.11	1.930	4	0.56	2.02	2.64	2.1	869
200.12	2.930	4	0.54	2.63	3.87	2.1	970
200.13	3.930	4	0.54	2.70	4.01	2.1	936
200.15	4.930	4	0.54	2.58	3.82	2.1	873
200.17	5.930	4	0.53	3.26	5.12	2.1	746
200.19	6.930	4	0.53	2.98	4.60	2.1	588
210.13	1.004	4	0.57	2.01	2.52	2.1	690
210.13	2.004	4	0.54	1.90	2.50	2.1	592
210.13	3.004	4	0.54	2.90	4.40	2.1	824
220.15	1.006	4	0.55	2.20	2.98	2.1	814
220.15	2.006	4	0.52	1.11	1.16	2.0	785
220.15	3.006	4	0.51	7.88	14.53	2.0	774
220.15	4.006	4	0.50	1.09	1.18	2.0	781
210.15	5.006	4	0.52	3.22	5.17	2.0	811
210.15	1.009	1	0.56	2.67	3.75	2.1	1375
		2		2.70	3.80		1334
		3		2.90	4.17		1107
		4		2.73	3.86		812
		5		3.04	4.40		658
		6		2.87	4.11		556

Table II Experimental Results (continued)

Configuration	Run	Station	$\dot{m}_1$ (pps)	$\dot{m}_3$ (pps)	$\dot{m}_2/\dot{m}_1$	$\frac{P_{noz}}{P_{atm}}$	U_{cl} (fps)
		7		2.98	4.29		490
200.15	2.009	4	0.53	3.28	5.21	2.05	857
		7		3.27	5.17		495
220.15	3.009	7	0.52	1.45	1.76	2.05	244
222.15	4.009	4	0.53	2.25	3.24	2.1	776
		7		1.60	2.01		243
210.10	1.011	7	0.54	2.17	3.03	2.05	432
210.10	2.011	7	0.50	1.91	2.84	1.9	445
210.10	3.011	7	0.41	1.77	3.29	1.6	344
210.10	4.011	7	0.41	1.77	3.29	1.6	349
210.10	5.011	7	0.41	1.90	3.63	1.6	331
210.10	1.013	7	0.42	1.87	3.41	1.6	346
200.10	2.013	7	0.42	1.79	3.30	1.6	334
220.13	3.013	7	0.42	0.81	0.94	1.6	158
220.15	4.013	7	0.54	1.26	1.32	2.1	215
210.15	5.013	7	0.53	3.38	5.32	2.1	392
200.15	6.013	7	0.54	2.39	3.47	2.1	393
200.15	7.013	7	0.37	1.54	3.19	1.45	248
200.17	8.013	7	0.37	1.62	3.42	1.45	248
200.19	9.013	7	0.36	1.77	3.84	1.45	258
200.13	10.013	7	0.36	2.27	5.23	1.45	280
202.13	1.015	7	0.38	2.03	4.40	1.45	290
201.13	2.015	7	0.37	2.02	4.45	1.45	280

Table II Experimental Results (continued)

Configuration	Run	Station	$\dot{m}_1$ (pps)	$\dot{m}_3$ (pps)	$\dot{m}_2/\dot{m}_1$	$\frac{P_{noz}}{P_{atm}}$	U_{cl} (fps)
200.13	3.015	7	0.22	1.20	4.60	1.15	169
200.13	4.015	7	0.29	1.67	4.83	1.28	232
200.13	5.015	7	0.42	2.44	4.83	1.62	352
200.13	6.015	7	0.46	2.67	4.86	1.78	394
200.13	7.015	7	0.50	3.03	5.12	1.94	432

Table III shows the inlet configurations tested, and Table IV lists the inlet configuration identification code.

If it becomes necessary to install turning vanes in a given test cell, the designer may have to provide means of increasing the turbulence level of the secondary air prior to its entry into the augmenter or build a longer augmenter to provide distance needed to achieve complete mixing.

The compressor used for the experiments was capable of producing a total pressure in the nozzle of up to 2.1 atmospheres. The nozzle total pressure was determined by entering the calibration curve shown in Fig. 14 with the total pressure measured in the supply pipe.

Figure 15 shows the velocity profiles measured at various augmenter stations for configuration 210.15 with a nozzle pressure ratio of 2.1 atmospheres. Station 1 was located 3" from the nozzle exit plane; station 7 was located 25" from the nozzle and 1" from the augmenter exit plane. The profiles were calculated using data obtained in run 1.009. The mass flow rates calculated at the various stations indicate an accuracy of about 10 percent. Prior to run 1.009, pressure and temperature measurements used to calculate the mass flows were obtained from station 4. After this run most of the remaining data were collected from station 7. The velocity profile is seen to have very much lower gradients at station 7 than at station 4. The centerline velocity at station 7 was below Mach 0.3 so that the assumption of incompressible flow is valid there. Additionally, the absence of large pressure gradients

Table III Dual Mode Inlet Configurations

Run	Inlet Configuration
1.929	1321.413543
2.929	1213.113543
3.929	1131.413543
4.929	1131.213543
1.004	1322.313542
2.004	1122.113542
3.004	5132.413542
1.006	5132.713342
2.006	1121.313342
3.006	1121.213342
4.006	1121.113342
5.006	1313.313342
1.011	1131.213442
2.011	5134.213442
3.011	5134.513442
4.011	5124.513442
5.011	5124.113442

Table IV Inlet Configuration Identification Code

Configuration Number: ABCD.EFGHIJ

A. INLET	B. INLET COVER	C. ACOUSTICS	D. ACOUSTIC POSIT.	E. TURNING VANES
1 vertical	1 none	1 none	1 before turn and transverse	1 none
2 horizontal	2 faired	2 flat baffle	2 after turn, vert.	2 one (#3)
3 none	3 bi-directional	3 staggered baffle	3 none	3 four
4 vert. w/o stack	4 flat plate	4 tubular	4 before turn, and axial	4 seven
5 S-turn	5 bi-dir, sideways	5 stag. baffle, crossways	5 *top of stack*	5 one (#5)
				6 one (#1)
				7 one (#3) in turn 2

F. FLOW STRAIGHTENER	G. ENGINE BELLMOUTH	H. AUGMENTATION	I. POWER MODE	J. ENGINE POWER LEVEL
1 none	1 neither	1 none	1 t/s-blower	1 maximum
2 rect. Xsection	2 engine w/o bell	2 zero	2 eng-blower	2 medium
3 screen before ac.	3 engine + bell	3 low	3 end+aug-blow.	3 lowest
4 screen after ac.		4 medium	4 dual mode	
5 both screens		5 high		
6 distort screen				
7 honeycomb				

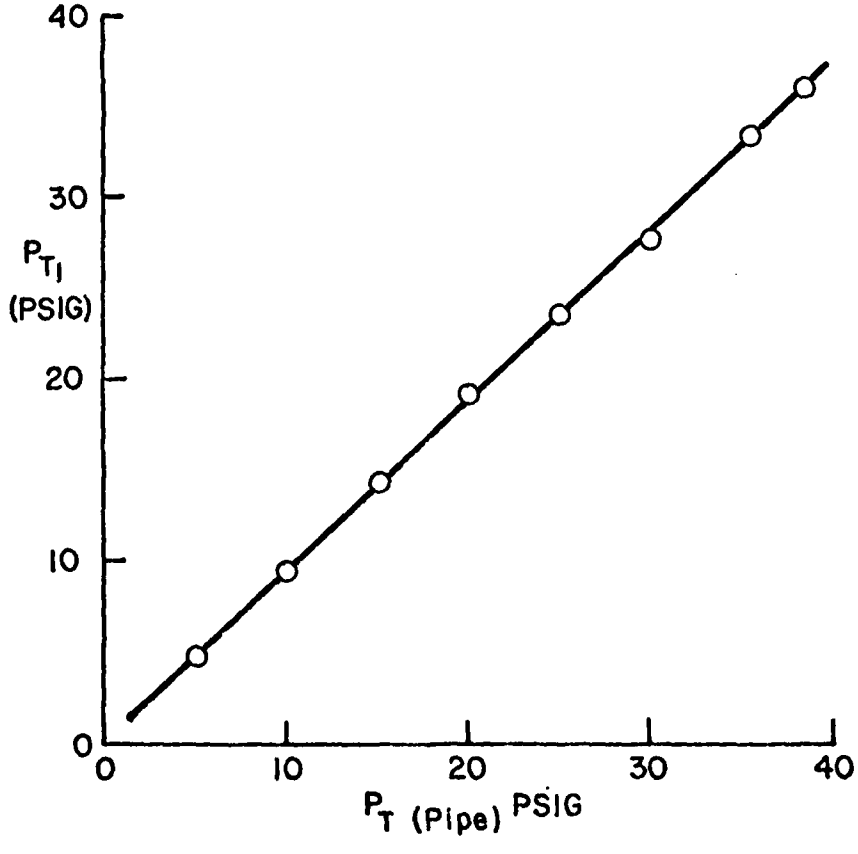

FIGURE 14 VARIATION OF NOZZLE TOTAL PRESSURE WITH TOTAL PRESSURE AT ORIFICE INLET

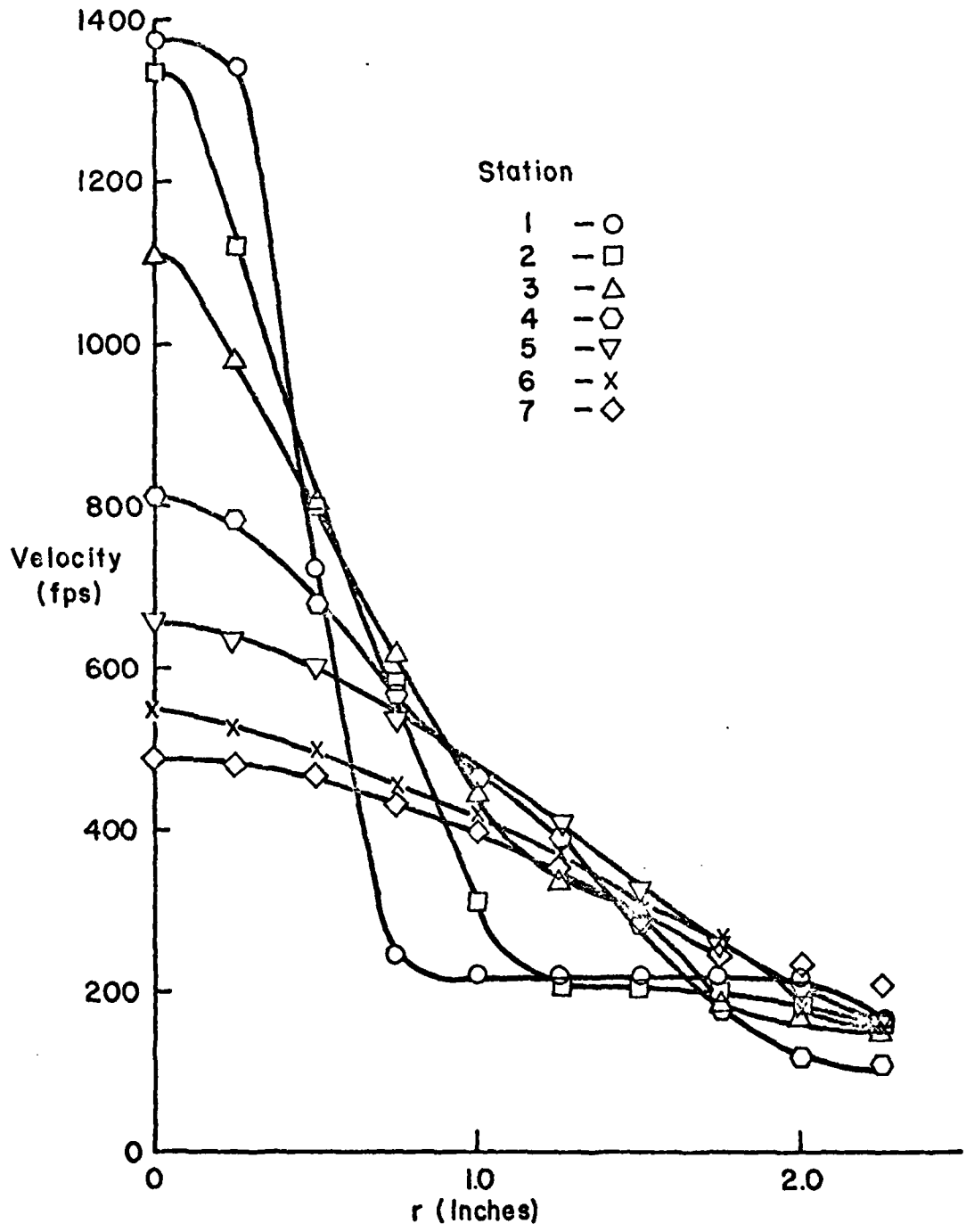

FIGURE 15 VELOCITY PROFILES FOR CONFIGURATION 210.15, P_{T_1} = 2.1 atm

and the proximity of station 7 to the augmenter exit indicated the validity of assuming constant static pressure at a cross section when calculating mass flow.

Figure 16 shows the rate of decay of centerline velocities as flow progresses in the augmenter. The velocities shown also were obtained from data of run 1.009 and are normalized to the centerline velocity at station 1. Figure 17 shows the nondimensional velocity profiles at stations 1 and 7 for run 1.009.

Some configurations yielded unusual velocity profiles. Figure 18 shows a profile where the maximum velocity occurs at a point other than on the centerline. Monroe [Ref. 6] encountered the same phenomenon and attributed it to the presence of oblique shocks at the nozzle. A second factor is the probable presence of a swirl component in the primary flow as it leaves the nozzle. The swirl component, if present, was probably caused by the three 90° turns in the inlet pipe between the orifice and the nozzle. It is recommended that if further work is carried out with the experimental apparatus, tubular flow straighteners should be installed in the nozzle section.

Experimental results were in close agreement with theoretical predictions. Figure 19 shows secondary mass flow as a function of primary mass flow for configuration 200.13. The experimental results closely match the theoretical predictions when no entry loss (ENTLOS) was included. The predictions which used an entry loss factor of 0.85 were less than the experimental results, which indicates that the loss

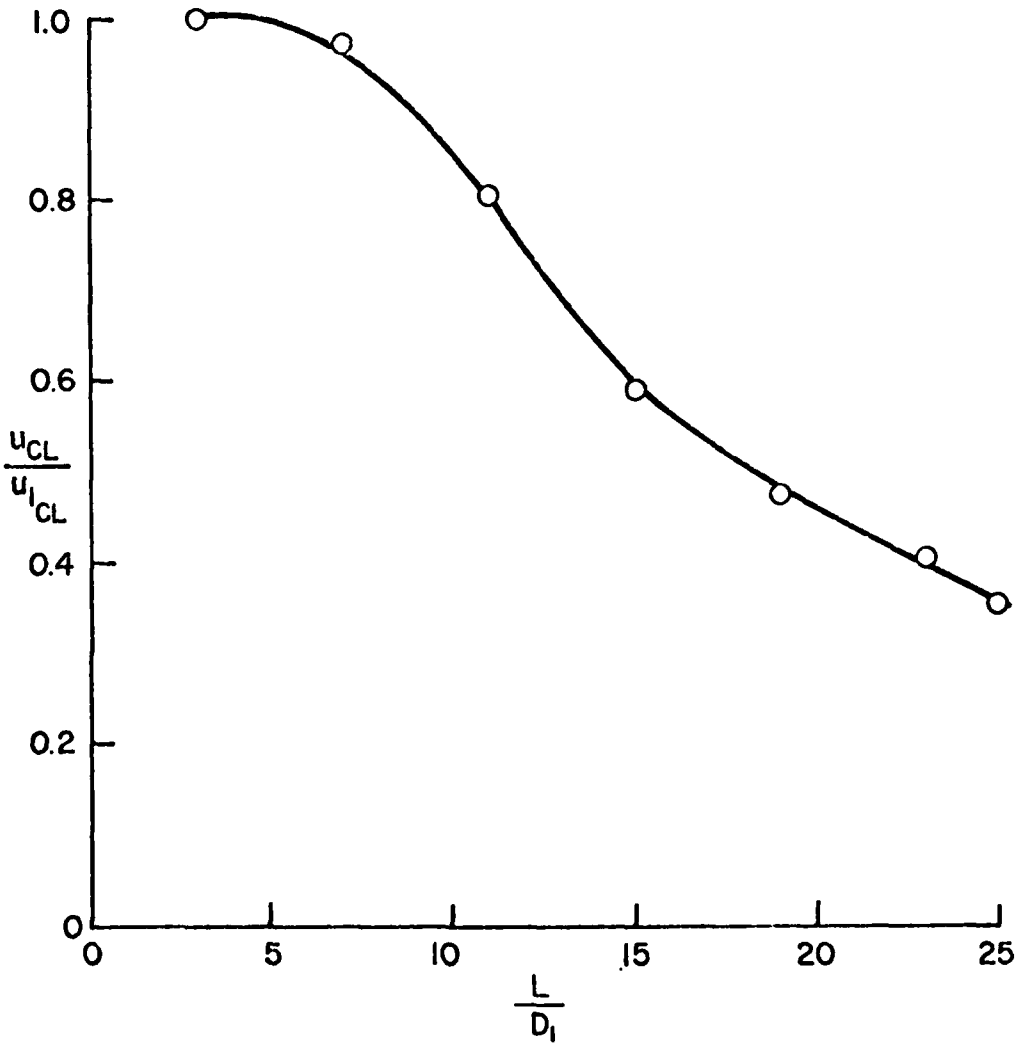

FIGURE 16 CENTERLINE VELOCITY DECAY,
P_{T_1} = 2.1 atm

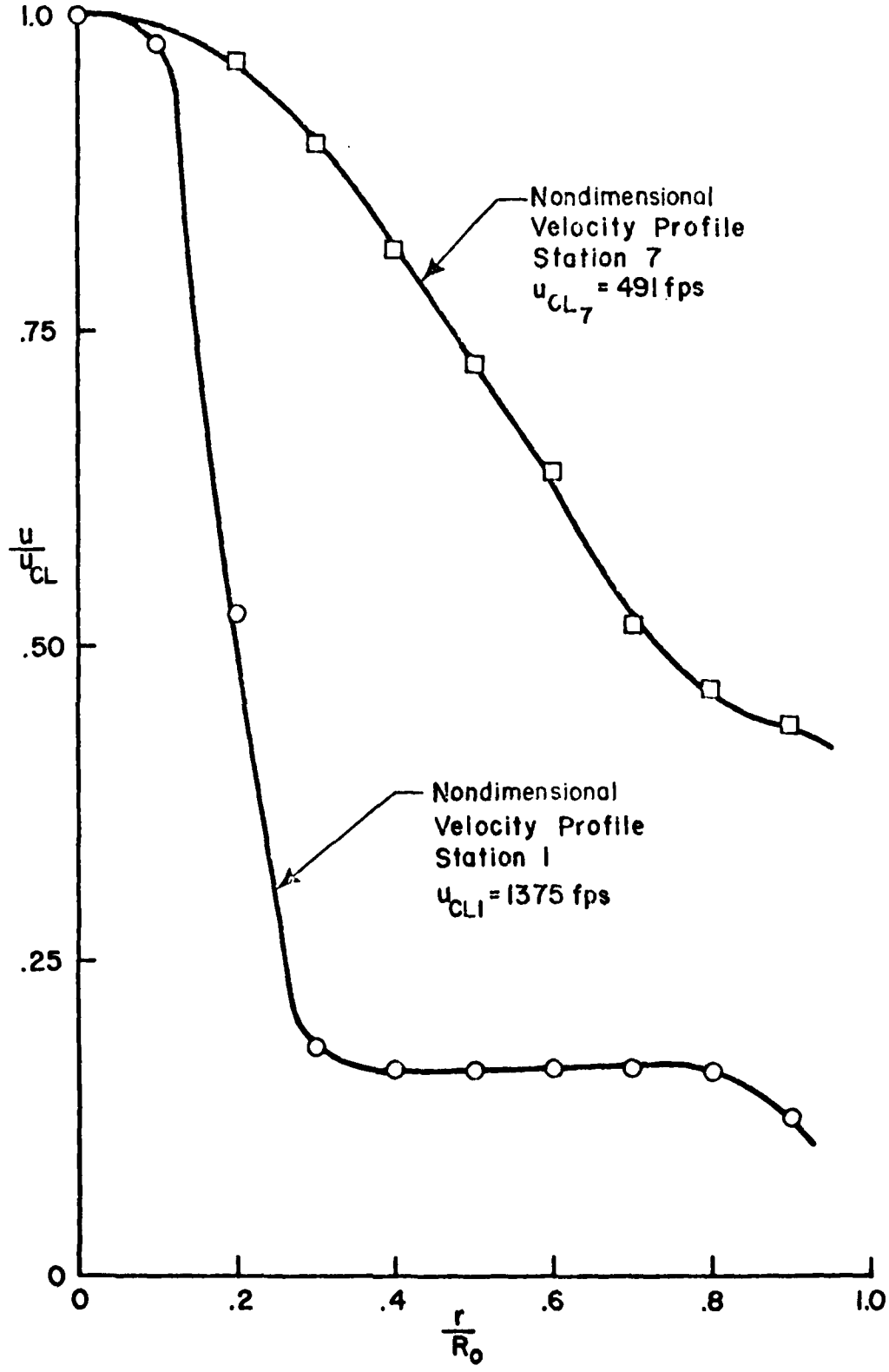

FIGURE 17 NONDIMENSIONAL VELOCITY PROFILES, P_{T_1} = 2.1 atm

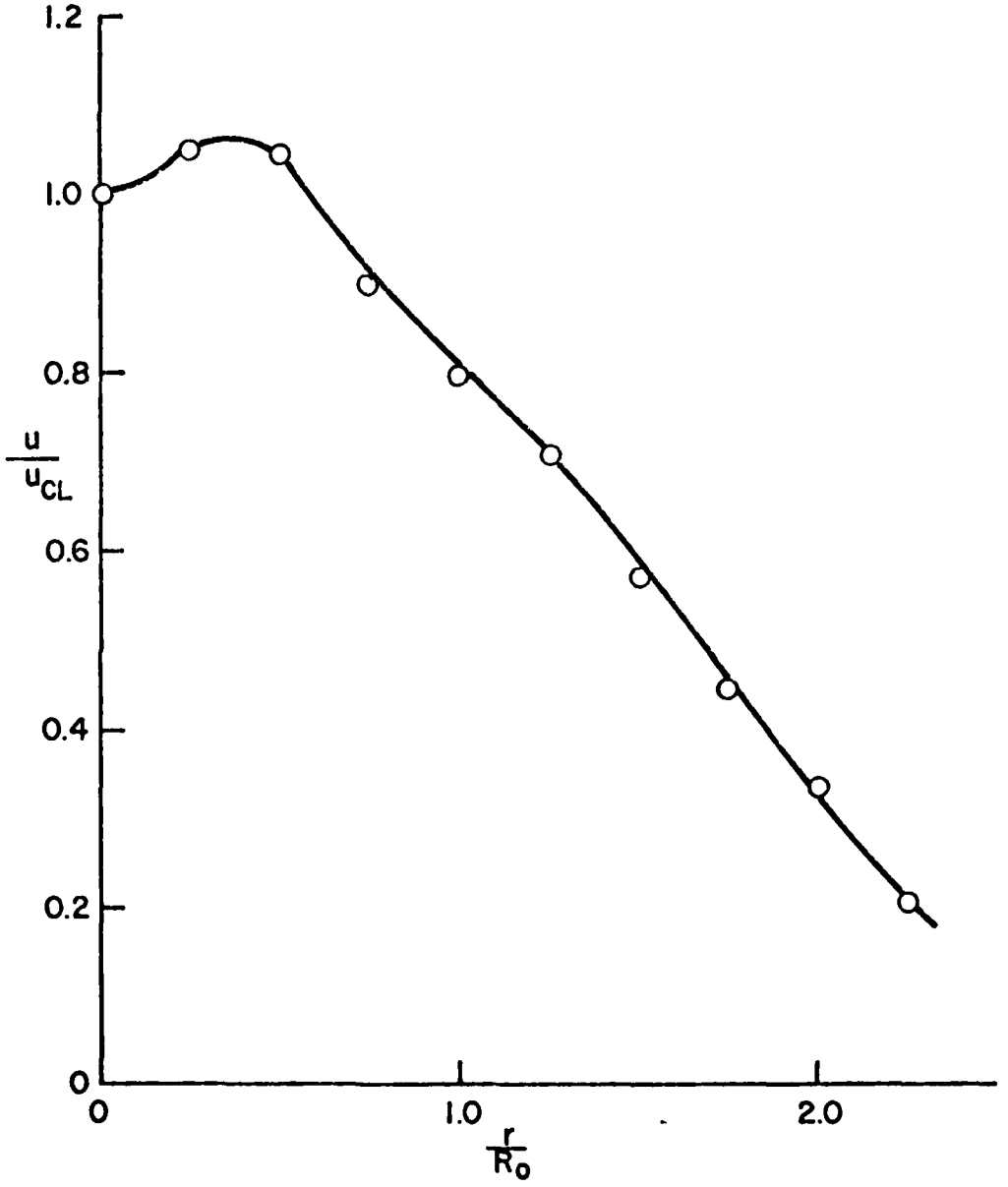

FIGURE 18 NONDIMENSIONAL VELOCITY PROFILE, STATION 4, CONFIGURATION 200.19, RUN 6.930

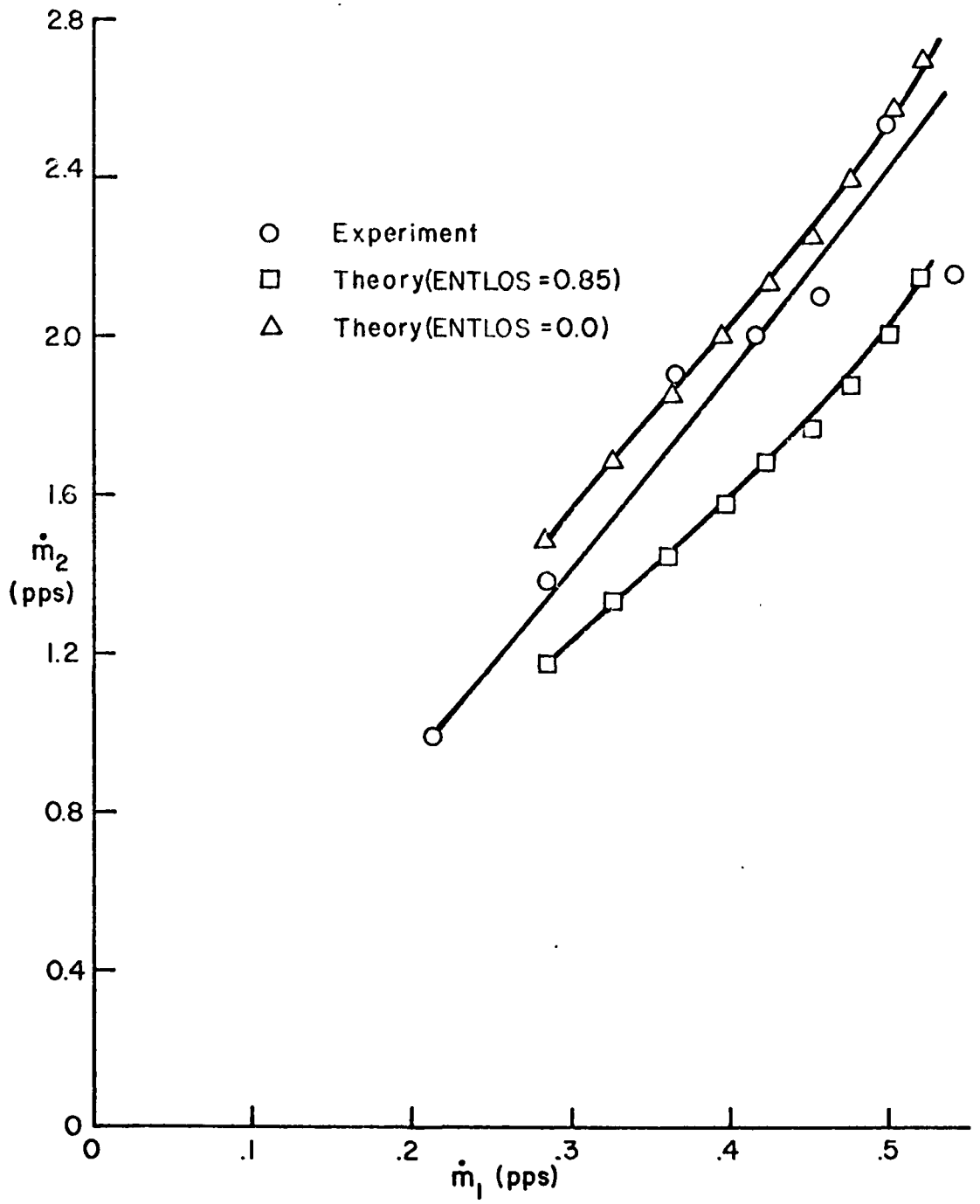

FIGURE 19 SECONDARY MASS FLOW VS PRIMARY MASS FLOW FOR CONFIGURATION 200.13

factor was too severe. Table V compares experimental and theoretical results pertaining to inlet configuration effects. It is seen that closest agreement is obtained when the loss factor is effectively equal to zero.

Experimental results indicated that the conical inlet lowered the augmentation ratio when installed rather than improved it. The reason for this phenomenon is that when the conical inlet was installed, it had the effect of moving the augmenter inlet away from the back wall of the test cell. Some turbulence or recirculation exists in the area between the inlet and the wall. It is thought that the change produced by moving the inlet caused some interference to occur in the streamlines into the augmenter decreasing the secondary flow rate. The particular model design tended to block the flow into the augmenter from the area behind the inlet. Future work with the main computer program should include a factor which accounts for the position of the augmenter inlet in relation to the back wall of the test cell.

Figure 20 compares experimental and theoretical results of the dependence of augmentation ratio of nozzle pressure P_{T_1}. Figure 21 shows the variation of P_1, nozzle exit static pressure, with P_{T_1}. In both figures good agreement between experimental and theoretical results is evident. Figure 22 compares the results showing variation of augmentation ratio with P_1. The experimental results agreed with the trend predicted for supersonic flow (P_1 less than 0.97 in Fig. 22) but did not follow the predicted trend for subsonic flow. The probable cause for the disagreement is that the computer program assumed that complete mixing

Table V Inlet Configuration Effects

Experimental Results			Theoretical Results		
Configuration	P_{T_1}	$\dot{m}_2/\dot{m}_1$	Entry loss	P_{T_1}	$\dot{m}_2/\dot{m}_1$
200.15	2.1	5.2	0.85	2.1	4.0
210.15	2.1	4.3	0.03	2.1	5.0
220.15	2.1	1.75	0.85 (D_2 = 3.0")	2.1	1.8
200.13	1.6	4.8	0.0	1.6	5.1
			0.5	1.6	4.3

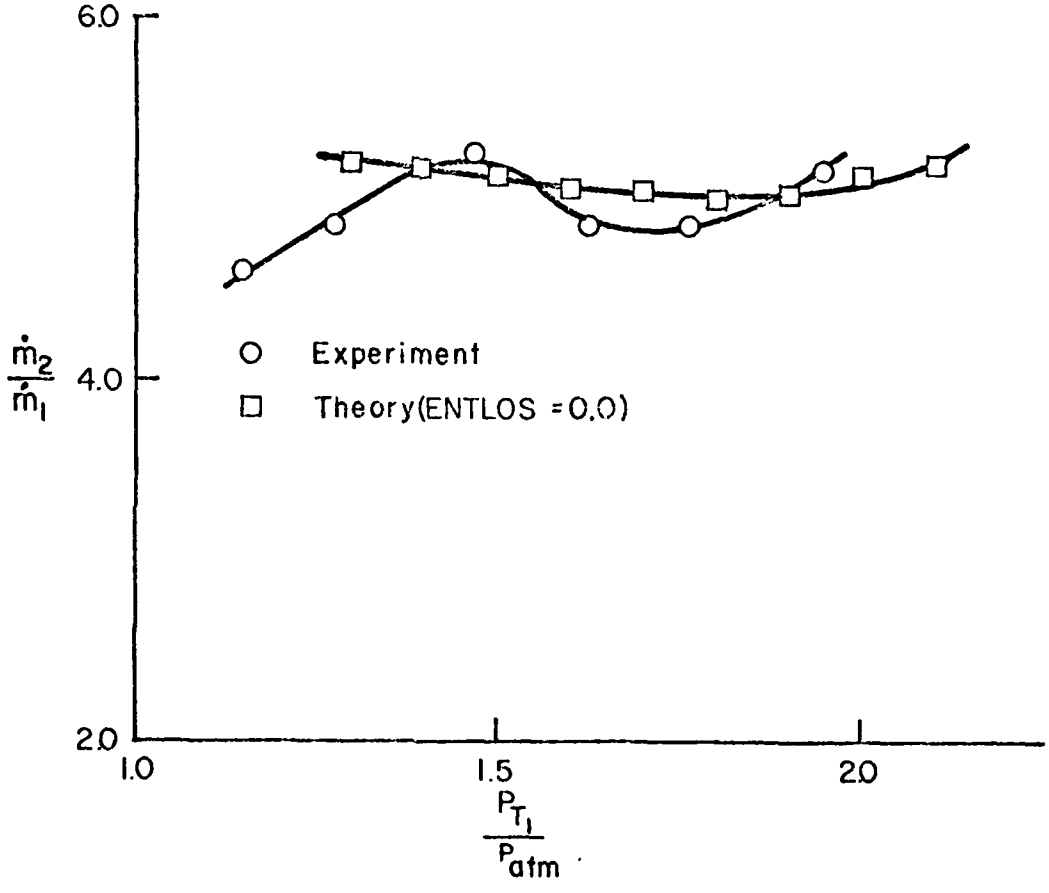

FIGURE 20 VARIATION OF AUGMENTATION RATIO WITH P_{T_1}, CONFIGURATION 200.13

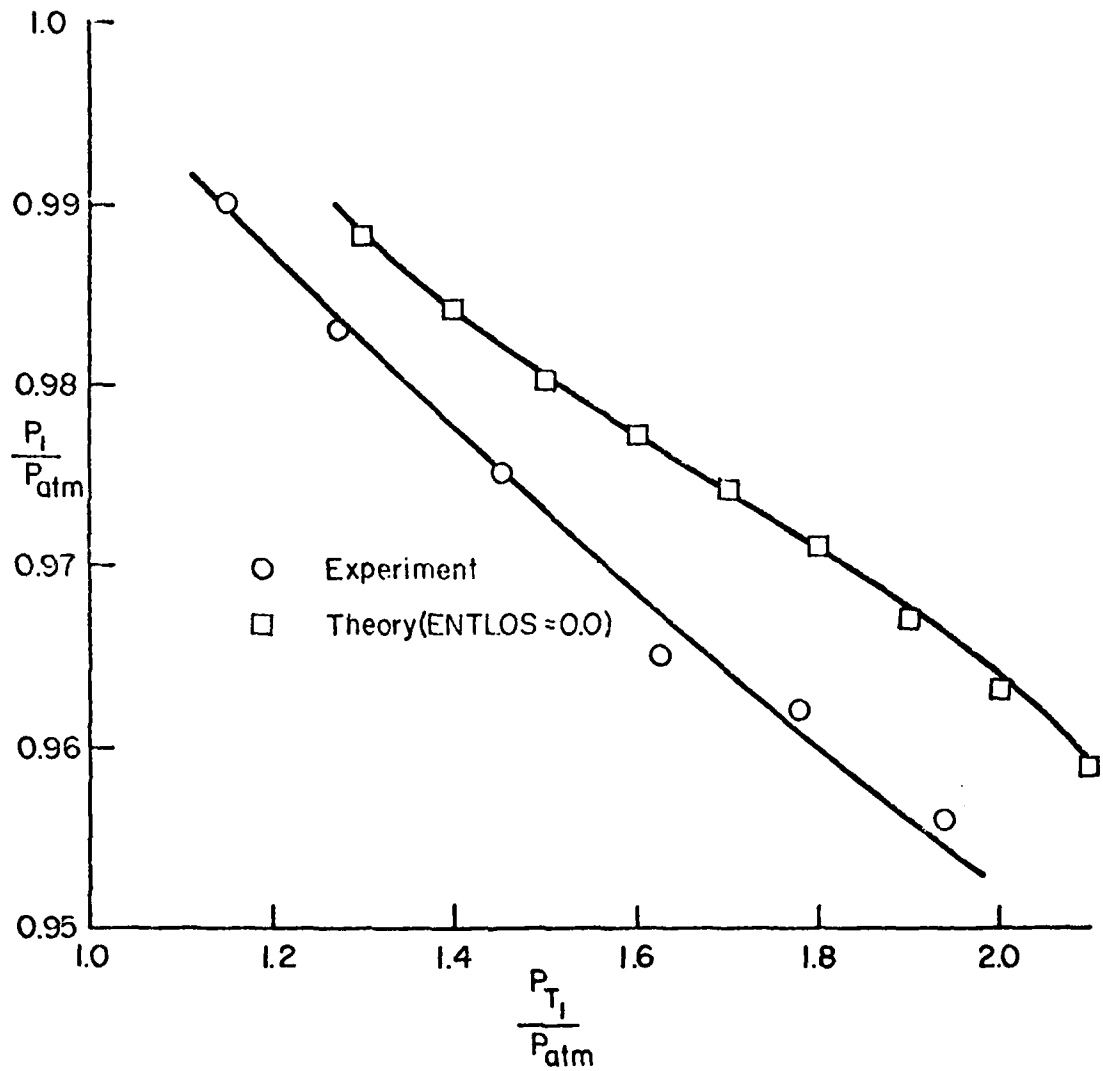

FIGURE 21 P_1 VS P_{T_1} FOR CONFIGURATION 200.13

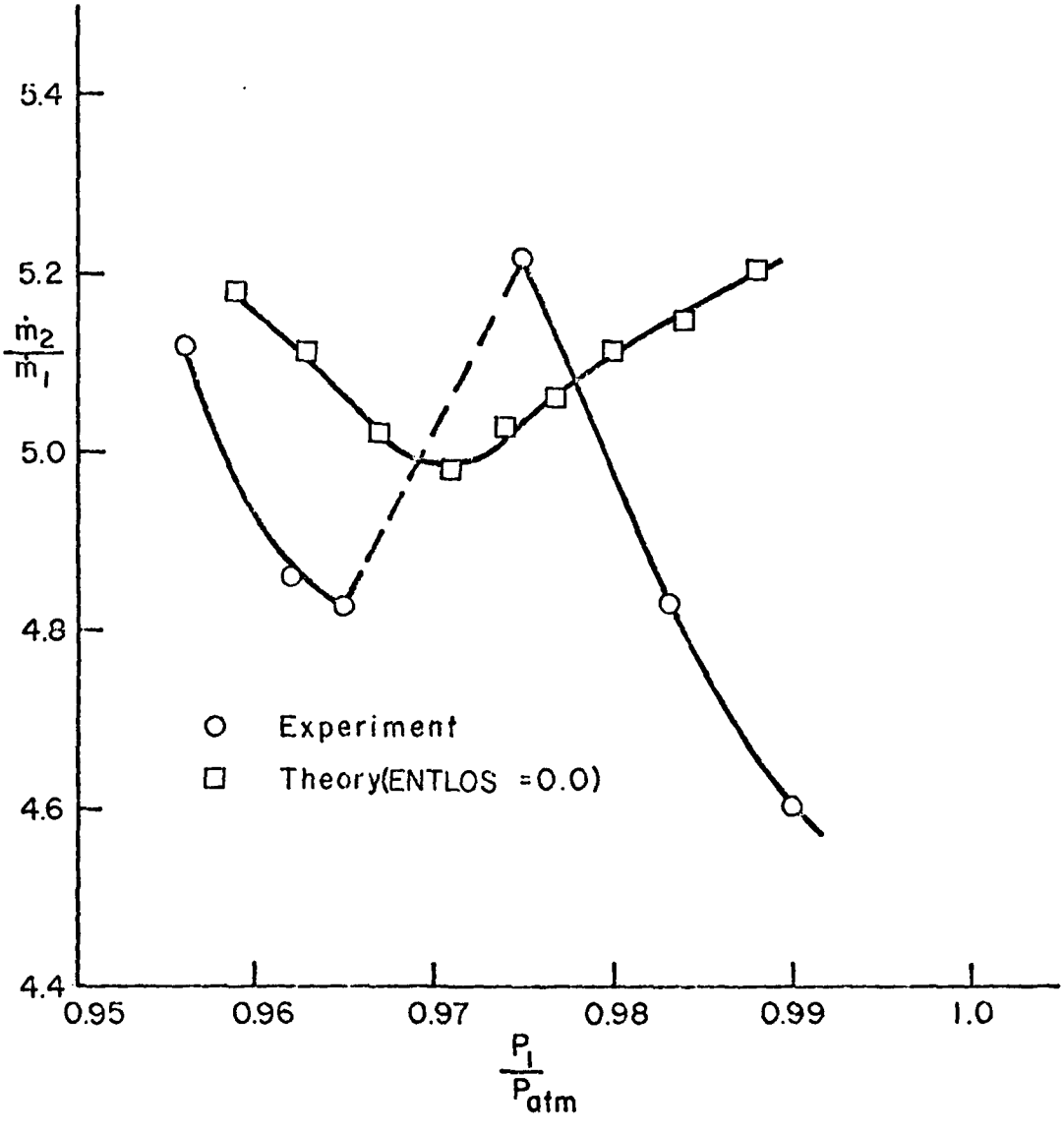

FIGURE 22 VARIATION OF AUGMENTATION RATIO WITH NOZZLE EXIT PRESSURE, CONFIGURATION 200.13

occurs at station 3 of the jet pump model, while in the experimental apparatus the amount of mixing that had been accomplished in the augmenter varied with the nozzle pressure ratio. An improvement might be made in the program by incorporating the jet spread parameter into the analysis. The present analysis only used the jet spread parameter to indicate the effect of nozzle position. The parameter is effectively a measure of the turbulence level and, as previously discussed, increased turbulence causes higher augmentation ratios.

Figure 23 shows theoretical predictions of the dependence of augmentation ratio on area ratio A_3/A_1. Present experiments have covered only one area ratio, so that further work is needed to validate the computed results.

Figure 24 illustrates the variation of augmentation ratio with nozzle displacement. The scatter of the data precludes any decision as to the validity of the predicted results. More data need to be collected for various nozzle displacements in subsonic flow situations. A form of the main computer program containing an improved turbulence factor should improve agreement between theory and experiment. A major addition needs to be made to the program in order to predict augmentation ratio as a function of nozzle displacement in the supersonic flow regime. At the present time the program is limited to zero-displacement in cases involving supersonic flow. It is thought that by applying the method of characteristics to the primary nozzle flow it will be possible to predict exhaust system performance for all levels of supersonic flow as nozzle displacement is varied.

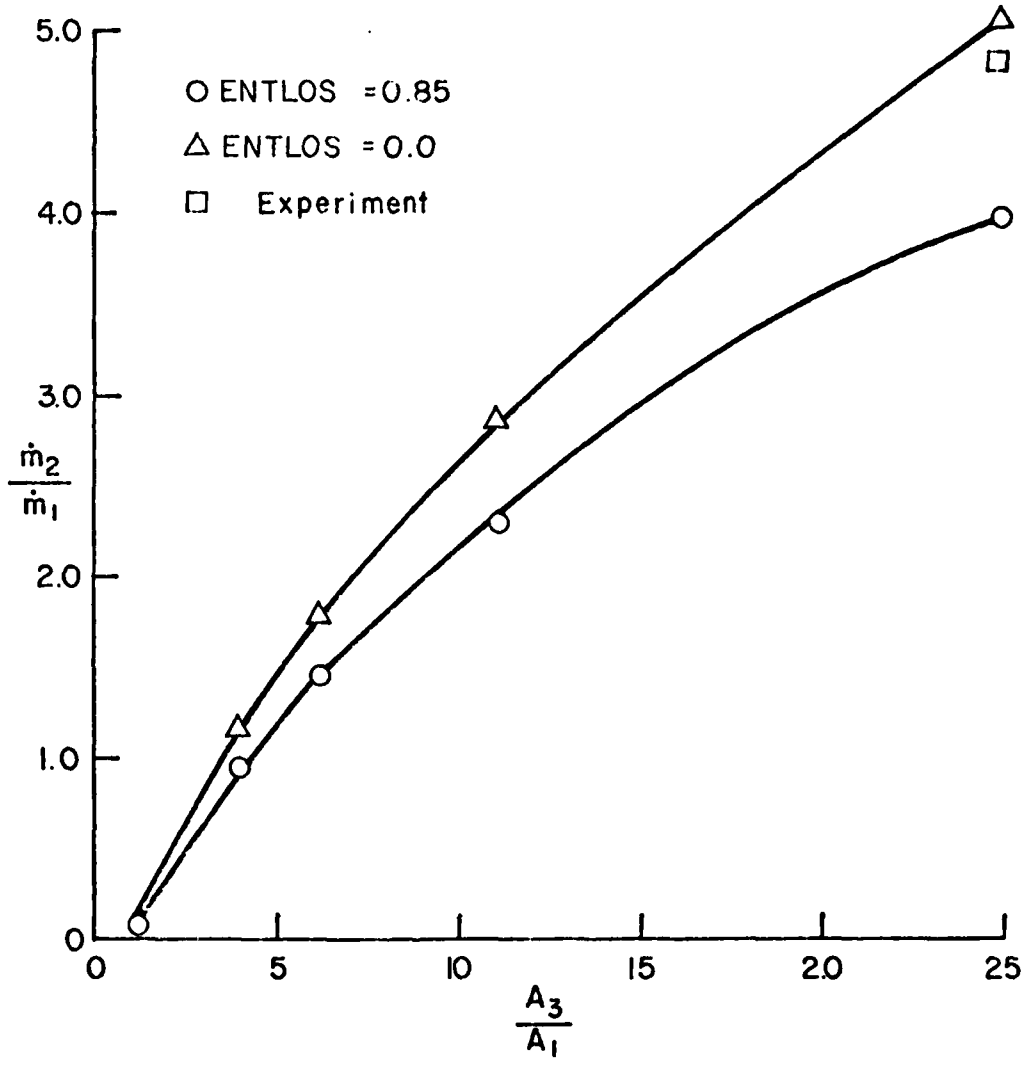

FIGURE 23 AUGMENTATION RATIO VS A_3/A_1, P_{T_1} = 1.6 atm

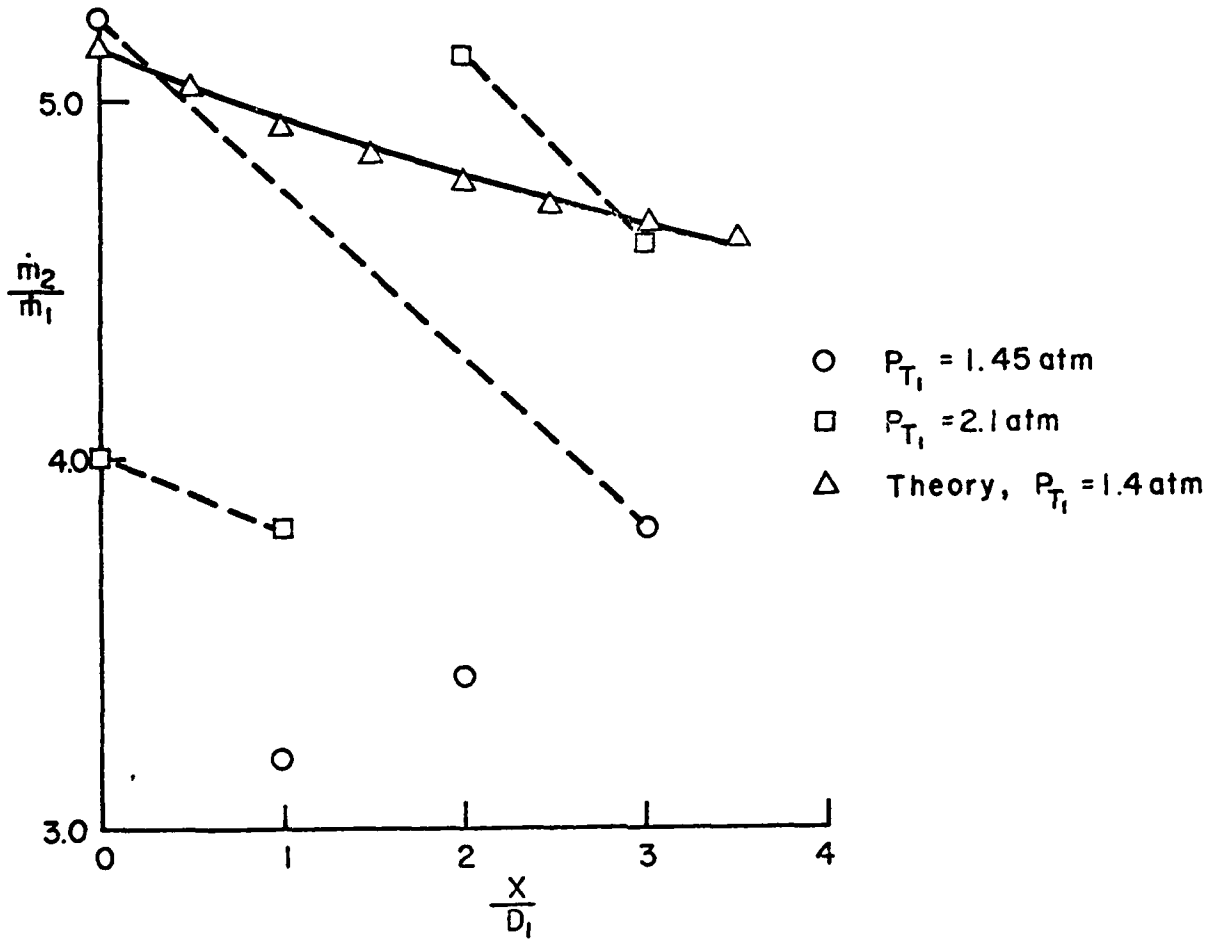

FIGURE 24 AUGMENTATION RATIO VS NOZZLE DISPLACEMENT

The back pressure against which the exhaust system operates greatly affects the augmentation ratio as seen in Fig. 25. In its present form the computer program is able to predict the maximum back pressure allowable without encountering exhaust gas recirculation. This is particularly useful in situations where P_{T_1} is low, such as an engine at idle power. Figure 26 shows the pressure rise in the augmenter system with various configurations.

Experimental results showed that the presence of a colander did little to enhance the amount of mixing that occurred in the augmenter. Figures 27 and 28 show nondimensional velocity profiles at station 7 for various configurations and nozzle pressure ratios.

The maximum length augmenter required in a given system may be calculated with the jet spread parameter. The criteria for minimum length should be that all the secondary air is entrained into the main mixing region, or in other words that the mixing zone has touched the augmenter wall. Figure 29 shows the jet spread parameter as a function of area ratio A_3/A_1. The outer boundary of the mixing zone was defined to be $\eta = 1.84$, where η is the nondimensional coordinate in the y direction

$$\eta = \frac{\sigma y}{x} \qquad \text{(V-1)}$$

To find the minimum augmenter length define y_{max}

$$y_{max} = \frac{D_3 - D_1}{2} \qquad \text{(V-2)}$$

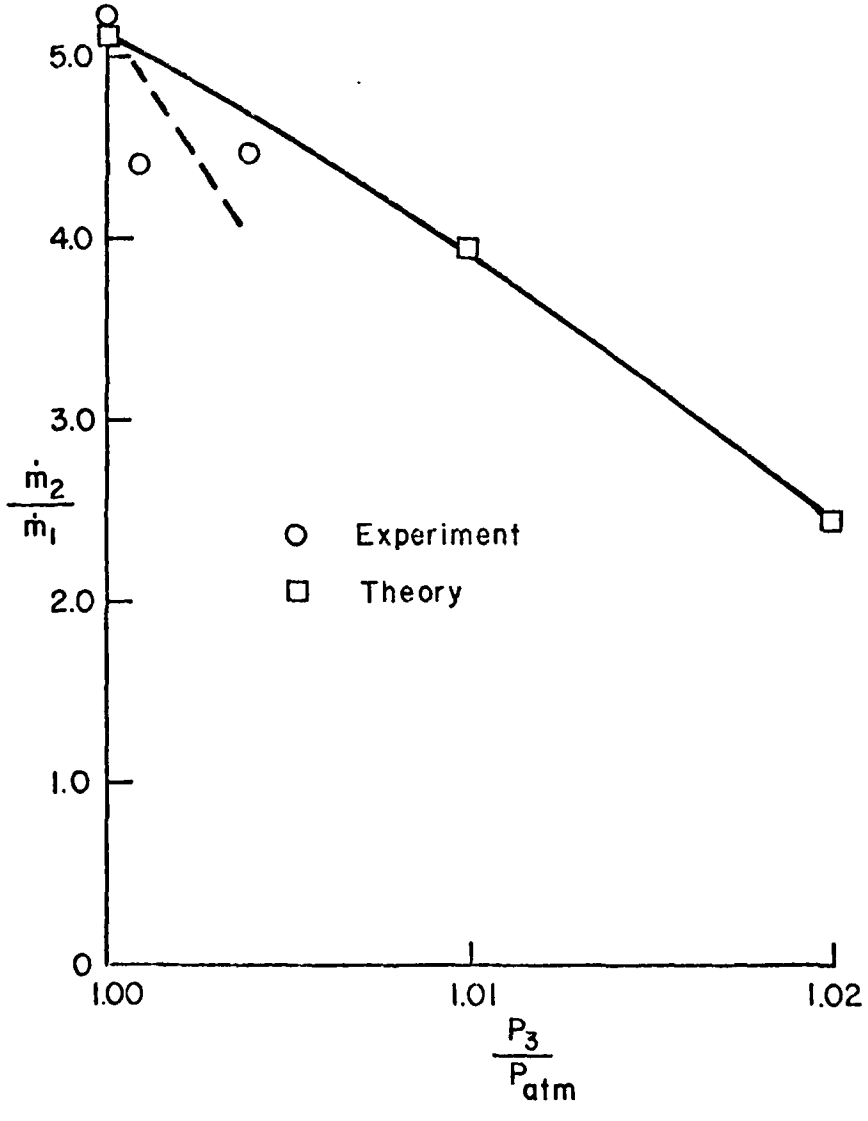

FIGURE 25 AUGMENTATION RATIO VS AUGMENTER BACK PRESSURE, P_{T_1} = 1.45 atm

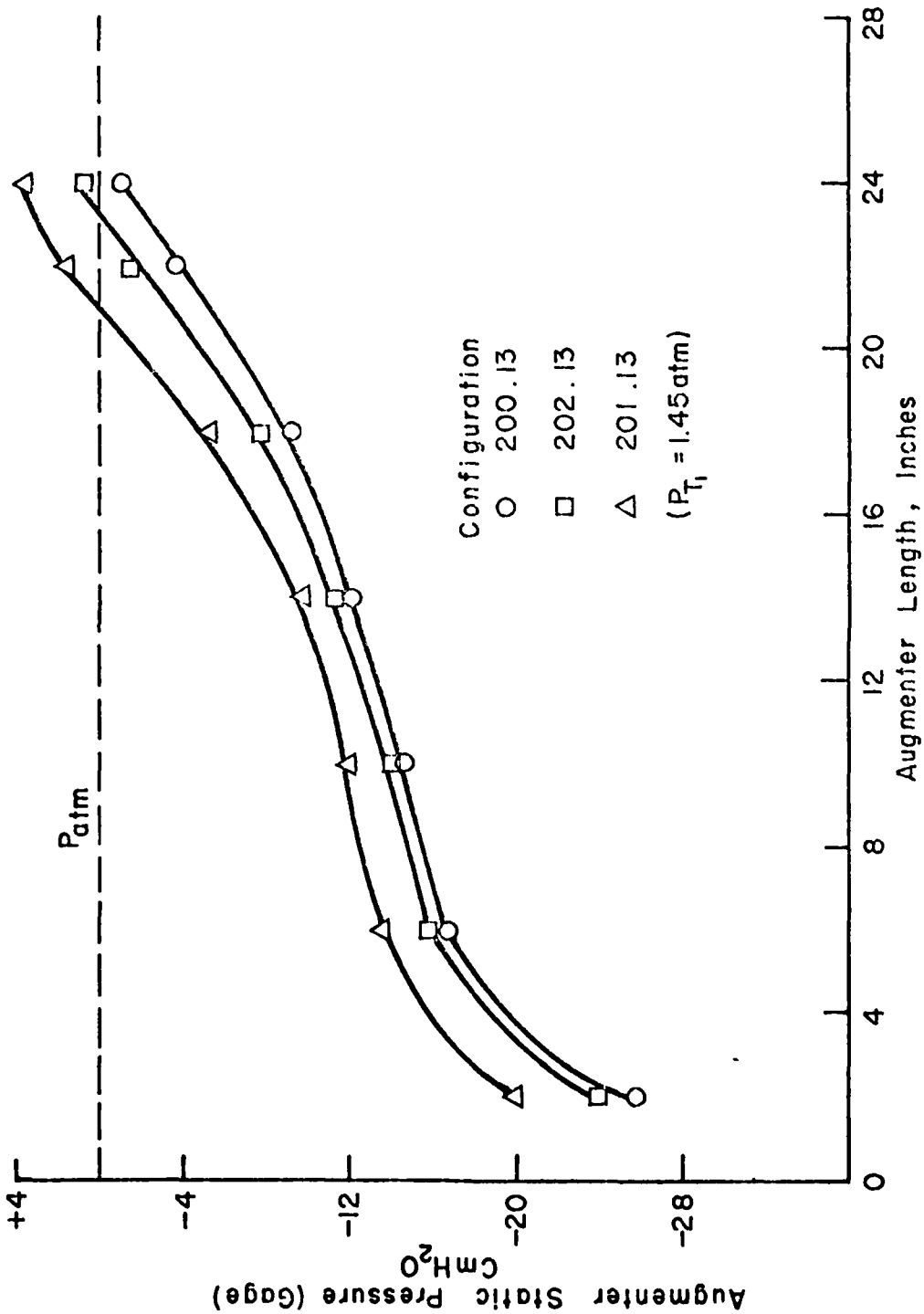

FIGURE 26 AUGMENTER PRESSURE RISE WITH COLANDERS INSTALLED

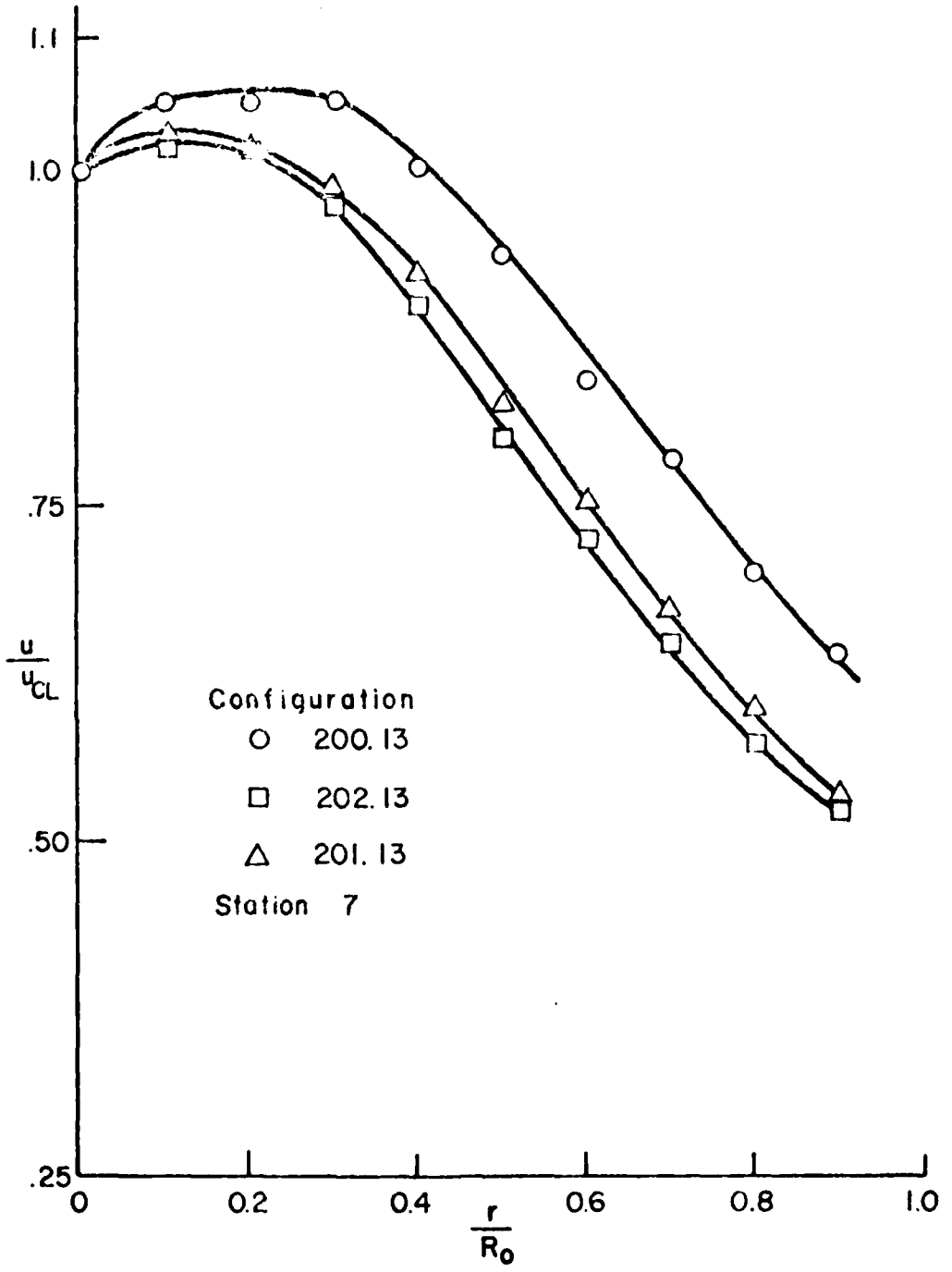

FIGURE 27 EFFECT OF COLANDERS ON NONDIMENSIONAL VELOCITY PROFILE, P_{T_1} = 1.45 atm

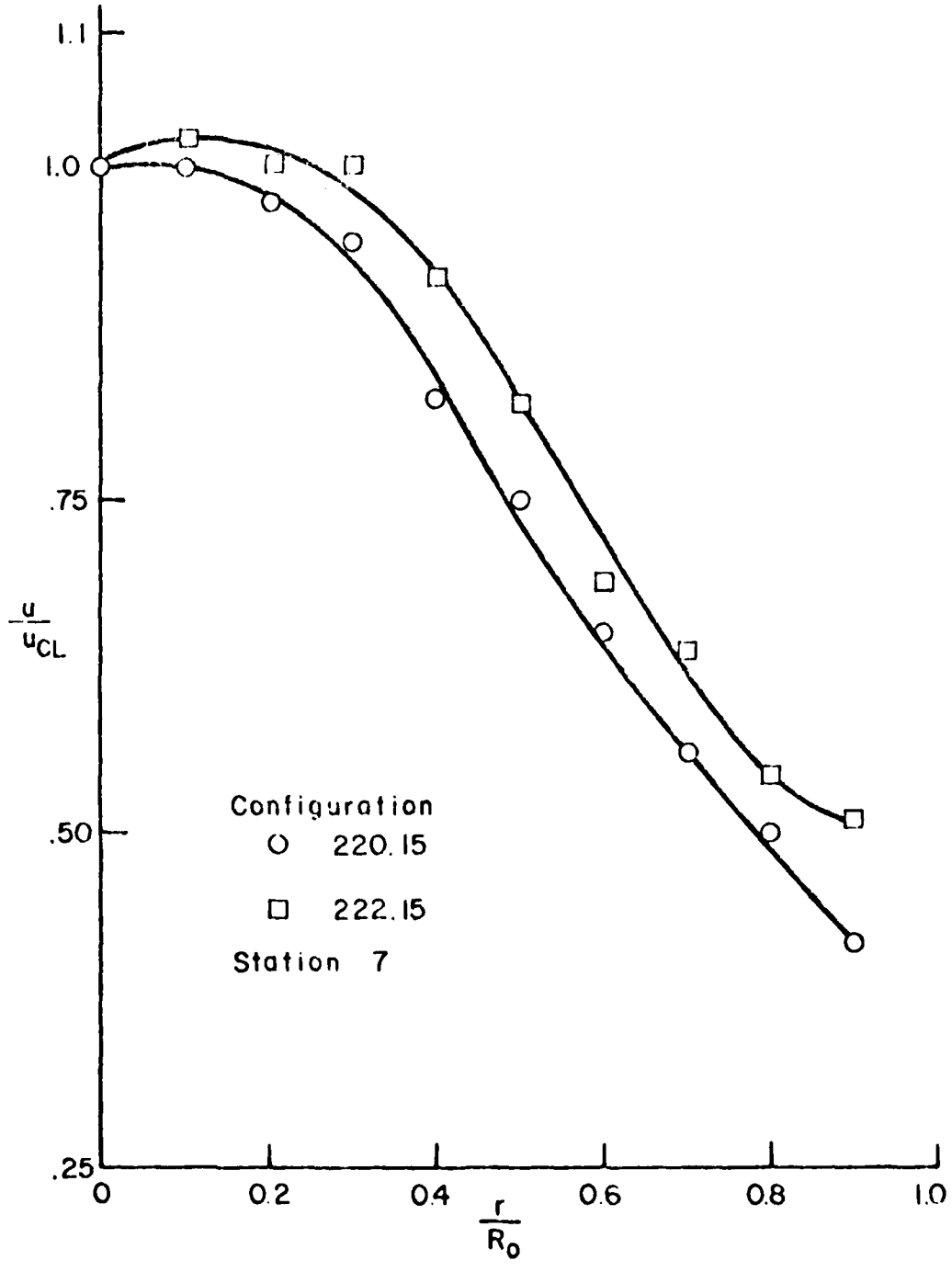

FIGURE 28 EFFECT OF COLANDER ON NONDIMENSIONAL VELOCITY PROFILE, $P_{T_1} = 2.1$ atm

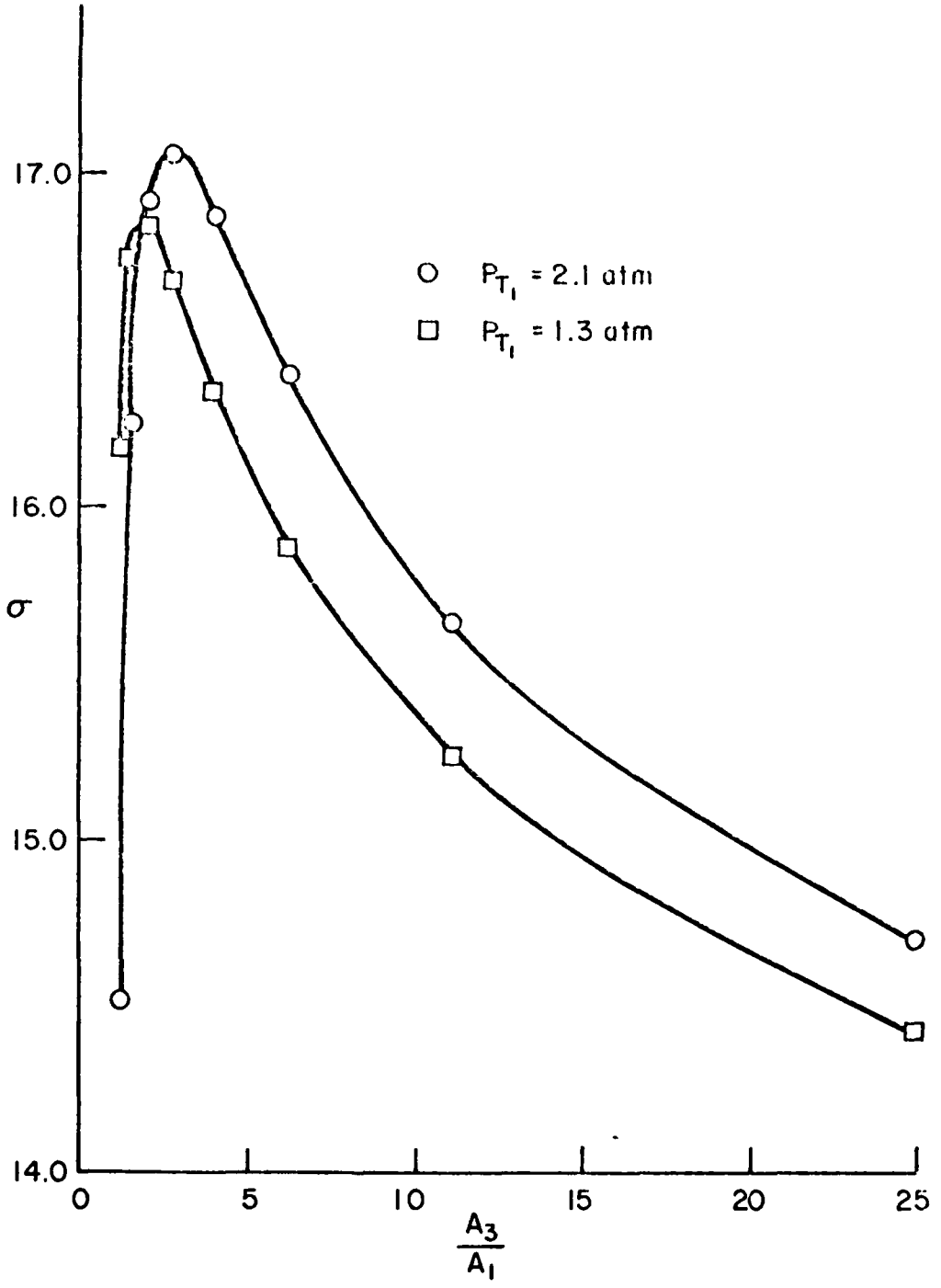

FIGURE 29 JET SPREAD PARAMETER AS A FUNCTION OF A_3/A_1

D_3 is the augmenter diameter and D_1 is the diameter of the nozzle. Pick σ from Fig. 29 using $A_3/A_1 = D_3^2/D_1^2$. Define x_{min} as the required augmenter length

$$x_{min} = \frac{\sigma (D_3 - D_1)}{3.68} \qquad \text{(V-3)}$$

For example, consider an exhaust system with an augmenter 10' in diameter in conjunction with a turbojet engine that is 3' in diameter, operating with a nozzle pressure ratio large enough for supersonic flow. Figure 29 indicates a value of σ of about 15.5. Equation (V-3) then indicates a maximum augmenter length of 30' for effective mixing.

B. CONCLUSIONS AND RECOMMENDATIONS

The performance analysis of the test cell exhaust system based on the conservation equations for mass, momentum and energy successfully predicted general trends when flow characteristics of the augmenter and engine were varied. The theoretical predictions slightly underestimate actual system performance. The probable cause is that neither the actual turbulence level in the augmenter nor the amount of mixing that occurs in the system was accounted for. Predictions concerning the effect of system back pressure were accurate.

The use of flow conditioners necessary for minimizing engine inlet distortion decreases the augmentation ratio but increases the augmenter length required for complete mixing.

The assumption of incompressible flow for calculating flow rates in the augmenter was validated at station 7, where centerline velocities were consistently below Mach 0.3.

Theoretical loss factors for the augmenter inlet configuration did not accurately predict performance. The analysis did not account for the position of the augmenter inlet with respect to the back wall of the test cell.

A method is available to compute the minimum augmenter length required for adequate mixing to occur.

The following recommendations for improving the analysis and experimental apparatus are made:

1. Develop an analysis for incorporation into the main computer program that will account for the turbulence level in the flow field and the amount of mixing that takes place in a given augmenter length.
2. Develop an analysis that will model the relative position of augmenter and the test cell wall.
3. Develop an analysis based on the method of characteristics that will allow prediction of test cell performance as the engine position relative to the augmenter is varied for supersonic flow.
4. Develop an analysis to predict the effect of injecting cooling water.

5. Reduce the swirl component in the primary flow by installing flow straighteners in the nozzle section.

6. Experimentally investigate various area ratio relationships.

7. Build models of exhaust system acoustic and pollution abatement systems for testing with the present apparatus.

8. Investigate system performance with higher pressure ratios by utilizing a more highly rated compressor.

APPENDIX A

TEST CELL EXHAUST SYSTEM

The following discussion was extracted from Ref. 13. Other discussions which are pertinent to test cell design were covered by Tower [Ref. 8].

1. PRESENT PHILOSOPHY

The basic philosophy of present exhaust treatments is to remove the majority of the kinetic energy from the jet exhaust, to cool the exhaust by mixing with secondary air or water, and to lower the noise level of the exhaust. Removing the kinetic energy is also a method of acoustic treatment. The most common method of accomplishing the first two objectives is to utilize the kinetic energy of the exhaust to pump secondary air through the cell and into the exhauster or augmenter tube where mixing of the two streams occurs. Augmentation ratio, defined as the ratio of secondary air mass flow to engine air mass flow, is an important consideration in determining overall cell design. With an excessive augmentation ratio, the depression limits of the cell may be exceeded; with too small a ratio, desired cooling may not be accomplished, and temperature limits of test cell exhaust components such as installed acoustic treatment may be exceeded. Present design goals for augmentation ratios are 2:1 for turbojet engines and 0.25:1 to 0.5:1 for high bypass turbofan engines [Refs. 10, 15, and 31]. Some facilities, however, still have augmentation ratios as large or greater than 1:1 for

large turbofan engines [Ref. 32]. Turbulent mixing phenomena are not well understood, and much work remains to be done in analyzing the ejector system.

Water cooling is usually required for an engine operating with afterburner; the augmentation ratio required to cool the exhaust without water is greater than 6:1. The minimum amount of water usage is desirable in order that water supplies be preserved. Many cells utilize spray rings mounted inside the augmenter. These operate very inefficiently because of the difficulty of penetrating the hot, high speed core of the exhaust [Ref. 33]. Several attempts have been made to inject the water from within the core itself. The water sparger [Ref. 34] is an example. Care must be taken in the design of such items since they can produce undesirable acoustic phenomena if their natural frequencies correspond to the driving frequencies of the exhaust. Further development of water injection is a necessity for economical future operation.

One method available for removing the kinetic energy of the jet exhaust is the "brute force" method. At NARF North Island in cells 13 and 14 the exhaust impinges on a solid concrete block which is lined with steel plate. This is effective in destroying the continuity of the stream but has failed to prevent serious damage to the walls of the plenum chamber. In the newer cells at North Island the exhaust impinges on a perforated steel plate. Figures 30 and 31 illustrate the cells.

A newer method of treating the flow and one coming into more general use [Refs. 32 and 35 - 37] involves a colander in the form of

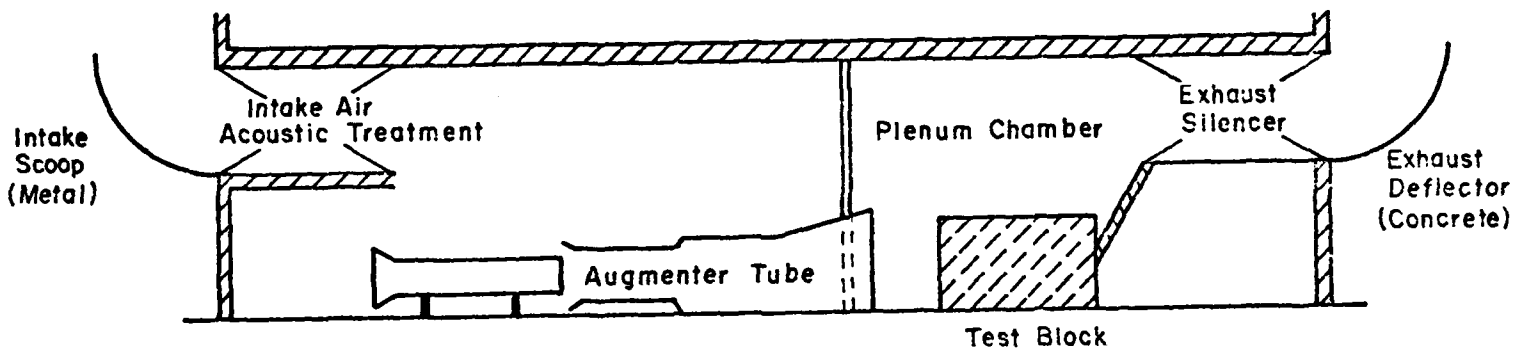

FIGURE 30 TEST CELLS 13 AND 14, NAS NORTH ISLAND

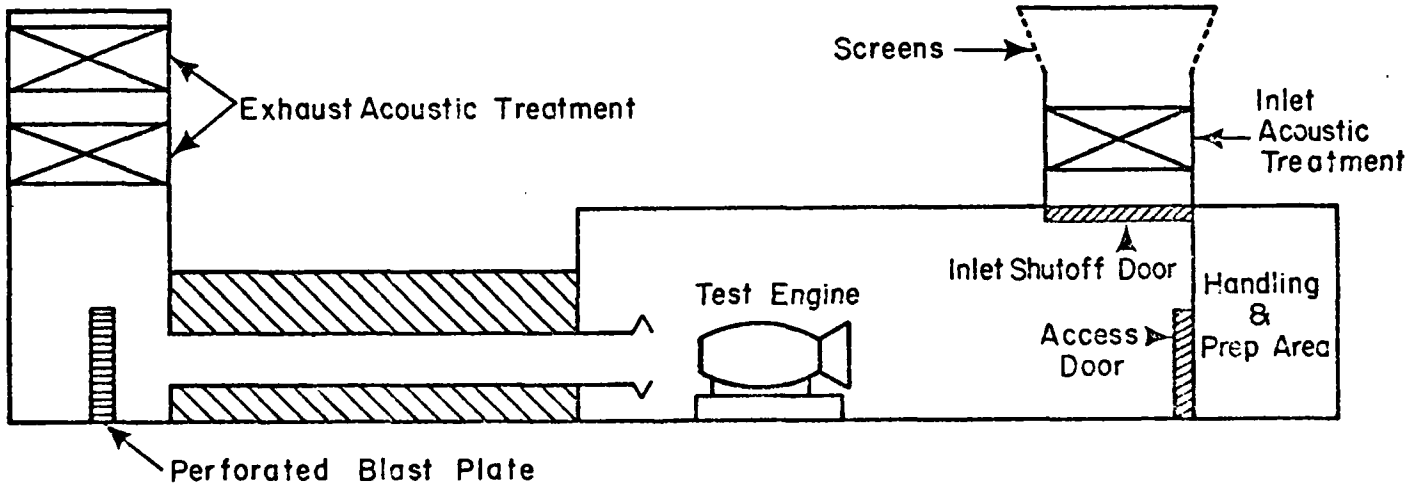

FIGURE 31 TEST CELLS 19 AND 20, NAS NORTH ISLAND

a cylinder or a cone. The colander is the last section of the ejector tube and is perforated with holes, usually on the order of 1-1/4" in diameter [Ref. 31]. This serves to break up the flow and changes the low frequency noise of the exhaust into more easily attenuated higher frequencies. Work remaining in this area involves the study of placement and sizing of the holes so that uniform flow in the exhaust stack is attained.

Other methods of exhaust treatment will become necessary in the future. Environmental protection standards will require pollution abatement systems for engine test facilities. These systems will require close matching between the engine nozzle and the exhauster because any excess mass flow will unnecessarily load the abatement equipment. Also, in some cases, the flow needs to be properly conditioned before it reaches the abatement system [Ref. 38].

Since many different engines are tested in one cell, consideration must be given to the ease with which cell hardware can be adjusted for various engine sizes. NARF North Island utilizes the movable augmenter concept. The United Air Lines facility uses a jackscrew arrangement to adjust the thrust bed position. The range of adjustment will depend on the size of engines projected to be tested, and the means of providing adjustment is up to the option of the designer.

Modern test facilities are being equipped with automatic data acquisition and processing capability. AiResearch Manufacturing Co. has an excellent example of a system designed for developmental

engine testing, and United Air Lines possesses a system designed for production testing of overhauled and repaired engines [Refs. 32 and 37].

2. NEW DESIGN OPTIONS

a. General

An efficient, flexible, and reliable exhaust system is perhaps the most critical segment in test cell design, yet the present level of engineering sophistication in this area is still elementary. Justification for the above statement is the recent change in the design criteria of cell exhaust treatments. Early designs were primarily built to lower exhaust temperatures to levels that would not shorten the life of installed noise abatement systems. This was accomplished by mixing the jet exhaust with secondary air.

Additionally, attention is now being focused on reducing the air pollution levels of jet engine test cells. Generally, test cells are placed in a different regulatory category than are jet aircraft themselves. They are classed with other stationary sources [Ref. 39].

b. Test Cell Aerodynamic Design

A poorly designed augmenter system may be one that acts as an unnecessarily powerful jet pump. In this situation too much secondary or cooling air is entrained with the engine exhaust, causing higher than designed cell airflows and cell depressions. Also, larger than design airflows will increase distortion levels and possibly disrupt smooth engine operation [Refs. 11, 31, and 40]. Large airflow also can cause errors in thrust measurement.

At the other end of the design spectrum is the system that fails to induce enough secondary airflow and thereby fails to prevent the problem of recirculation of exhaust gases. Excessive exhaust temperature also may result.

The problem of excess secondary airflow has been encountered at several facilities. At North Island a flange has been added to the augmenter bellmouth, restricting the flow of secondary air. This is not a smooth design aerodynamically, and the capability of this facility to handle large bypass fan engines or other high flow rate engine types is severely limited with the present flow restriction. A second solution is to install orifice plates within the augmenter itself to reduce the available flow area [Ref. 35]. This addition is slightly more flexible than the former since various size plates may be installed depending on the flow characteristics of the particular engine under test.

At the United Air Lines facility in San Francisco, secondary airflow in their new large jet engine test facility has been estimated as being almost twice as high as was originally anticipated [Ref. 32]. This condition has not exceeded cell structural limits with the present engines being tested, (JT9D, CF6), but the cell performance will be marginal with advanced technology engines which may reach the 100,000 pound thrust category. This situation indicates the need for close attention to augmenter design and more thorough analysis of the ejector process.

Secondary air provides the necessary cooling of the engine exhaust and prevents recirculation. For a turbojet engine operating without

afterburner an augmentation ratio of 2:1 has been set as a reasonable design goal [Refs. 15 and 31]. Augmenter performance is a function of the area ratio of the augmenter and exhaust nozzle, the length of the augmenter, the position of the exhaust nozzle relative to the entrance of the ejector tube, and velocity ratio. Most recommended test cell augmentation ratios for fan engines vary from 0.25:1 to 0.5:1 for high bypass engines and up to 1:1 for low bypass types [Refs. 10, 15, 31, and 41].

Besides the function of providing a means of mixing and cooling the engine exhaust, the ejector system must overcome the various pressure drops in the inlet and the exhaust systems. Figure 32 shows the general pressure pattern within the test cell. Basically, momentum is transferred to the secondary air, thereby increasing its pressure.

Studies have been made to determine the mixing characteristics of jet pumps [Refs. 6, 7, 22-25, and 42-45]. These indicate that for each characteristic exhaust and secondary airflow combination there is an optimum length and diameter mixing tube. However, because of the cost of construction of the exhaust facilities, many trade-offs must be made, and a flexible design must be selected that will work reasonably well over the range of engines to be tested.

A second method of cooling the exhaust is to use water spray cooling. This method is mandatory for engines operating with afterburner mode but may be used in other modes as well. Studies have been carried out [Refs. 31 and 46] which indicate the amounts of air, water, or both

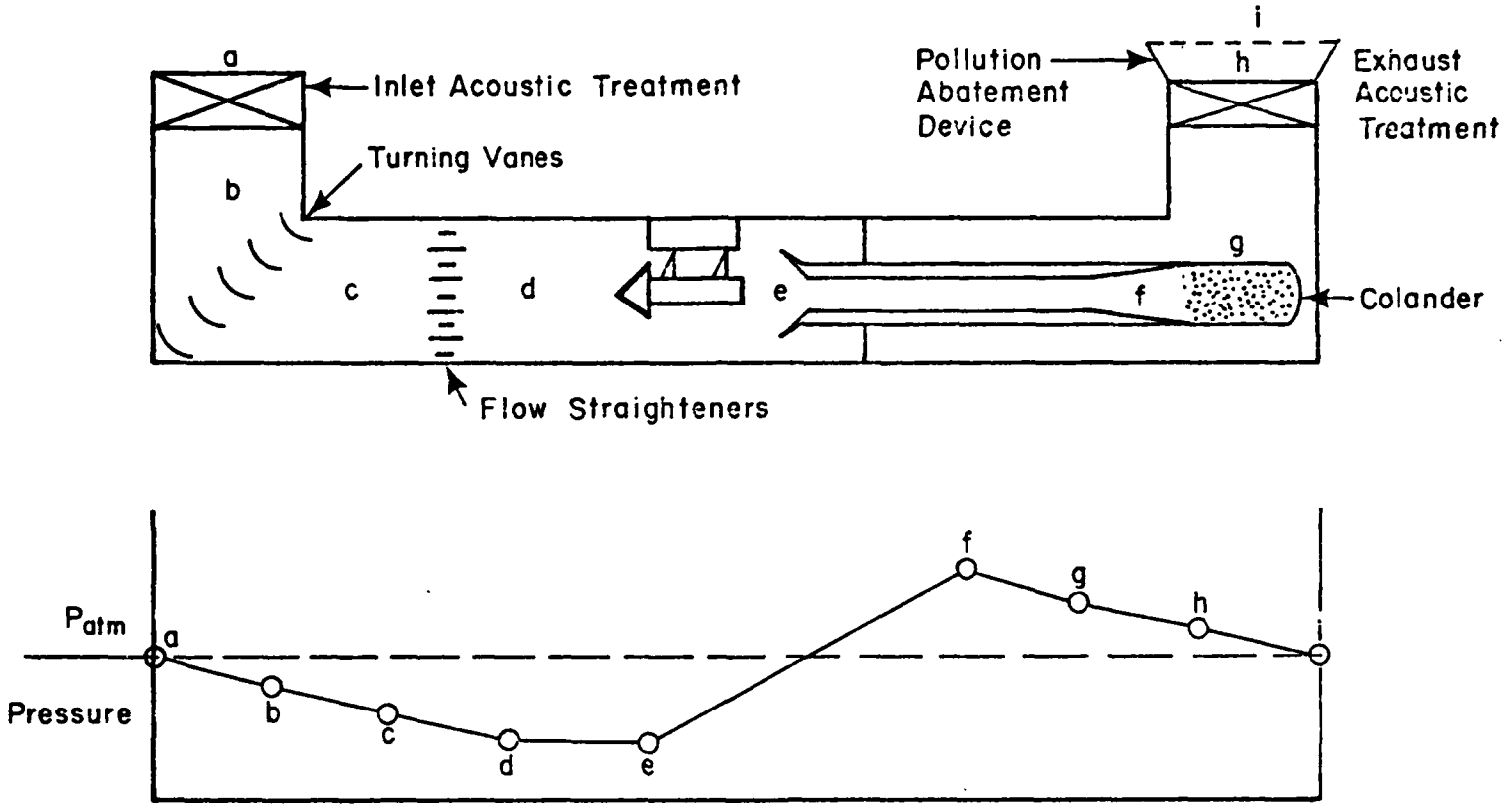

FIGURE 32 TEST CELL PRESSURE PROFILE

which are required to cool exhaust gas temperatures to acceptable levels. When suitable amounts of water cooling are used, secondary airflow can become negligible. However, compromises must be made to determine the amount of water used. At the present time, most of the water used in spray cooling is lost through the stack. At several locations, including NARF North Island, fresh water supplies are at a premium; availability may dictate the design option chosen.

Where water cooling is necessary and available, difficulties remain in devising means whereby the high temperature jet core may be thoroughly penetrated by water streams. It is known [Ref. 33] that even high pressure water jets have little success penetrating into the core of a high speed flow. Various designs have been developed, including concentric rings, water spargers and bounce sprays [Refs. 34, 35, and 47]. These designs, however, have not been optimized for facilities required to test widely varying engine types.

Matching augmenter characteristics to individual engines will be difficult, particularly where low augmentation ratios are desired.

Variable area nozzles are common for afterburning engines. The exhaust from the fans of high bypass engines is at a relatively low energy level; and since it contains no products of combustion, separate ducting may be desirable. The Pegasus engine used in the Harrier aircraft requires complex ducting during test cell operation [Ref. 10].

Prevention of thermal damage to the augmenter must be considered. In the entrainment zone, the walls are subject to radiant heating, while

in the fully developed mixing zone they are heated by convection. Water jackets may be necessary during testing of afterburning or high turbine inlet temperature engines, particularly if the selected exhaust treatment system requires a low augmentation ratio.

c. Acoustic Treatment

Noise sources that must be treated by exhaust systems are turbo-machinery generated noise, combustion noise, turbulent noise generated by the interaction of the jet exhaust and the secondary air, and the turbulence in the exhaust itself [Refs. 48 - 53]. In the entrainment zone the shear stresses are high and the turbulence level is relatively low, creating most of the high frequency noise emanating from the jet [Ref. 54]. Most of the low frequency sounds, those which contribute the most to the overall sound level, come from the portion of the exhaust beyond the potential core; the peak of this sound is at a wavelength about three times the diameter of the jet. It is this low frequency sound that is most difficult to attenuate. The higher frequency noise of machinery is easily attenuated with standard techniques which include baffles of all types, lined passages and bends, and tubular exhaust passages [Refs. 31, 40, and 55].

The properly designed augmenter can contribute to the overall reduction of noise; experimental results [Ref. 56] have shown that jet noise can be reduced by a factor of 5 (7db) in an ejector noise suppressor. It was also shown that the initial mixing conditions and the length of the

injector are more important factors in obtaining this attenuation than the area ratio of the tube and jet or the position of the primary jet relative to the ejector inlet.

Methods of breaking up the continuity of the jet and increasing the frequency of the exhaust noise are discussed in Section 1. The utilization of a colander in the form of a cone or a cylinder is presently preferred over other options in modern cell designs. It has been found by experience that a hole size 1-1/4" in diameter is the smallest practical size [Ref. 31]. Holes smaller than this tend to be easily blocked due to impurities in cooling water as well as particulate matter present in the engine exhaust. Standard practice has been to space uniformly the holes over the surface of the colander, with total hole area 40 to 60 percent in excess of the cross sectional area of the augmenter tube itself [Refs. 31 and 36].

An exception to this practice has been introduced in some smaller Navy "C" cells [Ref. 36]. In these cells holes were placed only in the lower half of the colander. This design has exhibited a serious shortcoming in that flow through the exhaust stack is very non-uniform; in fact, some points in the stack exhibit zero velocity. This causes portions of the acoustic treatment to be exposed to higher than design flow rates, thereby shortening useful life and decreasing overall performance.

Analysis must be done during design to insure adequate flow conditioning over the operational range of the proposed test cell. The

designer must insure that enough pressure rise will be obtained to overcome any flow blockage that may be present under all operating conditions.

Unwanted acoustic energy may be generated by obstructions present in the ejector assembly. These include spray rings or nozzles, diffuser rings, and any other hardware installations. These obstructions increase the turbulence level of the flow, thereby increasing the noise sources within the flow. The merits of each proposed installation must be weighed according to the use intended for the individual test cell. Care must be taken that natural frequencies of installed components are not activated by the driving frequencies of the flow.

Possible exhaust stack treatments are as varied as those intended for use in the inlet. Options include lined bends and passages, tubular mufflers, sinuous passages or straight passages [Refs. 31, 37, and 58]. Steel Helmholtz resonators have been investigated by General Electric [Ref. 31] and have been found to be unsatisfactory for their own use; however, this approach has been successfully taken by Aero Systems Engineering [Ref. 59]. Differences in the cell utilization of the two operators and in the acoustic characteristics of the engines tested account for the different technical approach.

A primary concern is to develop a system which will withstand a moderate range of temperatures and wide range of velocities. Most installations have been designed to withstand exhaust stack temperatures in the 450-550°F range, with a maximum of 600° [Ref. 31]. At one time NARF North Island attempted to maintain temperatures below 200° in

the non-afterburning mode by water cooling. However, it was impossible, with the existing water spray design, to operate the afterburner and maintain stack temperatures below 450°. The installed acoustic treatments were subjected to such severe thermal shock that their useful life was drastically shortened. Within practical limits, a constant stack temperature should be maintained in all tests.

Because of the varied sizes and characteristics of engines that will be tested in new construction test cells, consideration should be given to the possibility of providing variable area exhaust stacks. Methods of accomplishing this include blanking unnecessary portions of the stack with pre-fitted metal shutters according to the flow requirements of the engine under test and a movable cover over the stack opening which is programmed to provide optimum flow area. By designing the basic exhaust system to handle the largest forecast airflow with the additional capability of efficiently handling much lower flows, the problem of test cell obsolescence caused by advances in engine technology can be avoided.

d. Emission Control Devices

In the future, major design effort must be devoted to pollution abatement systems. It has been established by Executive Order 11282, May 26, 1966, that Federal installations comply with local environmental protection requirements. At the present time most emission requirements which are applicable to test facilities deal with the particulate emissions which cause visible pollution. Future legislation

will limit emission levels of invisible noxious gases, carbon monoxide, oxides of nitrogen, and sulfur dioxide. Studies have been conducted to determine exhaust emissions of gas turbine engines [Refs. 39, and 60-66]; and although the exact emission levels are not agreed upon, most data agree within an order of magnitude.

The abatement system chosen for test cell operation must first remove visible particulate emissions. California legislation limits the deviation from a maximum of 20 percent obscuration (#1 on the Ringleman scale) to three minutes out of every hour.

Except at idle, gas turbine engines emit very low levels of unburned hydrocarbons and CO, so that attempts to reduce these should concentrate on low flow rate conditions [Ref. 60].

By 1975, Los Angeles County will limit emission of oxides of nitrogen to 225 ppm [Ref. 39]. New developments in engine technology resulting in high pressure ratios and high combustion temperatures have raised the levels of these oxides in engine exhausts [Ref. 60]. The chosen abatement system must at the very least not add to these levels and ideally should reduce them.

The installed system must be able to remove unburned fuel from the exhaust flow. Estimates are that turbojet afterburners exhaust about 10 percent unburned fuel. Also, the ability must be retained to purge unwanted fuel from the exhaust drainage system. Prior to light-off, it is Navy practice to "dry run" the engine; that is, the engine is

windmilled and the throttle fully opened to check for leaks. This results in relatively large amounts of fuel being dumped directly into the exhaust system.

Emissions of sulfur dioxide will not be a problem as long as the current restrictions on sulfur content of fuel are maintained. Present restrictions limit the sulfur content to .3 percent, and most fuels contain even less.

Although advances have been made in combustor technology, completely clean jet engines are not yet a reality. NARF Alameda was recently cited in violation of local standards while testing a high time engine configured with "clean" combustor cans. One source [Ref. 66] theorizes that reactions within the cell exhaust system change the character of particulate emissions, either in size or number, so that visibility obscuration is greater at the test cell exhaust stack than at the engine tailpipe.

Interim solutions for reducing smoke involve the use of fuel additives. Additives coat engine hot section parts, and the effect of adding heavy metallic vapors to the exhaust is under continuing investigation by the Environmental Protection Agency.

Early studies of pollution abatement systems have resulted in the selection and development of a nucleation scrubber [Ref. 47]. Other devices analyzed include filtering devices, venturi scrubbers, and electrostatic precipitators. These have been evaluated as unsatisfactory from considerations of safety, flexibility, and economy [Ref. 47].

Filtering devices alone present problems because of their tendency to become clogged by particles entrained in the exhaust. Additionally, they require extremely low flow velocities and are not effective in removing noxious gases.

The primary drawback to the venturi system is its inability to operate efficiently over greater than a 10 percent interval away from its design point, which is an unacceptable restriction in view of the fact that air flows vary as much as 60 to 70 percent from idle to full power setting. A possible solution to this would be the installation of a bank of venturis, entailing high initial costs and complicated flow controls.

The present shortcoming of electrostatic precipitators is the inability to completely prevent fuel buildup on and around the electrodes; this condition creates the danger of an explosive discharge. Also, these systems cannot remove noxious gases or oxides of nitrogen.

Nucleation scrubbers work by process of creating large particles by condensation of vapor from a saturated vapor. The nucleates are the particulate matter already present in the exhaust. The enlarged particles are then removed by impaction in the scrubbing system. A prototype scrubber system developed by Dr. A. Teller (Pat. #3,324,630) has been installed by the Navy at NARF Jacksonville. This particular scrubber has the capacity to handle large changes in flow volume, can reduce noxious gases and unburned fuel, and with modification can remove much of the oxides of nitrogen and sulfur if such action is required. Installation of this scrubber also is anticipated at NARF Norfolk. The primary drawback

at present with the scrubber system is its high initial costs. At its present level of development this system is not considered the ideal solution, and investigation is being carried out in other areas as well.

The nucleation scrubber as well as the other alternatives discussed are all similar in that they function by physically removing particulates and unwanted gases; a second class of installations acts by converting unwanted pollutants to harmless chemical species. These include afterburners and catalytic converters.

Northern Research and Engineering Corporation has proposed a thermal converter installation for test cells [Ref. 39]. This reference is a comprehensive discussion of the feasibility of such an installation and the justification for Navy procurement in light of future requirements for pollution control. At the present time much work remains to be done in conducting recommended studies and testing.

The installation of a converter system will require close matching of the test section, engine, and exhauster itself since the proposed system requires a low augmentation ratio.

The final selection of an abatement system will be based on its flexibility and economy. It must be able to operate over a wide range of exhaust velocities and temperatures. The initial cost of procurement and installation must be low, as must the cost of operation and upkeep. The system must be reliable enough to allow firm scheduling of cell down time with the minimum amount of unscheduled maintenance. An additional factor will be the ease with which the abatement system may be retrofitted to existing test cell structures.

The creation of secondary pollution must be avoided. Thermal pollution of natural water supplies is a real possibility in systems requiring heavy cooling. Also to be avoided is the creation of additional, unwanted noxious gases or other undesirable products of combustion if an additional combustion process is used.

Maximum allowable temperatures, pressures, and velocities will dictate the level of required protection of hardware exposed to the jet exhaust. Because of the temperatures encountered during afterburner runs, it may become necessary to water cool certain exposed parts. Refractory linings have been considered but were rejected for economic reasons [Ref. 39].

Complete acoustic analysis must be completed to insure that the natural frequencies of equipment exposed to the flow not be excited by the frequencies of turbulence generated noise.

Finally, the design of adjustable components should be kept as simple as possible. Operators are wary of too much gadgetry in test cell design [Refs. 32 and 35], and cell down time increases with the addition of mechanical sophistication. All facilities must be designed to operate with the minimum amount of required upkeep.

APPENDIX B

THEORETICAL ANALYSIS

1. BASIC PROGRAM

Consider the schematic diagram of a jet pump shown in Fig. 2. For the purposes of this analysis sections 1 and 2 will be coplanar. Assume inviscid flow so that the velocity profiles are as shown in Fig. 2. The analysis is based on the one-dimensional conservation of mass, energy and momentum. The perfect gas relation is assumed for primary, secondary and mixed flows

$$P = \rho RT \tag{B-1}$$

It was assumed that total pressure and temperatures were known at stations 1 and 2, and that $P_1 = P_2$. The model was developed for constant area mixing so that $A_1 + A_2 = A_3$. The back pressure, P_3, was arbitrarily set. Define

$$\beta_i = 1 + \frac{\gamma - 1}{2} M_i^2 \tag{B-2}$$

Then

$$\beta_i = [P_{Ti}/P_i]^{\frac{\gamma-1}{\gamma}} \tag{B-3}$$

and

$$T_i = T_{Ti}/\beta_i \tag{B-4}$$

From Eq. (A-5)

$$M_i^2 = (\beta_i - 1)\left(\frac{2}{\gamma - 1}\right) \tag{B-5}$$

From Eq. (A-4)

$$\rho_i = P_i/RT_i \tag{B-6}$$

The speed of sound, a, is equal to $(\gamma RT)^{1/2}$. For air, $a_i = 49.01(T_i)^{1/2}$ for T_i in degrees Rankine. Using the definition of Mach Number it follows that

$$U_i = 49.01\sqrt{M_i^2 T_i} \tag{B-7}$$

Primary and secondary mass flows were obtained with the assumption that $P_1 = P_2$

$$\dot{M}_i = \rho_i U_i A_i \tag{B-8}$$

After some manipulation, Eq. (III-2) may be used to solve for U_3

$$U_3 = [(P_1 - P_3)A_3 + \dot{M}_1 U_1 + \dot{M}_2 U_2]/\dot{M}_3 \tag{B-9}$$

Values for the density and static temperature at station 3 may be determined from Eq. (B-6) and (B-8). The energy of the system must also be conserved, requiring that Eq. (III-3) be satisfied. A second value for T_3 is then found

$$T_3 = \left(T_1 + \frac{U_1^2}{2C_p}\right)(\dot{M}_1/\dot{M}_3) + \left(T_2 + \frac{U_2^2}{2C_p}\right)(\dot{M}_2/\dot{M}_3) - \frac{U_3^2}{2C_p} \tag{B-10}$$

The program was made to perform an iteration on inlet static pressures until the separately computed values for T_3 were within 1°R of one another. It was found that when the value for T_3 computed from considerations of momentum and mass conservation initially was greater

than the value for temperature computed from (B-10), the value of P_1 was too high. The opposite was always true when energy considerations yielded the higher temperature. The inlet pressure was adjusted accordingly for the next step in the iteration. The first such correction was a fixed value. For each successive iteration in which P_1 was adjusted in the same direction, the correction remained constant. Each time the comparative value of the temperatures changed sign, the correction value was halved. The process was continued until the two computed values of T_3 were within the specified limit. The above equations were combined in a basic computer program which was to be the core of the overall program discussed below.

2. RELATIVE POSITION OF PRIMARY NOZZLE

One goal of the study was to analyze the effect of removing the primary nozzle from the coplanar position shown in Fig. 2. The analysis of section 1 above was valid for the position shown as well as the case where the primary nozzle was positioned inside the augmenter inlet. However, if the nozzle was positioned outside the augmenter, some knowledge of free jet performance is necessary. A jet spread parameter is used in the literature for this purpose [Refs. 22-25, 27, 44, and 67]. Bauer [Ref. 27] has shown that Abramovich's [Ref. 25] model for σ, the jet spread parameter, provides a good agreement with empirical data for axisymmetric jet mixing zones

$$\sigma = 24U_{mean}/U_{\infty} \qquad \text{(B-11)}$$

U_∞ is defined as the centerline velocity of the potential core of the primary flow as shown in Fig. 3. It was assumed that the velocity profile within the mixing zone could be modeled by an error function following Refs. 19 and 27. The nondimensional coordinate η was defined and used as the argument of the error function

$$\text{erf}\ \eta = \text{erf}\left(\frac{\sigma\, y}{X}\right) = \frac{2}{\sqrt{\pi}} \int_0^{\eta} e^{-a^2}\, da \qquad \text{(B-12)}$$

where σ is the jet spread parameter, $y = r_o - r_1$ or $r_i - r_1$ where r_1 is the radius of the primary nozzle and r_o and r_i are the outer and inner boundaries of the mixing zone; X is the axial position measured from the nozzle exit.

The edge of the mixing zone was defined as the point where the velocity is within one percent of the free stream value. A table of error functions yielded a limit value of $\eta = 1.84$ for the boundaries. The width of the mixing zone was defined as

$$\delta = 2Y_{max} = \frac{2\,\eta_{max} X}{\sigma} = \frac{3.68X}{\sigma} \qquad \text{(B-13)}$$

It was assumed for the case under consideration that

$$U_{mean} = 1/2(U_1 + U_2) \qquad \text{(B-14)}$$

After some manipulation it was found that the velocity within the mixing zone is expressed by

$$U(\eta) = \frac{U_1}{2}\left[\left(\frac{U_2}{U_1} + 1\right) + \text{erf}\ \eta\ \left(\frac{U_2}{U_1} - 1\right)\right] \qquad \text{(B-15)}$$

where U_1 is the velocity of the primary potential core and U_2 is the free stream velocity of the secondary flow.

Areas A_1 and A_2 were redefined to be the areas occupied by the primary and secondary flows at the station under observation. Equation (III-1) then becomes

$$\rho_1 U_1 A_1 + \rho_2 U_2 A_2 + \int \rho(\eta) U(\eta) dA = \rho_3 U_3 A_3 \qquad \text{(B-16)}$$

Areas A_1 and A_2 were found using the assumption that the mixing zone spread evenly into both the primary and secondary flow so that

$$A_1 = \frac{\pi}{4}(D_1 - \delta)^2 \qquad \text{(B-17)}$$

and

$$A_2 = \frac{\pi}{4}\left[D_2^2 - (D_1 + \delta)^2\right] \qquad \text{(B-18)}$$

where D_1 and D_2 are the diameters of the primary and secondary nozzles. Before Eq. (B-16) could be utilized, an assumption had to be made concerning the density within the mixing zone; this was expressed by

$$\rho(\eta) = \frac{\rho_1}{2}\left[\left(\rho_2/\rho_1 + 1\right) + \text{erf}\ \eta\ \left(\rho_2/\rho_1 - 1\right)\right] \qquad \text{(B-19)}$$

This relatively simple approximation was made because the expected values of density in the experimental apparatus were very close to one another. That is $\rho_1 \cong \rho_2$. A better approximation might be made if one considered heat transfer rates in the mixing zone and assumed a given temperature distribution in the mixing zone. If temperatures were known, the perfect gas law could be used to calculate densities since the static pressure was assumed constant across the mixing zone.

The mixing zone was divided into incremental areas, and the mass flow in the mixing region was taken to be the sum of the mass flows in the incremental areas.

The mass flow in each area is found from the equation

$$\dot{M}_i = \frac{\rho_i U_i \pi}{4} \left\{ \left[D_1 + 2\left(\eta_i + \frac{1.84}{INT} \right) \right]^2 - \left[D_1 - 2\left(\eta_i - \frac{1.84}{INT} \right) \right]^2 \right\} \tag{B-20}$$

where η_i is the coordinate of the center of the area and INT is the total number of intervals into which the mixing zone was divided. The mass flow within the mixing region is the sum of all the $\dot{m}_i$'s

$$\dot{M} \text{ (mixing zone)} = \sum_{i=1}^{INT} \dot{M}_i \tag{B-21}$$

Similar manipulations of the momentum and energy equations yielded the following results

$$U_3 = [(P_1 - P_3)A_3 + \rho_1 U_1^2 A_1 + \rho_2 U_2^2 A_2 + \sum_{i=1}^{INT} \rho_i U_i^2 A_i]/\dot{M}_3 \qquad \text{(B-22)}$$

and

$$T_3 = \frac{\dot{M}_1}{\dot{M}_3}(T_1 + \frac{U_1^2}{2C_p}) + \frac{\dot{M}_2}{\dot{M}_3}(T_2 + \frac{U_2^2}{2C_p})$$

$$+ \frac{1}{\dot{M}_3} \sum_{i=1}^{INT} \dot{M}_i (T_i + \frac{U_i^2}{2C_p}) \qquad \text{(B-23)}$$

Note that by utilizing the perfect gas law

$$T_i = \frac{P}{\rho_i R_i} = \frac{\rho_1}{2} R[(\frac{\rho_2}{\rho_1} + 1) + \text{erf } \eta\ (\frac{\rho_2}{\rho_1} - 1)]P^{-1} \qquad \text{(B-24)}$$

The velocity and density in each incremental area were computed using Eqs. (B-15) and (B-19) in the form

$$U_i = A + B \cdot \text{erf } \eta \qquad \text{(B-15a)}$$

and

$$\rho_i = C + D \cdot \text{erf } \eta \qquad \text{(B-19a)}$$

where

$$A = (\frac{U_1}{2}) \cdot (U_2/U_1 + 1) \qquad C = (\rho_1/2) \cdot (\rho_2/\rho_1 + 1)$$
$$B = (\frac{U_1}{2}) \cdot (\frac{U_2}{U_1} - 1) \qquad D = (\rho_1/2) \cdot (\rho_2/\rho_1 - 1) \qquad \text{(B-25)}$$

The incremental flow areas were computed from the following equation

$$A_i = (\pi/4)\,(D_{out}^2 - D_{in}^2) \tag{B-26}$$

where

$$D_{out} = D_1 + 2(\eta_i + \frac{1.84}{INT})\frac{X}{\sigma}$$

$$D_{in} = D_1 + 2(\eta_i - \frac{1.84}{INT})\frac{X}{\sigma} \tag{B-27}$$

Equations (B-15), (B-19), and (B-26) make it possible to solve the conservation equations for two values of outlet static temperature and to iterate as before on inlet static pressure.

3. WALL FRICTION COEFFICIENT

It was necessary to find a system of equations to compensate for the friction losses at the walls of the augmenter. Equation (B-22) was modified to include the drag term as a momentum loss

$$U_3 = [P_1 - P_3)A_3 + \dot{M}_1 A_1 + \dot{M}_2 A_2 + \sum_{i=1}^{INT} \dot{M}_i U_i - Drag]/\dot{M}_3 \tag{B-28}$$

where

$$Drag = C_D \frac{\overline{\rho U^2}}{2} A_{ref} \tag{B-29}$$

C_D is the drag coefficient and A_{ref} is the area over which the drag acts. Since the flow in the augmenter does not resemble developed pipe flow, flat plate drag coefficients were chosen. Schlichting [Ref. 28] indicates that flat plate drag coefficient is

AD-A106 890 NAVAL POSTGRADUATE SCHOOL MONTEREY CA F/G 14/2
AN ANALYTICAL AND EXPERIMENTAL ANALYSIS OF FACTORS AFFECTING EX--ETC(U)
DEC 72 D L BAILEY

UNCLASSIFIED NL

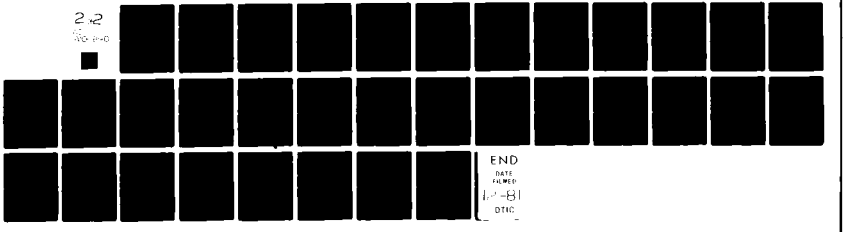

END
DATE FILMED
1-82
DTIC

$$C_D = 0.455/(\log Re)^{2.58} \qquad \text{(B-30)}$$

where Re is the flow Reynolds number based on the length. For computational purposes, the velocity used to compute the Reynolds number was taken to be the average of the inlet and outlet wall velocities or $(U_2 + U_3)/2$.

Values for kinematic viscosity were also found in Schlichting and were approximated in the following equations. If the reference temperature is below 564°R

$$\nu = (0.639T-177.4)\times 10^6 \qquad \text{(B-31)}$$

If the temperature is greater than 564°R

$$\nu = (0.667T-193.2)\times 10^6 \qquad \text{(B-32)}$$

so that ν is obtained in units of ft^2/sec.

The dynamic pressure term in Eq. (B-29) was taken to be the average dynamic pressure of the secondary and outlet flows, or

$$\overline{\rho U^2} = \frac{(\rho_2 U_2^2 + \rho_3 U_3^2)}{2} \qquad \text{(B-33)}$$

The initial drag term was set to zero, and all conservation equations were solved as previously discussed. A new value of drag was computed and inserted in Eq. (B-28). The process was continued until the new value for drag differed from the old value by less than one percent.

4. AUGMENTER CONFIGURATION

Several inlet configurations are in existence in engine test facilities. This analysis was developed to take the varying effects of these configurations into account.

Reference 29 discusses the effects of re-entry and bellmouth inlets of large ducting systems on the inlet head loss associated with the two different inlets. Loss factors of 0.85 and 0.03 for re-entry and bell-mouth inlets are given. The pressure loss of a system is defined to be the loss factor times the velocity head at the inlet

$$\Delta P = n \frac{\rho U^2}{2} \tag{B-34}$$

where n is the inlet loss factor. This concept was incorporated into the program. Since the secondary total pressure was assumed to be 1.0 atmosphere, the secondary total pressure immediately after an installed inlet would be equal to $1.0 - 1/2\ cn \cdot \rho \cdot u^2$ atmosphere, where c is an appropriate constant that converts the velocity head to atmospheres. An iteration is performed until two successive values of total pressure loss are within 0.0001 atmosphere of one another. It was found that the iteration process converged rapidly when the following equation was used

$$P_{T_{2\ new}} = 1/2\ (1.0 - \frac{cn\ \rho_2 U_2^2}{2} + P_{T_{2\ old}}) \tag{B-35}$$

The new value of P_{T_2} was used to re-evaluate Eqs. (B-2) through (B-7) for new density and velocity values at station 2. Reference 13 discusses

the restricted inlet configuration in use at one Naval Air Rework Facility. Allowances for this configuration were made by permitting variable values to be read in for D_2, the diameter of the secondary inlet, and assuming that the inlet was of the re-entry type.

5. BACK PRESSURE CONSIDERATIONS

Exhaust pressures at the augmenter exit are generally higher than ambient pressures because of the presence of installed acoustic and pollution controls. The computer program was able to run at any back pressure up to a specified value. This point was considered to have been reached when the secondary static pressure exceeded the secondary total pressure. This condition corresponds to the onset of exhaust gas recirculation in an actual installation.

6. MAIN COMPUTER PROGRAM

The program reads primary and secondary inlet conditions P_{T_1}, T_{T_1}, P_{T_2} and T_{T_2}; nozzle and augmenter diameters D_1, D_2, and D_3; the entry loss factor; and primary nozzle separation distance. The back pressure P_3 is set within the program.

The output includes inlet static conditions P_1, T_1, T_2; outlet static temperature T_3; primary and secondary mass flows $\dot{M}_1$ and $\dot{M}_2$; non-dimensional ratios P_{T_1}/P_3, P_{T_2}/P_3, P_{T_1}/P_{T_2}, X/D_1, A_3/A_1, A_2/A_1, T_{T_1}/T_{T_2}, T_3/T_2, ρ_2/ρ_3, D_{in}/D_1, D_{out}/D_1, D_{DIV}/D_1; sigma; and YDIV. D_{DIV}/D_1 is the location of the dividing streamline as determined by comparing the nozzle mass flow with the mass flow at distance X

from the nozzle. YDIV is the radial distance that the jet has spread at distance X. Table B-I is a listing of the algebraic symbols used and the corresponding Fortran symbols. A copy of the Main Computer Program follows Appendix C.

Table B-I Symbols for Main Computer Program

Algebraic	Fortran	Remarks
U_1	U1	
ρ_1	RHO1	
T_1	T1	
$\dot{M}_1$	M1DOT	
P_1	P1	
β_1	BETA1	$\beta_1 = 1 + \frac{\gamma - 1}{2} M_1^2$
M_1^2	M1SQ	
C_p	CP	Constant pressure specific heat of air
γ	GAMMA	1.4 for air
R	R	Gas constant for air
η	NU	Nondimensional radial variable $= \sigma\, y/x$
σ	SIGMA	Jet Spread Parameter
U_{mean}	UM	$UM = (U_1 + U_2)/2$
erf η_i	ERFNU(I)	Error function integral
A_i	AMZ(I)	Incremental area of the mixing zone
ρ_i	RHOMZ(I)	Values in the mixing zone in incremental A_i
U_i	UMZ(I)	

Table B-1 Symbols for Main Computer Program (continued)

Algebraic	Fortran	Remarks
$\dot{M}_i$	MDOT(I)	
$\dot{M}_{\text{mixing zone}}$	MZDOT	$\dot{M}_{mz} = \sum \dot{M}_i$
INT	INT	Number of intervals into which mixing zone is divided
X	X	Axial position of primary nozzle relative to augmenter
D_{out} D_{in}	DOUT DIN	Outer and inner dia. of mixing zone
C_D	COFRIC	Wall friction drag coefficient
ν	V	Dynamic viscosity of air
$\overline{\rho U^2}$	RUSQBR	$1/2(\rho_2 U_2^2 + \rho_3 U_3^2)$
n	ENTLOS	Loss coefficient for inlet configuration
ΔP	DELHD	Pressure loss through augmenter inlet
$\dot{M}_2/\dot{M}_1$	M2M1	Augmentation Ratio
P_{T_1}/P_3	PT1P3	
P_{T_2}/P_3	PT2P3	
P_{T_1}/P_{T_2}	PT1PT2	
X/D1	XD1	
A_3/A_1	A3A1	

Table B-I Symbols for Main Computer Program (continued)

Algebraic	Fortran	Remarks
A_2/A_1	A2A1	
T_{T_1}/T_{T_2}	TT1TT2	
T_3/T_2	T3T2	
ρ_2/ρ_3	RO2RO3	
D_{in}/D_1	DIND1	
D_{out}/D_1	DOUTD1	
D_{div}	DDIV	Diameter of streamtube defined by $\eta = 0$
D_{div}/D_1	DDIV/D1	
y_{div}	YDIV	DDIV = D_1 + 2 YDIV
R_e	REYNOZ	Nozzle Reynolds number
L	AUGL	Augmenter length
D	DRAG	Augmenter wall friction
T_3	T3COM T3ENR	Exit static temperatures from mass and momentum conservation and energy considerations
ν_{noz}	VNOZ	Dynamic viscosity at the primary nozzle

APPENDIX C

DATA REDUCTION PROGRAMS

1. PRIMARY MASS FLOW RATE

The mass flow of air through the primary nozzle was measured by means of a stainless steel sharp edged orifice plate installed in a section of 3" pipe upstream of the nozzle. The installation was constructed to meet ASME standards as set in Ref. 30. Pressure measurements were obtained from flange taps. The upstream static pressure was measured on a mercury manometer and the pressure drop across the orifice was measured on a water manometer. The total temperature was measured in an 8" pipe upstream of the orifice.

The orifice was chosen over other methods of flow measurement because of its availability and ease of installation. Facilities were not available for calibration of primary elements of the proper capacity. This fact dictated the use of an orifice since it possesses a well established coefficient of discharge. The high head losses associated with orifice plates did not interfere with test results.

Equation (C-1) was used to solve for mass flow rates.

$$W_h = 359\ CFd^2F_aY\sqrt{h_w\gamma} \qquad \text{(C-1)}$$

The weight rate of flow, w_h, is calculated in pounds per hour, C is the coefficient of discharge, F_a is the thermal expansion factor, d is the orifice diameter, F is the velocity of approach factor, Y is the net expansion factor for orifices, h_w is the pressure drop across the orifice

in inches of water, and γ is the specific weight, in pounds per cubic foot, of flowing fluid at the orifice inlet. Since the orifice used in the experimental setup was not calibrated, it was necessary to use the flow coefficient K where

$$K = CF \tag{C-2}$$

Values of K are tabulated in Table 4 of Ref. 30 as a function of pipe Reynolds number and diameter ratio β where

$$\beta = D/d \tag{C-3}$$

D is the pipe diameter. Orifice diameter d was 2.096" so that $\beta = 0.665$ when installed in a 3" pipe. Figure 38 of Ref. 30 is a curve of F_a as a function of temperature. Over the range of outlet temperatures expected, the values of F_a were obtained from the following equation for a straight line approximation to Fig. 38

$$F_a = (0.001T_1/70) + 0.9991 \tag{C-4}$$

Figure 40b of the same reference plots Y as a function of the ratio h_w/P_1 where P_1 is the orifice inlet pressure in pounds per square inch. The curve very closely fit the following straight line approximation for Y

$$Y = 1 - 0.037\, h_w/3P_1 \tag{C-5}$$

The specific weight of air was found by assuming a perfect gas

$$\gamma = P_1 \cdot g/RT_1 g_c \tag{C-6}$$

where P_1 is in pounds per square foot, T_1 is in °R and R is the gas constant for air, 1715.63 ft lbf/lbm °R.

Once input data were acquired, it was possible to begin a computer program which rapidly converged. Initial calculations involving expected flow rates indicated a probable Reynolds number based on pipe diameter D between 100,000 and 500,000. Table 4 of Ref. 30 indicated that a flow coefficient of 0.68 would give good results when used as a starting point. This value for K, along with measured values of inlet temperature and pressure and the pressure drop across the orifice, may be put in Eq. (C-1) to get a first solution for flow rate. Equation 8, page 58 of Ref. 30, yields the flow Reynolds number

$$R_{eD} = (0.004244\ w_h)/Dg\mu \qquad \text{(C-7)}$$

where μ is the viscosity of air in lbf-sec/ft^2. Figure 33 of the same reference plots values of $g\mu$ as a function of temperature. Over the expected range of temperatures

$$g\mu = (0.001832T_i + 1.0835) \times 10^{-5} \qquad \text{(C-8)}$$

Interpolation of Table 4 will yield a more precise value for K, the flow coefficient, from one of the following equations. If the Reynolds number is less than 100,000, then

$$K = 0.6865 - 0.0051(R_{eD}/50{,}000 - 1.0) \qquad \text{(C-9)}$$

and if the Reynolds number is greater than 100,000 but less than 500,000, then

$$K = 0.6814 - 0.004(R_{eD}/400{,}000 - 0.25) \qquad \text{(C-10)}$$

Two iterations were found to be all that were needed for convergence.

2. PROGRAM M1DOT

The data reduction M1DOT is included following Appendix C. Input data needed are the atmospheric and inlet pressures in inches of mercury, inlet temperature in °F, and the pressure drop across the orifice in inches of water. The output includes mass flow rate in pounds per second as well as the pipe Reynolds number.

Table C-I lists appropriate algebraic symbols and their Fortran counterparts used in the program.

3. AUGMENTER FLOW RATE

In order to determine the pumping effectiveness of the simulated engine, it was necessary to measure the total mass flow through the augmenter. Section IV discussed the positioning of data collection stations along the augmenter model and the probes used to measure total temperatures and pressures.

Program AUG1 was developed to process the raw data and calculate total augmenter mass flow. Input data to AUG1 include total pressures and temperatures measured at 1/4" intervals beginning at the center of the augmenter out to a position 1/4" from the wall. Velocities were calculated at each of the ten points. The dynamic pressure was calculated using Bernoulli's equation for incompressible flow

$$q = 1/2 \ \rho \ u^2 = P_T - P \qquad \text{(C-11)}$$

For one-dimensional flow

$$\dot{M} = \rho \, uA \qquad \text{(C-12)}$$

Table C-1 Symbols for Program M1DOT

Algebraic	Fortran	Remarks
d^2	DSQ	d = orifice diameter
K	K	Flow Coefficient
	KGUESS	Initial value of K = 0.68
P_{atm}	PA	Atmospheric pressure
P_1	P1G	Inlet gage pressure
T_1	T1	Inlet temperature
h_w	HW	Pressure drop across orifice
γ	SPWT	Specific weight
F_a	FA	Coefficient of thermal expansion
Y	Y	Net expansion factor for square edged orifices
w_h	M1DOT	Rate of flow, w_h in pounds per hour and M1DOT in pounds per sec.
$g\mu$	GNU	Viscosity term
R_{eD}	RE	Pipe Reynolds Number

or after substitution from Eq. (C-11)

$$\dot{M} = 2qA/u \tag{C-13}$$

From the perfect gas law and rearranging Eq. (C-11)

$$2q/u^2 = P/RT \tag{C-14}$$

Solving for u^2

$$u^2 = 2qRT/P \tag{C-15}$$

Using the isentropic flow relations

$$T/T_T = (P/P_T)^{\frac{\gamma-1}{\gamma}} \tag{C-16}$$

Substituting for T from Eq. (C-16) into (C-15)

$$u^2 = \frac{2qT_T(P/P_T)^{\frac{\gamma-1}{\gamma}}R}{P} \tag{C-17}$$

For T_T in °R and q, P, and P_T in identical units

$$u = [3431.26\ T_T(P/P_T)^{0.285}q/P]^{1/2} \tag{C-18}$$

With the velocity determined in Eq. (C-18), Eq. (C-13) was used to determine mass flow in the augmenter. The flow area was divided into ten circular increments of increasing radii beginning with a circle of 1/4" radius. The next circular segment had an inner radius of 1/4" and an outer radius of 1/2", continuing to the wall of the augmenter tube which was 5" in diameter. Values of velocity and q in each incremental area were taken to be the average of the values at the inner and outer boundaries of the area. The sum of the incremental mass flows represented the total augmenter mass flow.

4. PROGRAM AUG1

Data reduction program AUG1 is included in the following section. Input data required are the atmospheric pressure, static pressure at the station being surveyed, primary mass flow as determined by program M1DOT, and total temperatures and pressures measured at prescribed intervals across the augmenter. The program output includes primary and secondary mass flow rates, the augmentation ratio $\dot{M}_2/\dot{M}_1$, the centerline velocity, and the velocities at each point where temperatures and pressures were measured normalized to the centerline velocity.

Table C-II lists the algebraic and Fortran symbols used in program AUG1.

Table C-II Symbols for Program AUG1

Algebraic	Fortran	Remarks
r_i	R(I)	Radius of point I in augmenter
A_i	A(I)	Incremental flow area in augmenter
U_i	U(I)	Augmenter velocity at point I
U_{CL}	UCL	Centerline velocity in augmenter
P_{T_i}	PT(I)	Total values at point I in augmenter
T_{T_i}	TT(I)	
q	Q(I)	Dynamic pressure at I
$\dot{M}_i$	M(I)	Mass flow through area I
$\frac{\gamma - 1}{\gamma}$	GTERM	$\gamma = 1.4$
P_g	PG	Static gage pressure
P_{atm}	PA	Atmospheric pressure
$(P/P_T)^{\frac{\gamma - 1}{\gamma}}$	PTERM	
U_i^2	USQ	
$\dot{M}_3$	M3DOT	Augmenter mass flow
$\dot{M}_2/\dot{M}_1$	M2M1	Augmentation ratio
	ISTA	Augmenter station surveyed
	CONFIG	Test configuration
	RUNDAY	Date data were obtained and run number for that day

```
      IMPLICIT REAL*4 (M)
      REAL*4 MU
      DIMENSION NU(105),ERFNU(105),TMZ(105),RHOMZ(105),UMZ(105),AMZ(105)
     1,MDOT(105)
      DATA GAMMA/1.4/,EPS/1.0/,CP/6004.7/,R/1715.63/,P1S/0.95/,PT2S/1.0/
     1,P3S/1.0/,INT/100/
   73 FORMAT(6F10.5)
   74 FORMAT('0',///,' D1      D2      D3      PT1     TT1       TT2      P3
     1     AUGL      ENTLOS     X         P1         T1         T2         T3
     2CT      M2DOT',/,1F5.1,1F7.1,1F8.1,1F7.2,1F9.1,1F8.1,1F7.2,1F8.1,1F7
     3.2,1F10.2,1F8.3,1F9.1,1F8.1,1F9.1,2F9.4,/)
   75 FORMAT('0','M2M1     PT1P3     PT2P3     PT1PT2    XD1       A3A1      A2A1
     1    TT1TT2    T3T2    R02R03    DIND1    DOUTD1    SIGMA     YDIV      ODIV
     2D1')
   76 FORMAT(' ',1F5.3,3F8.3,1F9.3,2F9.2,1F7.2,1F9.2,1F8.3,1F9.3,1F8.3,1
     1F10.3,2F8.3,/)
   77 FORMAT('0','THE INNER CORE HAS BEEN EATEN UP WHEN X=',1F5.3,'INCHE
     1S')
   78 FORMAT('0','THE MIXING AREA HAS TOUCHED THE WALL FOR X =',1F5.2,'
     1INCHES')
   79 FORMAT('0','THE FRICTION DRAG =',1F7.2,' POUNDS, AND IS EQUIVALENT
     1 TO A BACK PRESSURE OF',1F6.2,' PSF')
   80 FORMAT('0',/,' SYSTEM WILL NOT WORK AGAINST A BACK PRESSURE OF',1F5
     1.2,'  ATMOSPHERES',//)
   90 FORMAT('0','THE PROGRAM HAS FAILED FOR X=',1F5.3,'  INCHES AND A B
     1ACK PRESSURE OF',1F5.3,'  ATMOSPHERES')
   91 FORMAT(3F10.5)
   95 FORMAT('0','NOZZLE REYNOLDS NUMBER =',1F8.3,' X 10**6')
      ATM=14.7*144.
      AMULT=3.141592653/4./144.
      GEXP=(GAMMA-1.)/GAMMA

      PUT ANY DO LOOP COMMANDS HERE.  ALL CONSTANTS SHOULD BE READY

      DO 100 J=1,9
      READ(5,73)D1,D2,D3,PT1,TT1,TT2
      READ(5,91)ENTLOS,X,AUGL
      P3=P3S
      A3=AMULT*D3*D3
      DO 100 N=1,50
      PT2=1.0
```

```
      P1=P1S
      P2=P1
      K=1
      L=1
      PCOR=0.01
      DRAG=0.0
   13 IF(L.GT.100) GO TO 100
   14 IF (P2.GT.PT2) GO TO 140
      GO TO 141
  140 CONTINUE
      WRITE(6,80)P3
      N=50
      GO TO 100
  141 CONTINUE
      BETA1=(PT1/P1)**GEXP
      BETA2=(PT2/P2)**GEXP
      M1SQ=(BETA1-1.)*2./(GAMMA-1.)
      M2SQ=(BETA2-1.)*2./(GAMMA-1.)
      IF(M1SQ.GE.1.0) GO TO 143
      GO TO 144
  143 X=0.0
  144 CONTINUE
      T1=TT1/BETA1
      T2=TT2/BETA2
      RHO1=P1*ATM/R/T1
      RHO2=P2*ATM/R/T2
      U1=49.02*SQRT(M1SQ*T1)
      U2=49.02*SQRT(M2SQ*T2)
      PT2OLD=PT2
      DELHD=0.0965*U2*U2*RHO2*ENTLOS/406.912
      PT2NEW=(1.0-DELHD+PT2OLD)/2.
      PDIF=ABS(PT2NEW-PT2OLD)
      PT2=PT2NEW
      IF(PDIF.LE.0.0001) GO TO 142
      GO TO 14
  142 CONTINUE
      UM=(U1+U2)/2.
      SIGMA=24.*UM/U1


      DEFINE THE WIDTH OF THE MIXING ZONE TO BE EQUAL TO DELTA
      DELTA IS BASED ON NU=1.84, OR THE NON-DIMENSIONAL Y COORDINATE
      WHERE THE VELOCITY IS APPROXIMATELY 99% OF THE FREE STREAM VALUE


      DELTA=2.*1.84*X/SIGMA
      IF(DELTA.GT.DL) GO TO 35
      GO TO 36
```

```
 35 WRITE(6,77)X
    N=50
    GO TO 100
 36 CONTINUE
    A1=AMULT*(D1-DELTA)*(D1-DELTA)
    A2=AMULT*(D2*D2-(D1+DELTA)*(D1+DELTA))
    IF(A2.LE.0.0)  GO TO 37
    GO TO 38
 37 WRITE(6,78)X
    GO TO 100
 38 CONTINUE
    M1DOT=RHO1*U1*A1
    M2DOT=RHO2*U2*A2
    IF(M1SQ.GT.1.0) GO TO 145
    GO TO 146
145 TSTAR=TT1*0.83333
    AASTAR=(((1./1.2)+(M1SQ/6.))**3.)/SQRT(M1SQ)
    ASTARA=1./AASTAR
    M1DOT=M1DOT*ASTARA*((TSTAR/T1)**3.)
146 CONTINUE

    DERIVE CONSTANTS FOR THE CONTINUITY EQUATIONS
    FROM UMZ=A+B ERFNU AND
    RHOMZ=C+D ERFNU

    A=(U1/2.)*(U2/U1+1.)
    B=(U2/U1-1.)*(U1/2.)
    C=(RHO1/2.)*(RHO2/RHO1+1.)
    D=(RHO2/RHO1-1.)*(RHO1/2.)
    XSIG=X/SIGMA
    HFINT=1.84/INT
    MZDOT=0.0
    AMIX=0.0
    IF(X.EQ.0.0) GO TO 41
    DO 40 I=1,INT
    NU(I)=1.84-HFINT*(2*I-1)
    ERFNU(I)=ERF(NU(I))
    DO=D1+2.*(NU(I)+HFINT)*XSIG
    DI=D1+2.*(NU(I)-HFINT)*XSIG
    AMZ(I)=AMULT*(DO*DO-DI*DI)
    AMIX=AMIX+AMZ(I)
    UMZ(I)=A+B*ERFNU(I)
    RHOMZ(I)=C+D*ERFNU(I)
    TMZ(I)=P1*ATM/R/RHOMZ(I)
    MDOT(I)=RHOMZ(I)*UMZ(I)*AMZ(I)
    MZDOT=MZDOT+MDOT(I)
```

```
 40 CONTINUE
 41 M3DOT=M1DOT+M2DOT+MZDOT
    MINT=0.0
    IF (X.EQ.0.0) GO TO 51
    DO 50 I=1,INT
    MINT=MINT+UMZ(I)*MDOT(I)
 50 CONTINUE
 51 U3=((P1-P3)*ATM*A3+M1DOT*U1+M2DOT*U2+MINT-DRAG)/M3DOT
    IF(U3.LE.0.0) GO TO 140
    RHO3=M3DOT/U3/A3
    DOLD=DRAG
    T3COM=P3*ATM/R/RHO3
    ENINT=0.0
    IF(X.EQ.0.0) GO TO 61
    DO 60 I=1,INT
    ENINT=ENINT+MDOT(I)*(TMZ(I)+UMZ(I)*UMZ(I)/2./CP)
 60 CONTINUE
 61 CONTINUE
    T3ENR=(T1+U1*U1/2./CP)*M1DOT/M3DOT+(T2+U2*U2/2./CP)*M2DOT/M3DOT+EN
   1INT/M3DOT-U3*U3/2./CP
    IF(AUGL.GT.0.0) GO TO 499
    GO TO 65
499 TBAR=(T3COM+T3ENR)/4.+T2/2.
    UBAR=(U2+U3)/2.0
    RHOB=(RHO2+RHO3)/2.0
    IF(TBAR.GE.564) GO TO 500
    V=0.639*TBAR-177.4
    GO TO 501
500 V=0.667*TBAR-193.2
501 CONTINUE
    COFRIC=0.455/((6.+ALOG10(UBAR*AUGL/12./V))**2.58)
    RUSQBR=(RHO2*U2*U2+RHO3*U3*U3)/2.
    DNEW=COFRIC*RUSQBR*AMULT*AUGL*D3*2.
    DDIFF=ABS(DNEW-DOLD)
    IF(DDIFF.GT.(0.01*DOLD)) GO TO 503
    GO TO 65
503 DRAG=DNEW
    GO TO 51
 65 COMP=T3COM-T3ENR
    IF(ABS(COMP).LT.EPS) GO TO 30
    IF(COMP) 20,30,21
 20 IF(K.EQ.3)  GO TO 23
    GO TO 22
 23 PCOR=PCOR/2.
 22 P1=P1+PCOR
    P2=P1
    K=2
    L=L+1
```

```
      GO TO 13
   21 IF(K.EQ.2) GO TO 24
      GO TO 25
   24 PCOR=PCOR/2.
   25 P1=P1-PCOR
      P2=P1
      K=3
      L=L+1
      GO TO 13
   30 CONTINUE
      MSAVE=M1DOT
       M1MZ=MSAVE
      M1DOT=RHO1*U1*D1*D1*AMULT
      M2DOT=M3DOT-M1DOT
      M2M1=M2DOT/M1DOT
      IF (X.EQ.0.0) GO TO 132
      IB=200
      DO 130 I=1,100
      II=101-I
      M1MZ=M1MZ+MDOT(II)
      IF(M1MZ.GT.M1DOT) GO TO 129
      GO TO 130
  129 IB=101-I
      I=100
  130 CONTINUE
      IF(IB.EQ.200) GO TO 135
      GO TO 131
  135 WRITE(6,90)X,P3
      GO TO 100
  131 CONTINUE
      YDIV=XSIG*(NU(IB)+HFINT)
      GO TO 133
  132 YDIV=0.0
  133 M1PPS=M1DOT*32.17
      M2PPS=M2DOT*32.17
      IF(T1.GE.564.) GO TO 134
      VNOZ=0.639*T1-177.4
      GO TO 136
  134 VNOZ=0.667*T1-193.2
  136 CONTINUE
      REYNOZ=U1*D1/VNOZ
      DIN=D1-DELTA
      DOUT=D1+DELTA
      PBACK=DRAG/A3
      T3=(T3COM+T3ENR)/2.
      PT1P3=PT1/P3
      PT2P3=PT2/P3
      PT1PT2=PT1/PT2
```

```
      XD1=X/D1
      A3A1=A3/A1
      A2A1=A2/A1
      TT1TT2=TT1/TT2
      T3T2=T3/T2
      RO2RO3=RHO2/RHO3
      DIND1=DIN/D1
      DOUTD1=DOUT/D1
      DDIV=D1+2.*YDIV
      DDIVD1=DDIV/D1
      M1DOT=M1DOT*32.2
      M2DOT=M2DOT*32.2
      WRITE(6,74)D1,D2,D3,PT1,TT1,TT2,P3,AUGL,ENTLOS,X,P1,T1,T2,T3,M1DOT
     1,M2DOT
      WRITE(6,75)
      WRITE(6,76)M2M1,PT1P3,PT2P3,PT1PT2,XD1,A3A1,A2A1,TT1TT2,T3T2,RO2RO
     13,DIND1,DOUTD1,SIGMA,YDIV,DDIVD1
      WRITE(6,79)DRAG,PBACK
      WRITE(6,95)REYNOZ
  201 CONTINUE
      P3=P3+0.01
  100 CONTINUE
  101 STOP
      END
```

PROGRAM M1DOT

```
      IMPLICIT REAL*4(K,M)
    8 FORMAT(1I2)
    9 FORMAT(6F10.5)
   10 FORMAT(' ',/,' NOZZLE FLOW =',1F7.4,' POUNDS PER SECOND, AND REYNO
     1LDS NUMBER IS',1F6.1,' X 10**3   DATA SET',1I4)
   11 FORMAT(' ',///,1F10.2,1F10.3,/)
      DSQ=2.096*2.096
      KGUESS=0.68
      READ(5,8) NSETS
      DO 17 J=1,NSETS

      PA AND P1G ARE IN INCHES OF MERCURY, HW IS IN INCHES
      OF WATER AND T1 IS IN DEGREES F

      READ(5,9)PA,P1G,T1,HW,CONFIG,RUNDAY
      WRITE(6,11)CONFIG,RUNDAY
      K=KGUESS
      P1=(PA+P1G)*14.67/29.92
      SPWT=P1*144./53.3/(T1+459.6)
      FA=(T1/10000.+6.994)/7.
      Y=1.-0.037*HW/P1/2.
      DO 16 I=1,2
      M1DOT=359./3600.*K*DSQ*FA*Y*SQRT(HW*SPWT)
      GNU=1.832*T1/1000.+1.0835
      RE=424.4*3.6*M1DOT/3./GNU
      WRITE(6,10)M1DOT,RE,J
      IF(RE.GT.100.) GO TO 15
      K=0.6865-0.0051*(RE/50.-1.)
      GO TO 16
   15 K=0.6814-0.004*(RE/400.-0.25)
   16 CONTINUE
   17 CONTINUE
      STOP
      END
```

PROGRAM AJG1

```
      IMPLICIT REAL*4(K,M)
      DIMENSION R(15),A(15),U(15),PT(15),TT(15),Q(15),M(15)
      READ(5,30)NSETS
   30 FORMAT(1I2)
      GTERM=0.4/1.4
      R1=0.0
      WRITE(6,29)
   29 FORMAT('0','CONFIG   RUNDAY   STA   M1DOT   M3DOT   M2M1    UCL
     1   U1UCL   U2UCL   U3UCL   U4UCL   U5UCL   U6UCL   U7UCL   U8UCL   U9UCL   U
     210UCL')
      DO 40 N=1,NSETS
      READ(5,31)CONFIG,RUNDAY,ISTA,PG,PA,M1DOT
   31 FORMAT(2F10.5,I110,3F10.5)

      TEMPERATURES ARE IN DEGREES F, PT'S AND PA ARE IN INCHES
      OF MERCURY AND PG IS IN CENTIMETERS OF WATER

      READ,(PT(I),I=1,10)
      READ,(TT(I),I=1,10)
      PG=PG/2.54/13.6
      P=(PG+PA)*14.67/29.92
      DO 34 I=1,10
      PT(I)=(PT(I)+PA)*14.67/29.92
      Q(I)=PT(I)-P
      IF(Q(I).LT.0.0) GO TO 41
      GO TO 42
   41 WRITE(6,37)N,I
   37 FORMAT(' ',2I10)
      Q(I)=-Q(I)
      TT(I)=TT(I)+459.6
      PTERM=(PT(I)/P)**GTERM
      USQ=2.*1715.63*TT(I)*PTERM*Q(I)/P
      U(I)=-SQRT(USQ)
      GO TO 34
   42 CONTINUE
      TT(I)=TT(I)+459.6
      PTERM=(P/PT(I))**GTERM
      USQ=2.*1715.63*TT(I)*PTERM*Q(I)/P
      U(I)=SQRT(USQ)
   34 R(I)=R1+(I-1)*0.25
      UCL=U(I)
```

```
      U(11)=0.0
      Q(11)=0.0
      R(11)=2.5
      M3DOT=0.0
      DO 35 I=1,10
      A(I)=3.14159*(R(I+1)*R(I+1)-R(I)*R(I))
      M(I)=(Q(I)+Q(I+1))*2.*A(I)/(U(I)+U(I+1))
      IF((U(I)+U(I+1)).GT.0.0) GO TO 32
      M(I)=0.0
   32 CONTINUE
   35 M3DOT=M3DOT+M(I)
      M3DOT=M3DOT*32.2
      M2DOT=M3DOT-M1DOT
      M2M1=M2DOT/M1DOT
      WRITE(6,36)CONFIG,RUNDAY,ISTA,M1DOT,M3DOT,M2M1,UCL,(U(I),I=1,10)
   36 FORMAT('0',1F6.2,1F8.3,1I6,1F9.3,2F8.3,1F8.1,1F8.1,9F7.1)
   40 CONTINUE
      STOP
      END
```

LIST OF REFERENCES

1. Engel, M. O., "Some Problems in the Design and Operation of Jet Ejectors," Proceedings of the Institution of Mechanical Engineers, v. 177, No. 13, p. 347, 1963.

2. Fabri, J., and Paulon, J., Theory and Experiments on Supersonic Air-to-Air Ejectors, NACA TM-1410, September 1958.

3. Fejer, A. A., Hermann, W. G., and Torda, T. P., Factors that Enhance Jet Mixing, Aerospace Research Labs., WPAFB, ARL-69-0175, October 1969.

4. Keenan, J. H., Neumann, E. P., and Lustwerk, F., "An Investigation of Ejector Design by Analysis and Experiment," Journal of Applied Mechanics, v. 17, No. 3, p. 299, September 1950.

5. Krenkel, A. R., and Lipowsky, H. H., Design Analysis of Central and Annular Jet Ejectors, ARL-66-0210, Polytechnic Institute of Brooklyn, October 1966.

6. Monroe, P. A., An Investigation of the Performance and Mixing Phenomena Associated with a Supersonic Exhauster Interacting with Subsonic Secondary Flow, Ae. E. Thesis, Naval Postgraduate School, Monterey, California, September 1967.

7. Wade, B. S., Parametric and Experimental Analysis of Ejector Performance, M.S. Thesis, Naval Postgraduate School, Monterey, California, July 1967.

8. Tower, P. W., The Dependence of Compressor Face Distortion on Test Cell Inlet Configuration, Ae. E. Thesis, Naval Postgraduate School, Monterey, California, December 1972.

9. Yaffee, Michael L., "Hybrid Fighter Engine Designed," Aviation Week and Space Technology, v. 95, No. 10, p. 40-42, 6 September 1971.

10. Pegasus Facilities Planning Manual, Rolls-Royce Limited Technical Report No. TP 148/B.E.D., Bristol, England, 1970.

11. Proposal for Development and Design Criteria and Model Test of a Universal Test Cell, FluiDyne Engineering Corporation Proposal No. P-1084, Minneapolis, Minnesota, October 1967.

12. Hieronymus, W. S., "Augmentor Wing Flight Tests Set," Aviation Week and Space Technology, v. 94, No. 1, p. 48-50, 4 January 1971.

13. Bailey, D. L., and Tower, P. W., Production Test Facilities for Turbojet and Turbofan Engines - 1975-1995, Naval Postgraduate School NPS-57 Ba, To72061A, Monterey, California, May 1972.

14. Gerend, R. P., and Roundhill, J. P., Correlation of Gas Turbine Weights and Dimensions, AIAA Paper 70-669.

15. FY71 MCP, Air Force Systems Command Advanced Engine Research Facility, WPAFB, 1970.

16. Beavers, T. E., An Engineering Analysis of Facilities for Altitude Testing of Large Turbojet and Turbofan Engines During the 1973-1990 Era, Arnold Engineering Development Center Report No. AEDC-TR-69-103, July 1969.

17. Schetz, J. A., Unified Analysis of Turbulent Jet Mixing, NASA CR-1382, July 1969.

18. Nagamatsu, H. T., Sheer, R. E., and Gill, M. S., Flow and Acoustic Characteristics of Subsonic and Supersonic Jets from Convergent Nozzle, NASA CR-1693, December 1970.

19. Korst, H. H., and Chow, W. L., Non-Isoenergetic Turbulent (P_{rt} = 1) Jet Mixing Between Two Compressible Streams at Constant Pressure, NASA CR-419, April 1966.

20. Morgenthaler, J. H., Zelazny, S. W., and Herendeen, D. L., Combustor Correlation Technique, Bell Aerospace Company Report No. 9500-920233, Buffalo, N.Y., February 1972.

21. Zelazny, S. W., Morgenthaler, J. H., and Herendeen, D. L., Shear Stress and Turbulent Intensity Models for Coflowing Axi-symmetric Streams, paper presented at AIAA 10th Aerospace Sciences Meeting, San Diego, California, 17-19 January 1972.

22. Pai, S. I., Fluid Dynamics of Jets, D. Van Nostrand Co., Inc., New York, 1954.

23. Birkhoff, G., Jets, Wakes and Cavities, Academic Press, New York, 1957.

24. Gurevich, M. I., The Theory of Jets in an Ideal Fluid, Translated by R. E. Hunt, Pergamon Press, Oxford, 1966.

25. Abramovich, G. N., The Theory of Turbulent Jets, M.I.T. Press, Cambridge, Mass., 1963.

26. Hanbury, W. T., The Performance of an Air-Air Ejector According to a Quasi-One-Dimensional Theory, Aeronautical Research Council of Great Britain, A.R.C. 29-341, April 1967.

27. Bauer, R. C., Characteristics of Axisymmetric and Two-Dimensional Isoenergetic Jet Mixing Zones, Arnold Engineering Development Center, AEDC-TDR-63-263, December 1963.

28. Schlichting, H., Boundary Layer Theory, McGraw-Hill, New York, 1968.

29. Carrier, W. H., and others, Modern Air Conditioning, Heating and Ventilating, Pitman Publishing Corporation, New York, 1959.

30. Supplement to ASME Power Test Codes, Chapter 4, Flow Measurement, p. 6-87, The American Society of Mechanical Engineers.

31. Airline Planning Guide: Test Facilities for Large Advanced Turbojet and Turbofan Engines, Flight Propulsion Division of General Electric, FPD-11-4/67, Lynn, Massachusetts, 1 April 1967.

32. Personal Communication with Mr. R. E. Totman, Staff Engineer, United Airlines Overhaul Facility, San Francisco, 17 December 1971.

33. Geery, E. L., and Margetts, M. J., Penetration of a High Velocity Gas Stream by a Water Jet, AIAA Paper No. 68-604, Presented at AIAA 4th Propulsion Joint Specialist Conference, Cleveland, Ohio, 10-14 June 1968.

34. Personal Communication with Mr. R. Boe, R. I. Corporation, Ogden, Utah.

35. Personal Communication with Mr. D. O'Dell, Naval Air Systems Command (Air 53431-D), Washington, D.C.

36. Personal Communication with Mr. G. Pulcher, Naval Air Propulsion Center, GSE Division, Philadelphia, Pa.

37. Olive, R. L., Modern Jet Engine Development Facility, ASME Paper 71-WA/GT-6, August 1971.

38. Personal Communication with Mr. G. Getter, Getter and Associates, New Rochelle, New York.

39. Preliminary Design, Model Testing and Installation of a Prototype of a Thermal Converter for the Control of Exhaust Emissions from Navy Jet Engine Test Cells, Northern Research and Engineering Corporation Report 950-313, Cambridge, Mass., 20 May 1971.

40. The Aeroacoustic Corporation, Bulletin B-37, R1, Amityville, N.Y., 1968.

41. Supplemental Airline Planning Guide: Test Facilities for Large Turbojet and Turbofan Engines, General Electric Report No. 4 DG 0006B01, Lynn, Mass., 1 June 1968.

42. Chriss, D. E., and Paulk, R. A., Summary Report: An Experimental Investigation of Subsonic Coaxial Free Turbulent Mixing, Arnold Engineering Development Center Report AEDC-TR-71-236, February 1972.

43. Pindzola, M., Jet Simulation in Ground Test Facilities, AGARDograph 79, Paris, November 1963.

44. Pai, S. I., "Axially Symmetrical Jet Mixing of a Compressible Fluid," Quarterly of Applied Mathematics, v. 10, No. 2, July 1952.

45. Ghia, K. N., Torda, T. P., and Lavan, Z., "Laminar Mixing of Heterogeneous Axisymmetric Coaxial Confined Jets," AIAA Journal, v. 7, No. 11, p. 2072, November 1969.

46. "Lockheed Research Aims at 50% Attenuation in Turbofan Noise," Aviation Week and Space Technology, v. 95, No. 3, p. 54-55, 19 July 1971.

47. Getter and Associates Report for the Naval Facilities Engineering Command, Pollution Abatement Study and Systems Analysis for Jet Engine Test Cells, Getter and Associates, New Rochelle, N.Y., February 1970.

48. Ribner, and others, Proceedings of a Short Course on Noise Generation and Suppression in Aircraft, 29 January - 2 February 1968, University of Tennessee Space Institute, Tullahoma, Tenn.

49. Acoustics Technology: A Survey, NASA SP-5093, 1970.

50. Aerodynamic Noise, Proceedings of AFOSR-UTIAS Symposium Held at Toronto, 20-21 May 1968, University of Toronto Press, 1969.

51. Richards, E. J., and Mead, D. J., Noise and Acoustic Fatigue in Aeronautics, John Wiley and Sons, Ltd., London, 1968.

52. Ferriss, D. H., and Johnson, R. F., "Turbulence in the Noise Producing Region of a Circular Jet," Journal of Fluid Mechanics, v. 19, part 4, p. 591, August 1964.

53. Lighthill, M. J., "Jet Noise," AIAA Journal, v. 1, No. 7, p. 1507, July 1963.

54. Westervelt, P. J., in Proceedings of a Short Course on Noise Generation and Suppression in Aircraft, 29 January - 2 February 1968, University of Tennessee Space Institute, Tullahoma, Tenn.

55. Standard Test Cell Design Study for Joint Airline Committee, Burns and Roe, Inc., April 1971.

56. Middleton, D., The Noise of Ejectors, Aeronautical Reserach Council, Reports and Memoranda No. 3389, October 1969.

57. Report on Standard Navy Depot Turbofan/Jet Engine Test Cell, Naval Air Systems Command/Naval Facilities Engineering Command, 1970.

58. The Aeroacoustic Corporation, Bulletin B-31, R1, Amityville, N.Y., 1968.

59. Personal Communication with Mr. L. B. Broberg, President, Aero Systems Engineering, Inc., St. Paul, Minn., Letter of 10 February 1972.

60. Sawyer, R. A., Atmospheric Pollution by Aircraft Engines and Fuels--A Survey, Department of Mechanical Engineering, University of California, Berkeley, 1 September 1971.

61. Analysis of Aircraft Exhaust Emission Measurements, Cornell Aeronautical Laboratory, Report No. NA-5007-K-1, Buffalo, N.Y., October 1971.

62. Assessment of Aircraft Emission Control Technology, Northern Research and Engineering Corporation, Report No. 11684, Cambridge, Mass., September 1971.

63. Heywood, J. B., Fay, J. A., and Linden, L. H., "Jet Aircraft Pollutant Production and Dispersion," AIAA Journal, v. 9, No. 5, p. 841, May 1971.

64. Henderson, R. E., Turbopropulsion Exhaust Smoke and Smoke Abatement, AFAPL Technical Memorandum APTC-TM-69-11, April 1969.

65. Report on Analysis of Exhaust Gases from Current Commerical Jet Engines, Study Group on Aviation Exhaust of the CRC Aviation Fuel, Lubricant and Equipment Research Committee, 23 July 1968.

66. Personal Communication with Mr. H. Lindenhofen, Naval Air Propulsion Center, Aero Engines Department, Philadelphia, Pa.

67. Channapragada, R. S., A Compressible Jet Spread Parameter for Mixing Zone Analysis (Part II), CETEC Corporation, TM-14-63-U31.35, San Jose, Calif., June 1963

INITIAL DISTRIBUTION LIST

		No. Copies
1.	Defense Documentation Center Cameron Station Alexandria, Virginia 22314	2
2.	Library, Code 0212 Naval Postgraduate School Monterey, California 93940	2
3.	Dean of Research Administration Naval Postgraduate School Monterey, California 93940	1
4.	Professor A. E. Fuhs, Code 57Fu Department of Aeronautics Naval Postgraduate School Monterey, California 93940	15
5.	LT David L. Bailey 721 Jamaica Ct. St. Louis, Missouri 63122	2
6.	LT Philip W. Tower 775 Santa Clara St. Alameda, California 49501	2
7.	John Adams AIR-4147B Naval Air Systems Command Washington, D. C. 20360	1
8.	Frank Freeman Code 642, Bldg. 94 Naval Air Rework Facility NAS North Island, California 92135	12
9.	Karl Guttman Code 330 Naval Air Systems Command Washington, D. C. 20360	1
10.	Commanding Officer Naval Air Rework Facility NAS North Island, California 92135	1

11. Harry Lindenhofen — 1
Naval Air Propulsion Center
AE Department, Bldg. 600
Philadelphia, Pa. 19112

12. Dennis O'Dell — 2
AIR-53431B
Naval Air Systems Command
1421 Jefferson Davis Highway
Washington, D.C. 20390

13. Eugene T. Pulcher — 2
Naval Air Engineering Center
GSE Division 76-1
Philadelphia, Pa. 19112

14. Chet Roscoe — 6
04 Group
Naval Air Systems Command
Washington, D. C. 20360

15. Irv Silver — 1
Code 03A
Naval Air Systems Command
Washington, D.C. 20360

16. Cyril S. Staub — 6
AIR-4147A
Naval Air Systems Command
Washington, D. C. 20360

17. Dr. R. W. Bell — 1
Chairman, Department of Aeronautics
Naval Postgraduate School
Monterey, California 93940

UNCLASSIFIED

Security Classification

DOCUMENT CONTROL DATA - R & D

(Security classification of title, body of abstract and indexing annotation must be entered when the overall report is classified)

1. ORIGINATING ACTIVITY (Corporate author)	2a. REPORT SECURITY CLASSIFICATION
Naval Postgraduate School Monterey, California 93940	Unclassified 2b. GROUP

3. REPORT TITLE

An Analytical and Experimental Analysis of Factors Affecting Exhaust System Performance in Sea Level Static Jet Engine Test Facilities

4. DESCRIPTIVE NOTES (Type of report and inclusive dates)

Engineer's Thesis; December 1972

5. AUTHOR(S) (First name, middle initial, last name)

David L. Bailey

6. REPORT DATE	7a. TOTAL NO. OF PAGES	7b. NO. OF REFS
December 1972		67

8a. CONTRACT OR GRANT NO.	9a. ORIGINATOR'S REPORT NUMBER(S)
b. PROJECT NO.	
c.	9b. OTHER REPORT NO(S) (Any other numbers that may be assigned this report)
d.	

10. DISTRIBUTION STATEMENT

Approved for public release; distribution unlimited

11. SUPPLEMENTARY NOTES	12. SPONSORING MILITARY ACTIVITY
This work was funded in part by AIRTASK Number A330330C/551B/ 2F00-432-302.	Naval Postgraduate School Monterey, California 93940

13. ABSTRACT

The study was motivated by a request from the Naval Air Rework Facility, NAS North Island, that work be conducted to obtain information on parameters affecting exhaust system performance in sea level static jet engine test facilities. The cost of pollution abatement devices makes it mandatory that accurate knowledge of flow parameters be developed. The study investigated by theory and experiment certain parameters of test cell design. A computer program based on the one-dimensional mass, momentum and energy conservation equations was developed. Components were designed to test on a scale of 24:1 the effects of varying exhaust system configurations. Theoretical results were found to be in good agreement with experimental data, indicating that the program may be used to analyze full scale systems. Recommendations for further development in the analysis and experimental program were made.

DD FORM 1 NOV 68 1473 (PAGE 1)

S/N 0101-807-6811

Security Classification

A-31408

14 KEY WORDS	LINK A		LINK B		LINK C	
	ROLE	WT	ROLE	WT	ROLE	WT
Test cell design						
Environmental protection						
Jet engine test facilities						
Jet mixing						
Jet pump						
Ejector design						